SANDIA REPORT
SAND2007-1871
Unclassified Unlimited Release
Printed March 2007

Macro-Meso-Microsystems Integration in LTCC: LDRD Report

Ken A. Peterson, Steven B. Rohde, Kamlesh D. Patel, Clifford Ho, Christopher D. Nordquist, Charles A. Walker, Brandon R. Rohrer, Stephen Buerger, Timothy S. Turner, Brian Wroblewski, Murat Okandan, Kent B. Pfeifer, Dennis De Smet

Prepared by
Sandia National Laboratories
Albuquerque, New Mexico 87185 and Livermore, California 94550

Sandia is a multiprogram laboratory operated by Sandia Corporation,
a Lockheed Martin Company, for the United States Department of Energy's
National Nuclear Security Administration under Contract DE-AC04-94AL85000.

Issued by Sandia National Laboratories, operated for the United States Department of Energy by Sandia Corporation.

Available to DOE and DOE contractors from
U.S. Department of Energy
Office of Scientific and Technical Information
P.O. Box 62
Oak Ridge, TN 37831

Telephone: (865) 576-8401
Facsimile: (865) 576-5728
E-Mail: reports@adonis.osti.gov
Online ordering: http://www.osti.gov/bridge

Available to the public from
U.S. Department of Commerce
National Technical Information Service
5285 Port Royal Rd.
Springfield, VA 22161

Telephone: (800) 553-6847
Facsimile: (703) 605-6900
E-Mail: orders@ntis.fedworld.gov
Online order: http://www.ntis.gov/help/ordermethods.asp?loc=7-4-0#online

SAND2007-1871
Unlimited Distribution
Printed March 2007

Macro-Meso-Microsystems Integration in LTCC LDRD Report

LDRD #04-1234, #05-1143, #06-1281 Project # 67008

Ken A. Peterson,[1] Steven B. Rohde,[2] Kamlesh D. Patel,[3], Clifford Ho[4], Christopher D. Nordquist,[5] Charles A. Walker,[1] Brandon R. Rohrer,[6] Stephen Buerger[6], Timothy S. Turner,[1] Brian Wroblewski,[1] Murat Okandan[5], Kent B. Pfeifer[5], Dennis De Smet[1]

Sandia National Laboratories
P.O. Box 5800
Albuquerque, NM 87185-0959

Abstract

Low Temperature Cofired Ceramic (LTCC) has proven to be an enabling medium for microsystem technologies, because of its desirable electrical, physical, and chemical properties coupled with its capability for rapid prototyping and scalable manufacturing of components. LTCC is viewed as an extension of hybrid microcircuits, and in that function it enables development, testing, and deployment of silicon microsystems. However, its versatility has allowed it to succeed as a microsystem medium in its own right, with applications in non-microelectronic meso-scale devices and in a range of sensor devices. Applications include silicon microfluidic 'chip-and-wire' systems and fluid grid array (FGA)/microfluidic multichip modules using embedded channels in LTCC, and cofired electro-mechanical systems with moving parts. Both the microfluidic and mechanical system applications are enabled by sacrificial volume materials (SVM), which serve to create and maintain cavities and separation gaps during the lamination and cofiring process. SVMs consisting of thermally fugitive or partially inert materials are easily incorporated. Recognizing the premium on devices that are cofired rather than assembled, we report on functional-as-released and functional-as-fired moving parts. Additional applications for cofired transparent windows, some as small as an optical fiber, are also described. The applications described help pave the way for widespread application of LTCC to biomedical, control, analysis, characterization, and radio frequency (RF) functions for macro-meso-microsystems.

---

[1] Manufacturing Science and Technology Center.
[2] Electronic Systems Center
[3] Biological and Energy Sciences Center
[4] Energy, Resources, and Systems Analysis Center
[5] Microsystems Science, Technology, and Components Center
[6] Security Systems and Technology Center

Contents

Figures

Tables

Acknowledgements

(in Alphabetical Order)

Chelsea Benally
Jon Bryan
Conrad James
Lucas McGrath
Richard Sanchez
Gayle Schwartz
David Saiz
Robert Stokes
Rose Torres
Chuck Walker
Gary Zender
Bernard Perini, Southwest Technical Sales
Luke Ferguson, Harmonics, Inc.

Executive Summary

Upon the recognition that LTCC technology can play an important part in integration of macro-, meso-, micro-, and nano- scale systems, several areas have been investigated. These include new sacrificial volume materials/methods (SVM), new structures, creative use of thermistors, and setter and jacketed setter materials to fabricate structures never before envisioned. These include moving parts that are self-assembling at the meso-scale. These parts have been actuated electrostatically, pneumatically, and directly mechanically.

In a sense, almost every use of solid SVM is crying out for a patterned definition. Many more ways to do this exist when the SVM is in the form of a fluid. SVMs have no real minimum thickness with respect to the scale of features envisioned for thick films. We have also investigated the upper end of features, successfully fabricating channels and volumes with mm scale dimensions. By using composite SVMs, there is essentially no limit. We have fabricated stacked parts in the form of washers of diameter approximately 1.2 cm. Evaluations have been performed on similar parts that are inches in diameter.

The application of sensitive materials has made it possible to fabricate smart channels. The bulk of this work has been carried out with polymeric chemiresistors, but new promise is held for cofirable sensitive materials as well. The two that were examined in detail include thermoresistive and piezoresistive materials.

The portions of the work that are suitable for open distribution are included in this report.

Nomenclature

Au = gold
Cr = chromium
FA = Failure Analysis
g (g's) = multiples of the earth's gravitational field used to quantify acceleration
HMC = Hybrid Microcircuit
HF = hydrofluoric
HTCC = High temperature cofired ceramic
In = indium
I/O = input/output
IP = Intellectual Property
LDRD = Laboratory directed research and development (Project)
LIGA = a German acronym for lithography, electroplating and molding
Lpm liters per minute
LTCC = Low temperature cofired ceramic
MEMS = Microelectromechanical systems
MCM = multichip module
Ni = nickel
NW = Nuclear Weapon
Pb = lead
PC = Patent Caution
RPA = resistor pair attribute
SCCM = standard cubic centimeter per minute.
SEM = Scanning electron microscope (microscopy)
SM = Surface Mount (device)
Sn = tin
TA = Disclosure of Technical Advance
TC = thermocompression
TCR = thermal coefficient of resistance
TFN = thin film network
TKN = thick film network
UCI = Unclassified Controlled Information

Macro-Meso-Microsystems Integration in LTCC LDRD Report

Introduction

The original milestone plan is shown below with comments. Several milestones were realized early and annually-updated proposals showed other milestones delayed to accommodate these adjustments of effort. In only one case did we decline to go into the detail originally specified—the incorporation of bulk metals. This was in order to give additional emphasis to the topic of meso-scale structures and sensor applications which turned out better than expected. This means that the applications were numerous and promising. Although no milestones were dropped, several were added and these are shown in underlined italics in Table 1. With technical contacts that permitted excursions into the realm of smart channels (both meso and micro scale), micro high performance liquid spectroscopy (mHPLC) and biological functions using small channels, the applications realized exceeded our expectations. Also fabricated were electro-microfluidic test fixtures, RF structures, and several structures that are the first of their type in the world.

Table 1. Project Milestones (underlined italics indicate milestones added during the project).

FY04 milestones:	**Projected date**	**Comments**
Discovery	1/4/04	
Selection of integration application	3/31/04	
Fabrication of prototype fluidic microsystem	6/30/04	Delayed 3 mos.
Incorporation of thick film materials	9/30/04	Advanced 3 mos.
Customization of chemiresistor sensor requirements	*9/30/04*	*New item*
FY05 milestones:		
Preliminary characterization of suspended thick film structures		*1/4/05 (new item)*
Preliminary characterization of μHPLC applications		*11/30/04 (new item)*
Incorporation of cofired bulk metals	1/4/05	Superseded by meso structures
Design of 3-D package application	3/31/05	Delayed 6 mo.
Prototype sensor thick film incorporation	6/30/05	
Design of new meso-scale structures	9/30/05	Advanced 3 mo.
FY06: milestones:		
Characterize existing structures	*1/3/06*	*New item*
Design of new meso-scale structures	1/3/06	
Prototype of meso scale structures	3/31/06	
Design of integration application	6/30/06	Advanced
Complete fabrication of integration application	9/29/06	Advanced
Complete SAND report.	9/29/06	Delayed

Results

Sacrificial Volume Materials (SVM)

Thermally fugitive materials have been used to fabricate parts of ceramic and other materials. Analogous to these are the materials that can be 'ashed' in an oxygen plasma in thin film technology. A technique was developed that augmented the common usage of sacrificial materials to create embedded unfilled volumes. Thick film materials were incorporated into these features to provide new functions. In addition, techniques were developed to incorporate other sensor and actuator structures, such as thermistors, heaters, and suspended and movable parts. As we learned more about sacrificial materials we also learned more about creating functional volumes without them, and where the relative advantages were. Perhaps the most significant development was the timely discovery of a material manufactured by Harmonics, Inc. This material was obtained in it's existing slurry form for early experiments—the slurry being the material that the vendor then tape-casts into tape form. We also procured the material in its tape form, and also acquired a paste that was more suitable for screen printing and stenciling due to changes in the organic vehicle and the loading which reduced the shrinkage upon drying. We have extensively described most of this work in several articles in the appendices. These techniques include the following list:

Dispensing
Stenciling
Screen printing
Screeding

We also saw that the list could include lithography, ink-jetting, spraying, flocking and several other techniques. With these materials we made suspended thick film structures which have valuable uses as outlined in the appendices.

A special class of the SVMs was the setter and separation materials which we also put to unconventional uses. These made it possible to make the first cofired movable parts in the world. Composite layers of these various materials also made it possible to preserve the best properties of each. An example is the ability for spaces to collapse partially while maintaining separation so structural elements intended to remain unattached (not sintered together) in fact do remain unattached.

Microfluidics

Extensive advantage was taken of LTCC to form many microfluidic solutions to integration problems—both with various types of SVMs and without. We showed a concept that asked the question 'What if surface topography is not limiting the end device?' Several manifolds have been made permitting the channel topography to appear at the surface of the part. Another useful structure is deformation that appears during lamination and gives rise to a conical port. By using sacrificial materials and creative lamination, we were also able to make flat parts and parts with tight control on the I/O port shape.

HPLC hardware
Applications undertaken pioneered the chip and board-scale use of LTCC for electrokinetic pumping and for high pressure liquid chromatography functions. This includes complex channel arrays, mixers, and LTCC parts with sapphire windows that would permit the observation of flowing fluids in the otherwise opaque or translucent board.

Cell Lyser
Biological cell lysers were developed which successfully lysed biological cells by using heat and pressure. The embedded heaters were tailored to the application and the inputs and outputs were arranged around them. This work is described in the appendices.

Chemiresistors
Smart channels were fabricated from LTCC that consisted of integrated temperature, flow and chemical sensing. Early prototypes demonstrated the use of LTCC as smart channels with different geometries and configurations of the substrate and sensors. Later, an optimized design was developed in the form of a small solid tube. The advantage of such a structure is that it permits a flexible tube to be attached to each end to convey fluid flow while maintaining access to the electrical leads in the center as discussed in the Appendices. The tube is strong enough to withstand the normal use conditions including fastening and loosening of flexible tubing. Other implementations have since included the use of flow sensing and chemiresistors in smaller channels of the type incorporated into microsystem boards. The chemiresistor smart channel samples had a heater as well as thermistors that were capable of measuring both the temperature and flow rate of gas moving through the tube (via “hot-wire” anemometry). In addition, the polymer-based chemiresistor sensors detected the presence and concentration of volatile organic compounds.

The only post-fabrication LTCC processing that needed to be performed following cofiring was soldering of leads onto the tube and deposition of the chemiresistor polymers. Techniques have since been developed to make the leads and connections socketable. The minimization of post-fabrication assembly processes is a huge advantage of using LTCC for smart channels and other micro/meso-system assemblies.

Microfluidic Interposers
A microfluidic interposer has been proposed as a manufacturability aid. The numerical punching technique has the ability to fabricate fine features consistent with geometries on microfluidic MEMS devices. An example would be a 300 micron diameter Bosch-etched counterbore with a wall thickness of 500 microns between openings.

Several aggressive pitches have been successfully punched in green tape. In addition, channels can be formed by a number of techniques. These include

sacrificial volume materials molded into the structure by lamination, SVMs used as placeholders in pre-punched channels, unsupported pre-punched channels with special lamination, and unsupported pre-punched channels without any special lamination procedures. An example of a complex prototype part consisting of a central chamber, perforated on both sides is shown in . The entire board is only 0.022" thick. Other thin boards comprising manifolds are shown in Figure 2 and Figure 3.

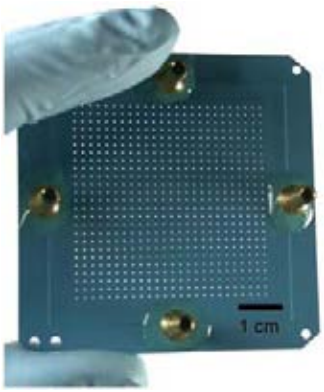

Figure 1. Thin, finely perforated microfluidic (pneumatic) boards are possible using SVMs.

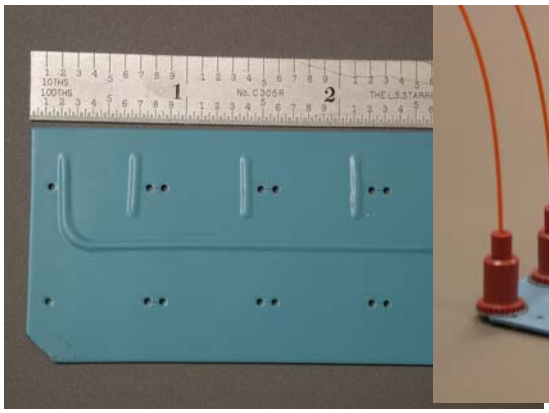

Figure 2. Microfluidic manifold

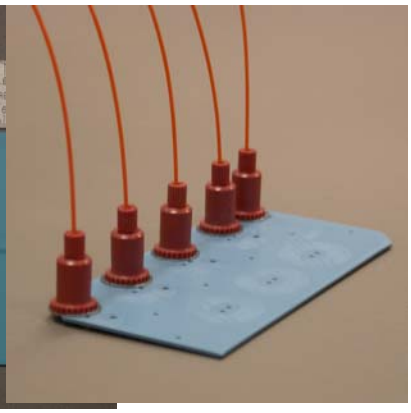

Figure 3. Test manifold

Incorporated metals

Work proceeded on incorporated metals. Other authors have also described work on incorporated metal structures. Our interest was drawn to an application where a TO-can type of package would be ideal. This was not ultimately pursued in detail as appealling alternatives became available using the abilities to perforate and fill appropriate segments of the LTCC. Additional work in the future would add more value to the preliminary results obtained.

Thermistors

We worked extensively with thermistors in order to use them for on-board temperature measurement and also as elements for anemometry. The anemometry was performed in prototypical smart channels that consisted of tubes with components on the inside walls. Later, the channels were made smaller and more like the channels in other devices we fabricated. Smart channels are described in the appendices. Thermistors were supplied to multiple applications as a result of this work.

Miniature heated tubes

Through involvement with an IMS program at Sandia we became aware that ceramic sample inlet tubes tubes were being used as inlet tubes for IMS samples. These tubes were then fitted with heaters which appeared to be rather bulky. We knew from earlier experience that we could make these tubes in LTCC and

incorporate heaters in the inner layers that would perform the necessary function. In addition, we were able to equip these tubes with thermistors that had the capability to read temperature of the tubes. An image of such a tube is shown in Figure 4.

Figure 4. Heated sample inlet tube for IMS application.

Heated platen

In microelectronics, several applications require a sealing technique that is served well by a rather high temperature solder, eutectic 80Au-20Sn, that melts at a temperature of 280° Celsius. Frequently, however, the device in the package can not go to the sealing temperature, and measures are taken to keep the device at a maximum temperature of about 150° Celsius. One popular tool for achieving this is a seam sealer that can weld two metal surfaces together or heat a region locally and impart enough energy to melt the solder sequentially around the seal ring.

Another technique for doing this employs a dynamic situation where sufficient heat is concentrated at the seal without heating the device excessively. When the seal is accomplished the removal of heat has always been the challenge, as heat in the package, and sometimes in the heater, will equilibrate resulting in a higher temperature than desired at the device.

We have fabricated a platen that accomplishes this goal in sealing microelectronic packages. The heater is a thick film heater buried in the matrix of LTCC. Because the mass of the heater and supporting structure is low, it can be cooled rapidly by a stream of air. At the same time, glands can be directed at the part itself to facilitate this cooling after the seal is accomplished.

Fluidic grid array (FGA)

Microelectronic parts have long been packaged in an assortment of packages including the common pin grid array (PGA). We have previously considered inclusion of tubes in packaging in place of pins to enable complementary electrical and electrical connections (Reference LDRD proposal)[1]. We had also long ago investigated packages designed after PGAs, but lacking the pin. We termed these

pad grid arrays (PaGA). Since that time, the advent of chip scale packaging has matured and similar packages are known as ball grid arrays (BGA). We have shown annular connections that can be arrayed across an area representing a fluidic grid array (FGA) by using the many layers possible in LTCC (detailed in appendices).

Suspended Cofired Structures

Review of the LTCC literature led to our analysis of a thermal flow sensor that needed thermal isolation and a microstrip application. Both were limited by construction of a thick film feature on a suspended bridge of the thinnest tape available. Both would benefit from the substrate being made negligibly small or eliminating the substrate entirely. Such structures have been fabricated in both a conductor and dielectric as shown in Figure 5. A related structure is illustrated in Figure 6.

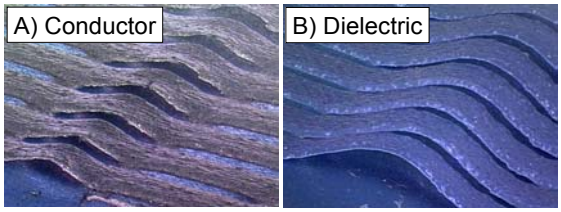

Figure 5. Freestanding conductor and dielectric structures.

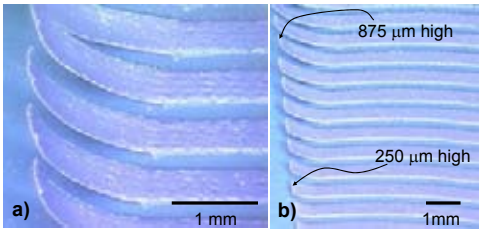

Figure 6. Isolated dielectric fingers.

These techniques, especially the ability to integrate airgaps and metal loops into LTCC structure, offer potential for fabricating unique structures for RF applications. Typical inductors in LTCC are fabricated with planar spirals, which typically have a low Q and a low self-resonant frequency. This is primarily due to the narrow spiraled conductors, which typically have a high resistance and a large inter-turn capacitance. Using these fabrication techniques, a 3-dimensional structure can be made to minimize the parasitic elements while maintaining the inductance of the structure. The result of this improved Q and self-resonance frequency is improved response, frequency range, and loss for filters and other circuits realized in the LTCC material. These lateral structures may also allow the fabrication of transformers and other coupling elements. Additionally, the straight open core may allow the insertion of a ferrite material, which will significantly increase the inductance of the structure over an air-core structure.

The SVM technique also presents the option of building air-gap stripline structures, in which a metal conductor line is placed in an airgap between two ground planes. These structures demonstrate lower-loss than traditional stripline fabricated with dielectric material in the gap, and much lower dispersion and loss than traditional microstrip on the same substrate. This will enable filters and delay networks with higher performance and lower loss than using other techniques in similar technologies.

Stacked tubes

Earlier work on a project paved the way for rolling and shaping of green structures, resulting in a rolled design for the IMS tube used in the Microhound project. Another effort within that project concentrated on a stacked design for the construction of the drift tube. It is our understanding that that design experienced cracking of the monolithic section of the drift tube (about 1cm cubed) that was to be assembled into the complete drift tube. Since that time, the specifications of the tube have changed, and the inner diameter of the current tube is 0.5 inch.

We have used a technique consisting of stacking to simulate a fabrication method for a tube that is comparable to the rolled tube. The successful burnout and firing of a 0.040" thick wall on a rolled tube suggested that a 0.040" wall on a washer embedded in a stack would also burnout and fire successfully. Individual washers are collated on a mandrel with a slight taper. This assembly is then buffered and restrained by a plastic film. The assembly is then laminated in a conventional manner in an isostatic laminator. Following lamination the green tube is removed from the mandrel and fired standing on it's end. Two such tubes have been fabricated using 300 washers that were each 0.001" thick. One was laminated at ~3000 psi and the second was laminated at 30,000 psi. Both tubes were successful on the first attempt. Additional tubes have been fabricated at the smaller diameter of the original IMS tube. All tubes have been checked for hermeticity of the union between layers and have passed with no detectable leak to a limit of 2.5 X 10-10 Atm cc/sec He.

An example of one of these tubes is shown in Figure 7. These tubes did not have any other thick film features that would complicate firing due to differential loading. The end shown in the photo is as-fired. Various end-support fixtures have been envisioned to improve planarity and finish at these tube ends.

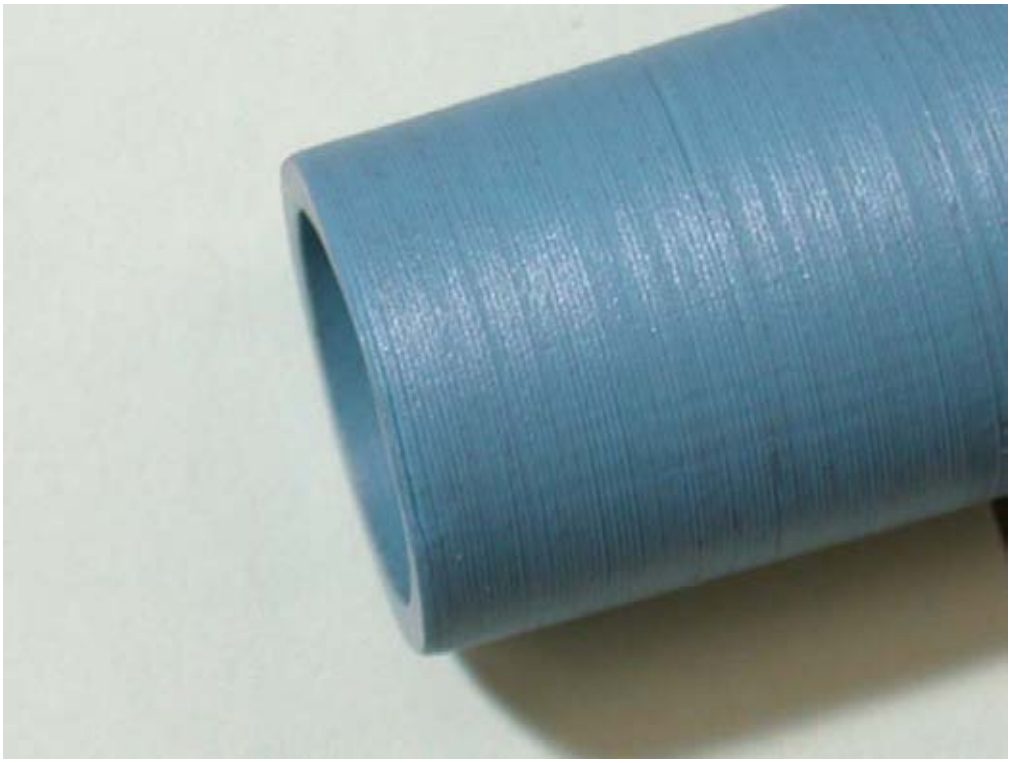

Figure 7. Fired tube fabricated from stacked washers.

Capacitive sensing

The ability to fabricate free-standing structures suggested the ability to perform capacitive sensing. Shows a small data set illustrating this capability. This is also covered in the appendices.

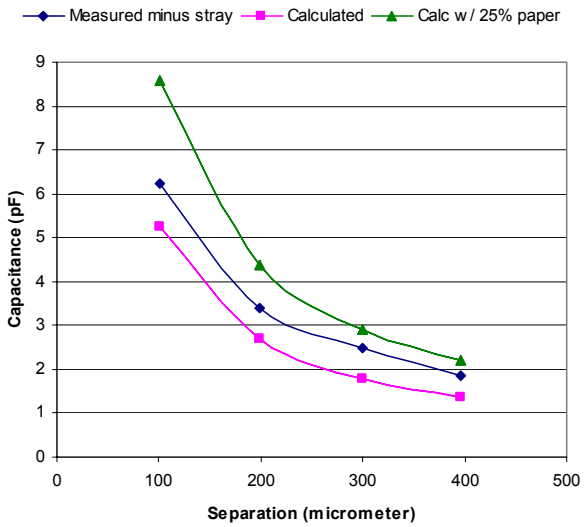

Figure 8. Plot of capacitance vs. separation for a movable parallel plate capacitor.

Other

Inductor Structures
Combination of electrostatic drive--capacitive sensing
Pressure sensors
RF Cavity Resonators
Electrostatic Actuation
Pressure regulators
Flow sensors
Simple accelerometer

Conclusions.

Low Temperature Cofired Ceramic, though mature in some applications, is in its infancy with regard to the many applications to microsystems. It provides a technique to interface to microscale mechanical features with mesoscale function and compatibility with nanoscale capabilities (i.e., coatings)—all the while providing the electrical, mechanical, fluidic, environmental, and other interfaces to the macroscale outside world. We have discussed processing techniques we have used to accomplish particular structures. These include the use of various sacrificial volume materials (SVM) to create structures such as moving parts, sensor cavities, microfluidic channels, and suspended thick films. We have also used forming and fabrication techniques to obtain structures such as rolled tubes. We have given examples of these structures in several applications where LTCC has been essential to microsystems and meso-scale-sensors. By tailoring processes to meet specific program needs, LTCC can meet microsystem components at their tiny scale and present them in usable form to the outside world. We have shown this for highly-electroded (closely spaced) high flow fluid analysis, microfluidic chip and wire manifolds, and interposer manifolds that are ideal for testing silicon MEMS die. We have shown promising early results for cofired, scalable pressure sensors. Windows in microfluidic circuits will greatly increase the acceptability in life sciences analytical applications. Radio frequency applications such as patch antennas and inverted microstrip are feasible in view of success with high aspect ratio channels. Finally, rolled tubes are reaching maturity and are ready for commercialization for devices such as the rolled IMS drift tube.

Appendix Descriptions

Appendix 0: Invited conference presentation and proceedings 2003

K.A.Peterson, S.B. Rohde, K.B. Pfeifer, T.S.Turner, “Novel LTCC Fabrication Techniques Applied to a Rolled Ion Mobility Spectrometer,” (Invited presentation and paper) Proc. 204th Mtg. (Electrochem. Soc. Series); v2003 no.27 156-171, Orlando, Florida, October 12-16, 2003.

Appendix I: Conference presentation and proceedings 2004

K.A. Peterson, S.B. Rohde, C.A. Walker, K.D. Patel, T.S. Turner, C.D. Nordquist, “Microsystem Integration with New Techniques in LTCC,” Proceedings, IMAPS/AcerS Conference Ceramic Interconnect Technology; The Next Generation, 2004; April 26-28, 2004, Denver, CO, p. 19-26.

Appendix II: Conference presentation and proceedings 2005

K. A. Peterson, K. D. Patel, C. K. Ho, S. B. Rohde, C .D. Nordquist, C.A. Walker, B.D. Wroblewski, M. Okandan, “Novel Microsystem Applications with New Techniques in LTCC,“ 1st International Conference on Ceramic Interconnect and Ceramic Microsystems Technologies (CICMT), Proceedings CD-ROM; Co-Published by IMAPS and ACerS, pp. 156-173; Baltimore, Maryland, April 10-13, 2005.
Also published in *Int. Journal of Applied Ceramic Technology*, 2 (5) 345-363, 2005.

Appendix III: Conference presentation and proceedings 2006

K.A. Peterson, K.D. Patel, C.K. Ho, B.R. Rohrer, C.D. Nordquist, B.D. Wroblewski, K.B. Pfeifer, “LTCC Microsystems and Microsystem Packaging and Integration Applications,”2nd International Conference on Ceramic Interconnect and Ceramic Microsystems Technologies (CICMT), Proceedings CD-ROM; Co-Published by IMAPS and ACerS, Denver, Colorado, April 25-27, 2006.
Also invited and published in *J. Microelectronics and Electronic Packaging*, 3 (3) 109-120, 2005.

Appendix IV: Conference presentation and proceedings 2006

Clifford K. Ho, Kenneth A. Peterson, Lucas K. McGrath, and Timothy S. Turner, “Development of LTCC Smart Channels for Integrated Chemical, Temperature, and Flow Sensing,” 2nd International Conference on Ceramic Interconnect and Ceramic Microsystems Technologies (CICMT), Proceedings CD-ROM; Co-Published by IMAPS and ACerS, Denver, Colorado, April 25-27, 2006.
Also invited and published in *J. Microelectronics and Electronic Packaging*, 3 (3) 136-144, 2005.

Appendix V: Conference presentation and proceedings 2006

Kamlesh D. Patel*, Kenneth A. Peterson, and Kyle W. Hukari, "Low Temperature Cofired Ceramic Microfluidic Microsystems for High Temperature and High Pressure Applications," 2nd International Conference on Ceramic Interconnect and Ceramic Microsystems Technologies (CICMT), Proceedings CD-ROM; Co-Published by IMAPS and ACerS, Denver, Colorado, April 25-27, 2006.
Also invited and published in *J. Microelectronics and Electronic Packaging*, 3 (3) 152-158, 2005.

References

[1] LDRD Proposal LDRD# 00-0620: MCM-C Technology Development, May 29, 1999, Lead PI: Fernando Uribe, Author: Ken Peterson.

NOVEL LTCC FABRICATION TECHNIQUES APPLIED TO A ROLLED MICRO ION MOBILITY SPECTROMETER

K.A. Peterson, S.B Rohde, K.B. Pfeifer, and T.S. Turner
Sandia National Laboratories, P.O. Box 5800
MS0959 (kap), MS1073 (sbr), MS1425, (kbp), MS0959 (tst)
Albuquerque, NM 87185-0959

peterska@sandia.gov, sbrohde@sandia.gov, kbpfeif@sandia.gov, tsturne@sandia.gov

ABSTRACT

LTCC is applicable to a broad range of micro systems. New LTCC techniques for micro-IMS fabrication have improved function, while simplifying the structure for better manufacturability at lower cost, which is critical to widespread implementation of robust sensing capability. A drift tube is fabricated by rolling unfired glass-ceramic tape with thick film features on both sides, including internal electrodes, external connections, seal rings, a buried heater, and an integral precision resistor network. The tube supports itself mechanically through burnout and firing. The assembly of internal components, including an ionizer, apertures, grids, and a target, is accomplished from the tube ends. The high aspect ratio of LIGA grids accomplishes low obstruction with high axial rigidity. Gas plumbing is also incorporated, and a sacrificial material technique which simplifies the exhaust porting is described. Integral transparent windows in LTCC as they may improve a future IMS are also described. Prototypes have detected ion peaks.

INTRODUCTION

This work describes the combination of an unconventional application of existing commercial infrastructure in Low Temperature Co-fired Ceramic (LTCC) technology for microelectronics with LIGA (a German acronym for lithography, electroforming, and molding) to provide improved functionality and simplicity to an ion mobility spectrometer (IMS). A miniaturized IMS that included a large number of stacked elements had been demonstrated previously. Success with the initial model indicated the need for a more producible implementation. It was also recognized, that the same function could be met by a number of other materials and configurations, including other stacked versions. A rolled LTCC tube concept was selected for further development.[1,2,3] A fired example of this approach, which eliminates more than 150 parts, is shown in Figure 1.

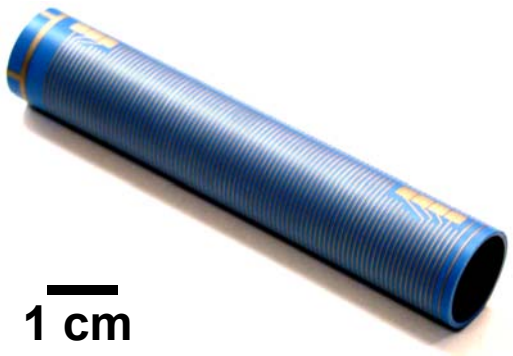

Figure 1. An LTCC IMS drift tube is rolled, laminated and fired to net shape.

BACKGROUND

Ion Mobility Spectrometer

An ion mobility spectrometer (IMS) is a device which can identify and quantify compounds by ionizing them and transporting them down a drift tube with an electrostatic potential gradient as the driving force. A counter flow of a carrier gas results in collisions that increase the time of flight to a biased target. A potential well is established in the drift section to trap negative ions. When the well is released, the ions travel toward the detector at a speed that is determined by the ion's mobility. The mobility is a complex function of the mass, shape, and other properties of the ion.[4] The time of flight to the target is measured using a sensitive amplifier and used to determine the species of the ion. The mobility is determined from the time of flight via the equations below where v_g is the speed of the ion, ϕ is the potential, κ is the mobility, L is the length of the drift region, E is the electric field, and t is the time of flight for the center of the peak.

$$v_g = \kappa E = -k\nabla\phi \tag{1}$$

$$\kappa = -\frac{L}{\nabla\phi t} = \frac{L}{t\frac{d\phi}{dx}} \tag{2}$$

$$\kappa \approx \frac{L\Delta x}{t\Delta\phi} \tag{3}$$

Figure 2a. shows the location of the ionizing chamber with respect to the

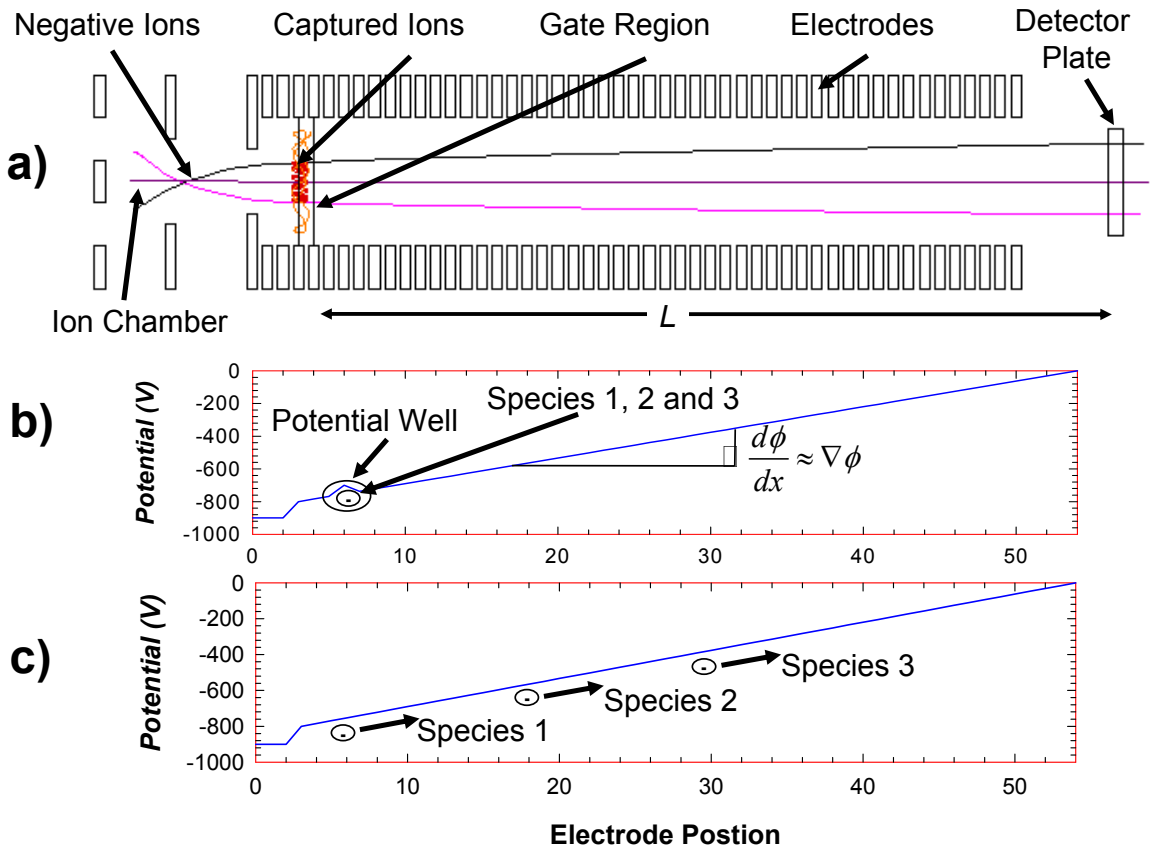

Figure 2. Schematic of operation of micro-IMS stacked version.

apertures, gate, and target in a schematic cross section of the IMS. Figure 2b. shows the gradient with the potential well in place and schematically illustrates the trapped ions for 3 species of compounds also represented in the earlier sketch in Figure 2a. Figure 2c. shows the gradient with the well released, and suggests that the three ionic species travel the length of the drift tube and strike the target with a time distribution that is characteristic of each species. Figure 3 shows what a plot of the output would look like, with species

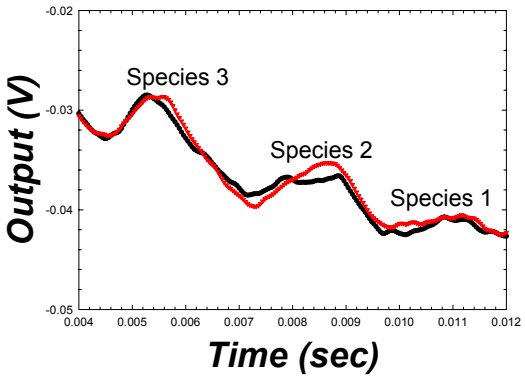

Figure 3. Diagram of raw and smoothed output from three species in IMS.

3 the first to arrive, followed by the others. The output is shown both as-detected and smoothed by averaging. Sharper peaks are desirable because more compounds can be resolved. Effects that would broaden peaks would obscure neighboring peaks. Statistics of collisions suggest additional practical considerations for the time of flight, including tube geometry, temperature, flow rates and triggering.

A perspective view of the baseline micro-IMS drift tube, consisting of a series of stacked metal and insulator plates, is illustrated in Figure 4. Electrical connections were made by spot-welded leads to the appropriate plates. In the baseline design, the grid consisted of a lattice of fine wires. Additional detail in the end-blocks at the front and tail end of the IMS facilitated plumbing of carrier gas, sample gas, and exhaust from the IMS. A separate heater was wrapped around the IMS and this assembly was then thermally insulated. The baseline IMS was assembled in a simple fixture by adhesively joining the

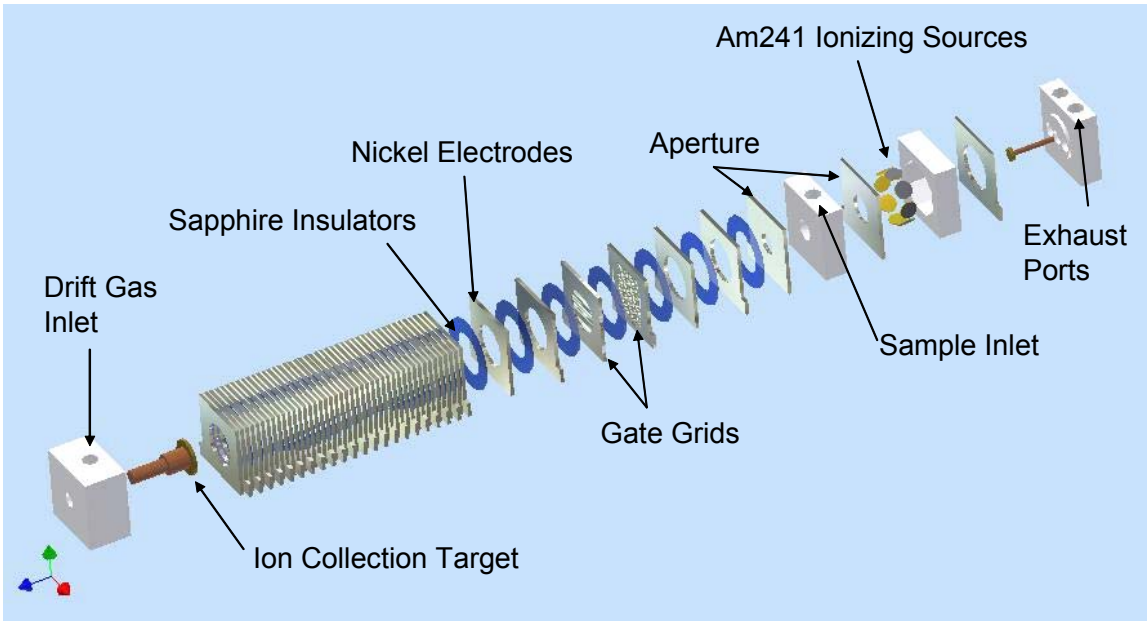

Figure 4. Stacked micro-IMS.

many plates together to form the drift tube. End-block assemblies were also joined to the drift tube with adhesive.

IMS Features/Requirements

Inertness. For implementation of an IMS detector, it is desirable to have a chemically inert internal surface with minimum porosity to reduce trapping of contaminates in the tube. The ceramic in the rolled tube is a good replacement for the inert insulating plates in the stacked version. The gold conductors are also inert compared to the edges of the conductive nickel plates. Polymeric adhesive joints between nickel and sapphire plates can provide trapping sites, leaks and can contribute contaminates to the drift tube in reactions with species that are present--not the least of which are chlorine ions.

Hermeticity. One of the major improvements that could be made to the IMS tube was to close leaks. Presently, the device is primarily operated as a positive pressure device. Because sample volumes can be small, the flow must be contained. In a negative pressure device, the same benefits would ensue.

Precision Voltage Divider. The IMS relies on a voltage divider consisting of a main and reference chain to establish and release the potential well at the drift tube gate. In laboratory models of the stacked tube, discrete precision resistors were matched so that corresponding resistors varied less than 1%.

Heater. The IMS is operated at an elevated temperature near 100C. A capability to increase the temperature even more, for the purpose of desorption and purging of compounds, is a useful consideration for the instrument.

Ionizer. Presently, the IMS uses a radioactive ionizer. The baseline used a number of discrete buttons coated with americium 241. The rolled design uses a coated metal strip which is coiled into a ring and spring loaded outward to hold itself in place. The ionizer must not have a line of site view to the outside world to prevent external radiation. The baseline design had right angle flow ports that aided this requirement.

Biased Exhaust. When the IMS operates in a selectable polarity, it is desirable to bias the ions of the opposite polarity to the exhaust ports to assist their exit from the device. This is also accomplished with internal electrodes in the end-piece.

Low-Temperature Co-fired Ceramic

An opportunity was seen to simplify the construction of the drift tube, improve performance, and include the end block functionality in a single monolithic structure. LTCC was attractive because it is an established technology with a considerable infrastructure and several commercial vendors—both for materials and for fabrication. Others are also developing new applications of LTCC to devices in general and an IMS in particular.[5,6] Because the thick films are tailored to the necessary attributes, one may select the most inert metallization for internal electrodes, high-conductivity metallization for buried signal lines, a metal for suitable resistor terminations, and more resistive internal metallization for a heater. One could select a product for solder leach resistance or for brazing, and could tailor material loading that

affects the subtle differences in the geometry of the tube. The conventional use of this system involves an organic binder burnout followed by an elevated temperature firing cycle—both in air. We have primarily used a cycle involving burnout at 450ºC and subsequent firing at 850ºC. We have adjusted ramp rates as required by various details of geometry and material loading.

Commercial tape and pastes were used. Because a rolled design is a unique case, where the inside of the unfired sheet is rolled onto the external surface of the layer below, it is possible to achieve interconnection between the two sides without vias. A nominal overlap distance for electrode lines suffices for this inside-to-outside connection. The lines facing inward on the inside of the tube are capable of setting up an electrostatic field equivalent to the conductive plate edge in the prior design. Areas where solder connections were to be made to prototypes received an additional printed thickness. Because thick film technology has had stable resistor infrastructure for many years, the resistors previously used on the printed circuit board were combined on the tape and even rolled onto the shape of the tube for co-firing. The detail of precision laser trimming was a minor inconvenience for which special fixtures were considered but are not yet needed. Internal structures were inserted into the rolled design with relative ease. Initial success with assembly of a micro-ion mobility spectrometer has been described elsewhere.[1,2]

We first demonstrated a small diameter micro IMS and are progressing well to scaling it to a larger diameter and length drift tube, since the larger diameter is thought to be beneficial to improve resolution.[7] There are only minor technical considerations in scaling up the IMS. The change to the larger design was a design change that provided an opportunity to incorporate additional functionality into the device. As such, the process description will include some steps from each types of prototype. The large diameter tube was shown in Figure 1, and the earlier tube is shown in Figure 5b in comparison to the stacked version it replaces, shown in Figure 5a.

The IMS shown in Figure 5b has been used to resolve actual ion peaks. Figure 6 shows an actual output plot showing the capability to detect both a reactive ion peak (Cl^-) from the carrier gas and an analyte peak including the species trinitrotoluene (TNT).

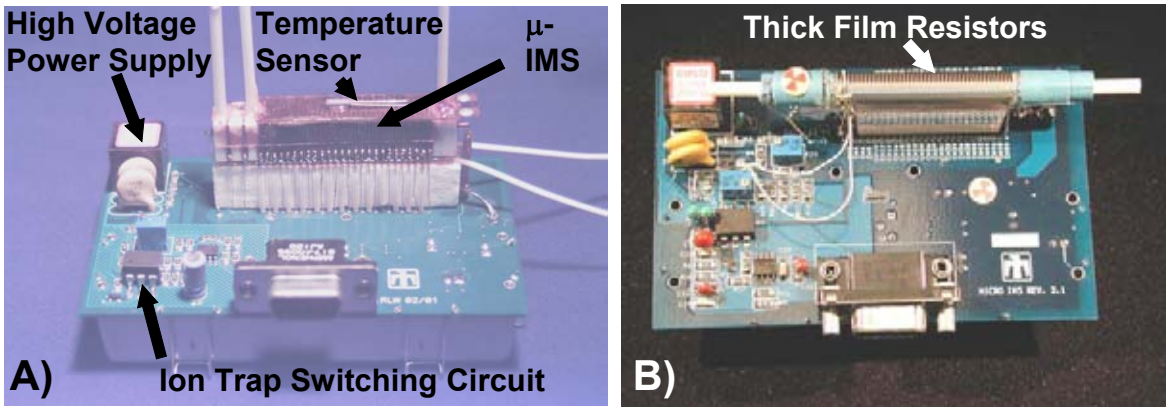

Figure 5. a) Baseline micro-IMS on printed circuit board. B) Rolled design demonstrated in 6 mm internal diameter shown for comparison.

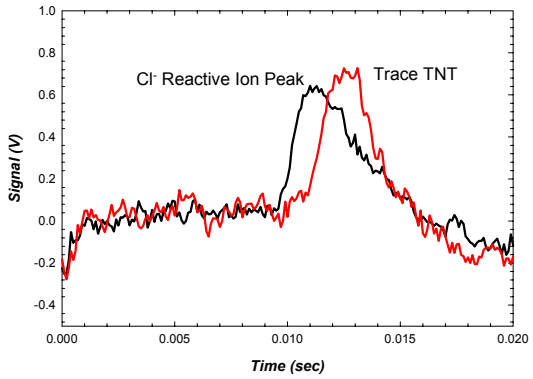

Figure 6. Output from a prototype rolled tube showing the ability to detect both a reactive ion peak (Cl^-) from the carrier gas and an analyte peak.

CONSTRUCTION DETAILS

Printing

Prototype models used conventional thick film screen printing. Additional work using an in-house direct write system and commercial capability (Ohmcraft, Inc.) will also be discussed. To preserve pliability of the unfired sheet, the thick film drying temperature was reduced from 125ºC to 75ºC. The print layers for the larger tube are shown in Figure 7. At left, the inside electrodes are printed. At center, the outside conductors are shown. Double printed areas are not visible, but improve the durability of soldered areas. The heater insert is a conductive serpentine on a separate tape.

Sizing, Edge Preparation

In preparation for rolling, critical edges, such as the leading edge, are prepared with a taper. Various techniques were used for this operation, including cutting, pressing, and abrasive definition. The latter was most effective in our practice. Without this taper, the underlying layer acts like a shear for the overlying layer during lamination. The structure of the green tape would recover from such an event—and this can be used in making novel parts—but any associated thick films might be irreparably severed. Even with a taper,

Figure 7. Completed step to print / direct-write layers for IMS tube.

or other mechanical discontinuity arising from creative layering, the bend radius needs careful attention when the bend places the dried paste in tension.

Rolling

Rolling to date has been performed manually, but in principle is well suited to automation such as even reel-to-reel processing. In early designs, a 6mm diameter tube was constructed in two wraps of 0.25 mm thick unfired tape. In a later design, a total of four wraps was used, incorporating a thick film heater. A cross sectional end cut in a laminated, unfired tube provides the view in Figure 8a, which highlights both the start of the roll and the termination of the roll with the heater layer incorporated at an intermediate level. The overlap area shown is the only joint contact required between inner conductors and outer conductors to bring electrical leads to the exterior. Figure 8b, at the opposite side of the tube, shows the technique for starting and terminating the mechanical incorporation of the heater layer. A taper at the edges prevents the mechanical damage alluded to above. The small dip in the contour of Figure 8b is due to the minor imperfections of the tapered layer overlap.

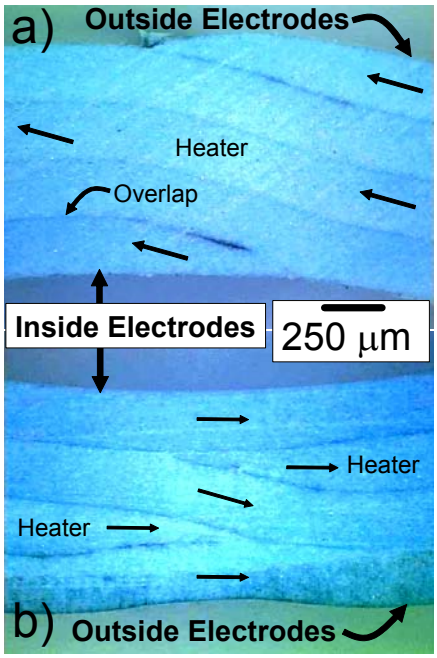

Figure 8. Unfired cross section showing wrap technique (a) near start and termination of wrap, and (b) at opposite side where heater is incorporated.

Conductor mechanical behavior needed special consideration. Because the internal electrodes were rolled onto a mandrel placing them in compression along their length, the thick film was driven into the tape somewhat during lamination without concern for electrical continuity. Subsequent firing of this material resulted in minor relief on the inside surface of the tube. The exterior unfired thick film lines were placed in tension on the exterior of the tube by the same rolling operation. This resulted in some crazing in the unfired state. This crazing healed satisfactorily for thinner prints with proper practice, but was seen to lead to electrical discontinuity and even cracking for excessively thick prints.

Following rolling, a commercial food wrap was an ideal engineering material when rolled onto the outside of the structure, and served the purpose of restraint to preserve the rolled tape position and alignment. When rolled in sufficient thickness, this material was also very effective as a mechanical buffer during lamination.

The heater layer is included with the thick film heater facing outward. It contacts no IMS electrodes as their path has been transferred to the outside lines. The heater contact pads are accessed through openings in overlying layers as shown in the image of a fired tube in Figure 9. As one might expect from the

earlier view in Figure 8, the internal seam is near perfect in that the electrode alignment is good and no mechanical problems are induced.

The heater is an 18 ohm distributed conductive thick film trace powered by a 12 V battery. Initial operation of the heater has been straightforward. It brings a still-air volume at the center of the tube length and diameter to the operating temperature of 100°C in two minutes. This assembly has been thermally insulated and power cycled between about 40°C and 200°C seventeen times with no apparent ill effects. The heater needs further design optimization to provide the proper thermal profile along the length of the IMS tube under actual flow conditions.

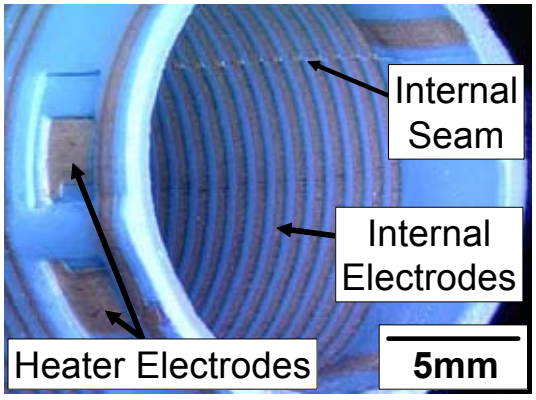

Figure 9. Access to heater terminations is through openings in overlying layers.

Lamination

Again using conventional infrastructure an isostatic press is commonly used to effect the lamination of the unfired tape. These structures were laminated at 68°C and 20.7 Mpa (3000 psi) for variable times around a nominal 10-15 minutes.

The assembly is prepared for lamination using a vacuum bagging technique to prevent contact of the pressurized water with the unfired tape. These bags would tend to pinch seams into the tube during lamination but that is mitigated by the buffer material. Attention to the ends of the mandrel also prevented perforation of the bag under pressure. We have also fabricated other fixtures to be able to use the convenience of vacuum bagging and isostatic pressing for special parts by tapering fixture edges. The laminated IMS structure is removed from the mandrel and has sufficient strength to be handled and mechanically trimmed as necessary.

Burnout and Firing

A variety of different burnout and firing cycles have been employed, depending on particular conditions. Slower ramp rates were beneficial as the wall thickness of the tube design and the loading with additional thick film features were increased. In addition, certain parts were burned out in a separate cycle from the firing cycle for the purposes of study. The burnout conditions and resulting success varied with the selection of materials used and the configuration of the sample and the furnace. Early samples were demonstrated in a belt furnace, but for subsequent samples a box furnace was preferred. This is because the tape is laminated into a structure with sufficient strength to support itself and provide excellent roundness when stood on-end for burnout and firing, as shown in. Figure 10. In Figure 10a, the tube has changed color due to the onset of burnout during the ramp to the 450°C burnout dwell. Dark stains near the bottom show that binder burnout, which consists of softening, melting, pyrolysis, and combustion, has commenced. Figure 10b shows the tube during the ramp to the 850C firing dwell. Figure

10c shows the tube near the end of the firing dwell, still glowing red and having shrunk approximately 12%.

To understand roundness, orthogonal diameter measurements were made at multiple internal and external locations. One diameter was keyed to the external seam for reference, and the other was orthogonal to it. Plotted in Figure 11 are points for a typical tube where the diameter in each direction was compared to the overall mean. It isn't surprising that there is a diameter gradient along the tube. The bottom is in contact with an LTCC setter, and the top is free. The diameter is greatest at the bottom of the tube. The diameter in the center, where the loading is most consistent is within 0.5% of the mean diameter. At the top of the tube, there is no thick film loading, and the minimum diameter is seen. The tubes are processed in a

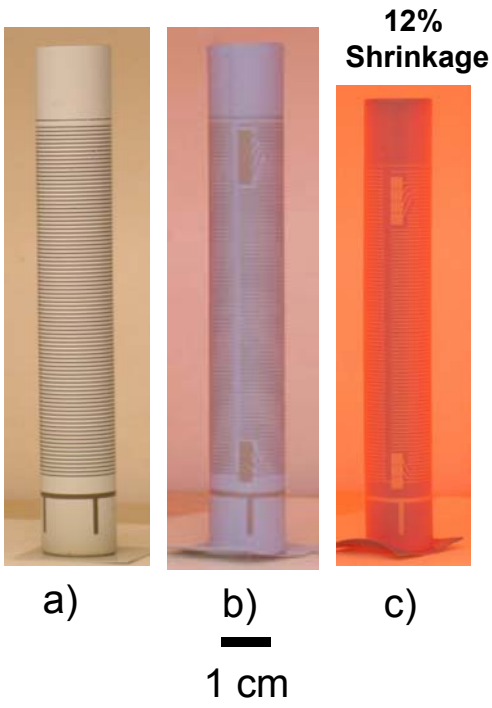

Figure 10. Burnout and firing cycle. a) 350°C on ramp up to 450°C burnout dwell. b) 550°C on ramp up to 850°C firing dwell. c) 850°C firing, note shrinkage.

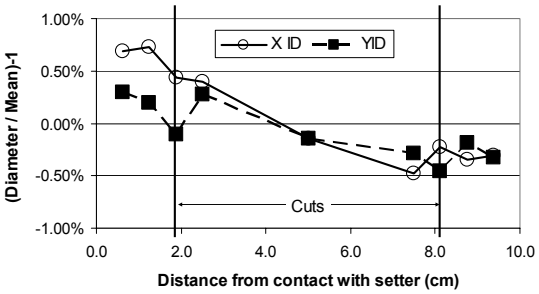

Figure 11. Roundness evaluation tubes.

length that permits the removal of both ends after firing—a throw away zone shown by the arrow on the plot. As such, sagging was not a problem, and the roundness of the tubes was more than adequate for operation of the IMS, and sufficient for the logistics of sizing the internal components.

In addition, the length was very predictable. In a sample of 8 of the 6mm diameter tubes, the average length was within 250 µm (0.010 inch) of the designed length of 3.81 cm (1.5 inch).

Resistor firing and trimming

Resistors were added to the structure to provide the main and reference chain voltage gradient required for the drift tube. The resistor paste is a commercial product with 1MΩ/square sheet resistance. We elected to use short, wide resistors, which provide a built-in trim structure, because they fit naturally on the tube in the spaces between the centers of the leads. We first used a simple band of resistor material that spanned the length of the tube. Because we are cofiring the resistors, it was preferred to not have them cover the electrodes completely. It was possible to routinely trim these resistors to better than 1% of nominal value—even when as fired resistor tolerances were rather coarse as shown in Figure 12. An index

was used to compare the difference between each resistor on the main and reference chain, normalized to the mean of all values. Here, the as-fired resistances are plotted for both the early 6mm diameter tube with 50 resistors and the more recent 12.7 cm diameter tube with 80 resistors, if only to show that in both cases the as-fired variance is large. The dark symbols plotted near the zero index for a trimmed tube with 50 resistors show that the trimmed result is more than adequate. This trimming was done both in house and commercially (Ohmcraft, Inc.). Direct writing was also considered in both the co-fired sequence and the post-fired sequence. Trimming of these resistors on a cylindrical surface was performed

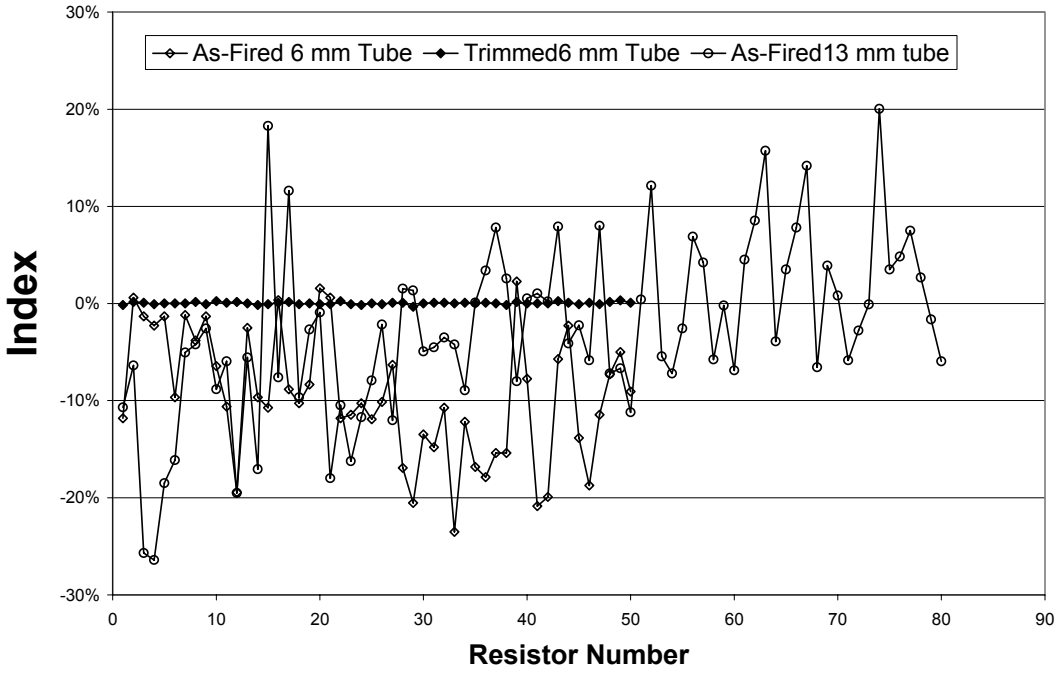

Figure 12. Laser trimming of resistors with large variances results index values less than 1%. The index is (Rmain –Rreference)/MEAN.

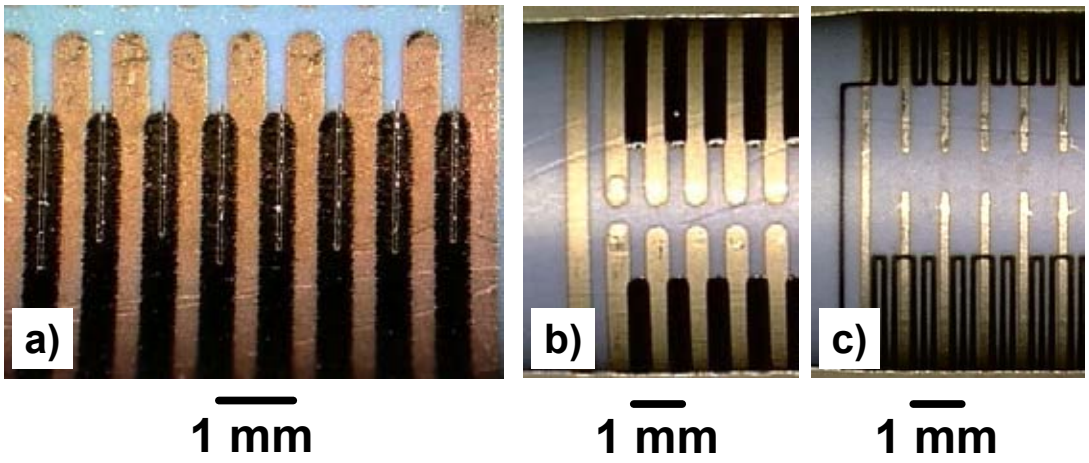

Figure 13. a) Trimmed resistors on a round tube. B) another early resistor design. C) Electrodes and resistors created by the direct-write technique (Ohmcraft, inc.).

routinely. A design wherein the trim distances are short enough that the curved surface is inconsequential is one approach. Trimmed resistors are shown in Figure 13a, while Figure 13b and Figure 13c show a comparison of printed features and direct-write features, respectively. We are working to improve the precision in hopes of eliminating the laser trim, including printing following firing, direct writing, and other techniques. Under the best of circumstances, we have post-fired resistors with every index value within 12% of the nominal). The key to eliminating trimming is control of the resistor geometry.

We have characterized the thermal coefficient of resistance for these resistors and have seen a 0.5% shift from room temperature to 150ºC. As this affects main and reference chain resistors, it is tolerable in the operation of the IMS. When post-fired features are being considered, we have looked at the effect of refiring, which increases resistor values,. Additional attention will be required as reliability of resistors is characterized, but presently no overglaze is employed.

ASSEMBLY

When fired, the structure is checked for continuity and isolation, and resistors are checked as part of our characterization during development. Geometrical details such as length, roundness, and straightness are also noted. The tube is sized appropriately for next assembly. The internal structures to be placed fall into three categories: The LIGA grids, apertures and target, and the ionizer.

LIGA grids

The use of a grid to create a potential well at the leading edge of the drift tube was desirable. Ideally, such a grid would have a very small cross section, especially near the center, and therefore be non-restrictive. In addition, the grid should have rigidity along the axis of the tube in order to minimize vibration sensitivity (microphonic effects) in the axis of the tube. These criteria were solved by the use of LIGA. Several designs were evaluated, and a number of these were built. Figure 14a shows the two main types that were used. A support ring near the perimeter supports the grid structure. At the perimeter of this support ring, several LIGA springs were designed, to assist holding the grids in place. Various techniques were used

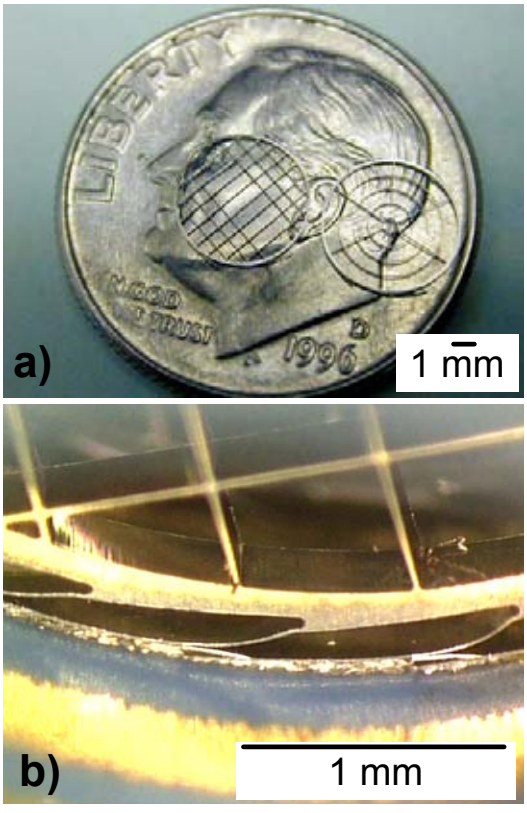

Figure 14. a) LIGA screens of orthogonal and radial design. b) LIGA screen installed and soldered in place at internal IMS electrode.

to alter the stiffness of the springs. At best, a spring loaded installed grid survived a simple impact test, estimated to impart more than 20 g's acceleration, without moving the grid. In addition, flow rates 100 times greater than the designed flows were tested on some of the weaker springs without any negative effect. Nevertheless, LIGA grids for prototypes were tack-soldered for additional strength. An insertion tool consisting of a wire electro-discharge machined support grooves on a mandrel tip, and a coaxial tapered compression feature resulted in simplifying screen insertion to a process taking a few minutes when performed manually.

Target and Apertures

The target and apertures were commercially photo-defined from a nickel plated kovar sheet (Towne Technologies, Inc.). The undercutting at edges was used to provide additional spring force to hold these components in-place as shown in Figure 15. The target is a central plate supported by small tabs at the perimeter. These structures were inserted manually with a simple mandrel. Care was taken not to scratch conductive traces onto the inside of the tube by placing components near their final position and rotating them into position. When so positioned, they were also tacked with solder to the appropriate electrodes.

Tube Ends

Tube ends were also fabricated from LTCC material, with appropriate electrodes. Both sleeve designs (primarily small diameter prototypes) and flange designs (primarily large

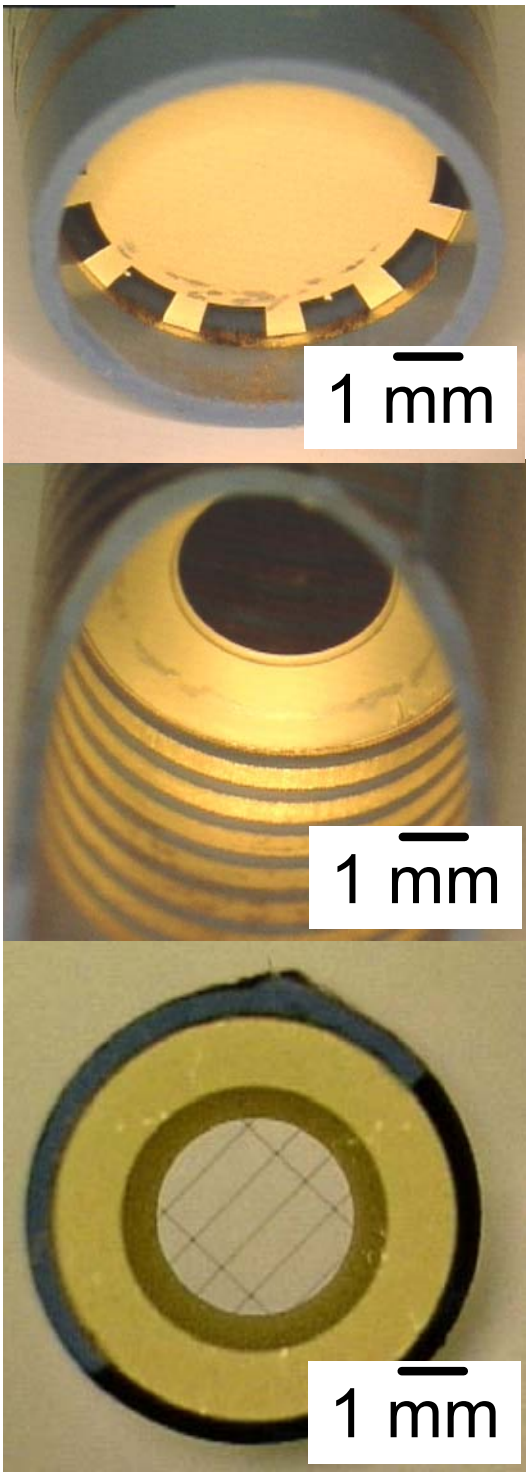

Figure 15. Targets (top), apertures (center), and apertures combined with LIGA grids are shown for illustration of assembly.

diameter prototypes) were used in the course of this work. At the target end, the tube end is basically in place to facilitate plumbing of the carrier gas, and as such was relatively simple. The combination of the central target area and the central gas port behind it blocked the line of sight from the opening to the ionizer. A mechanical sample of one prototype design is shown in Figure 16. At the left is the carrier gas inlet, which admits gas which flows around the perimeter of the target and up the tube. Note that in this mechanical sample, the tube ends are significantly smaller than the center, due to an attempt to expand the commercial thick film ink selection, and its unique loading and restraint of the diameter during firing. Also, this picture was taken at a time when blistering due to loading was not completely solved.

At the ionizer end, the tube end was a multipurpose design, which served to support the ionizer, plumb the sample gas to the appropriate drop-off point, and provide an exhaust port. In the smaller diameter design, spiral ports were crafted and cofired into the structure. The spiral prevented the line-of-sight to the ionizer. A sacrificial material technique was used in the larger diameter design as shown in Figure 17 to accomplish the same purposes. Figure 17a is a model of the use of the sacrificial material to form the exhaust ports. Figure 17b shows how the metal strip ionizer will be formed into a ring and placed in the tube end with the

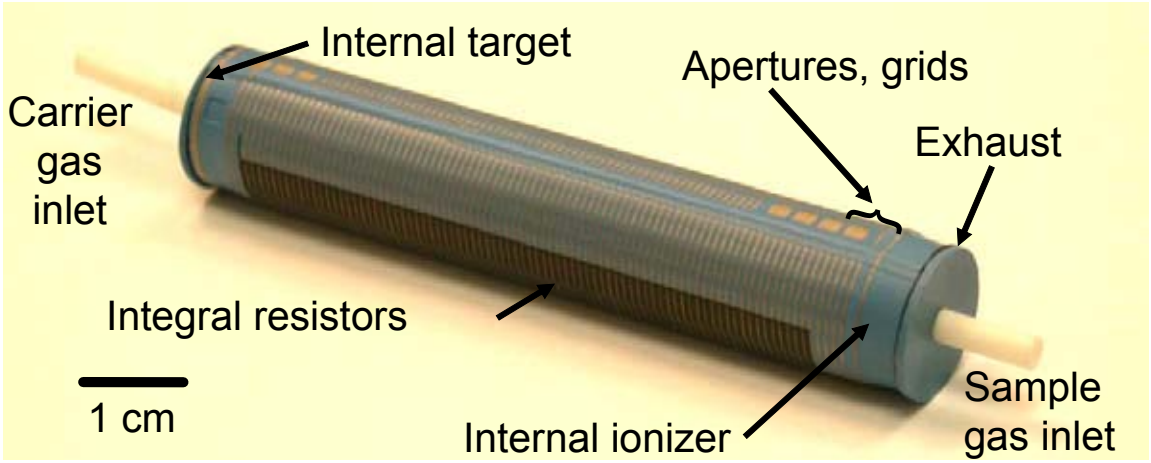

Figure 16. Mechanical sample of large diameter IMS design showing critical components.

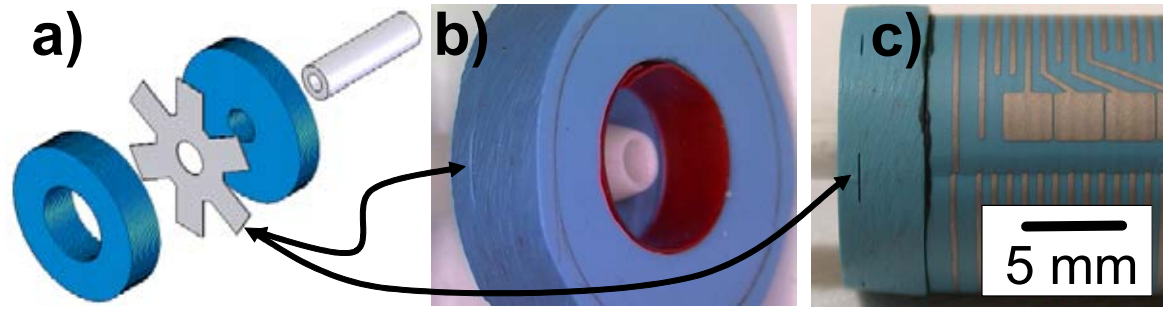

Figure 17. Tube end incorporating ionizer and sacrificial volume exhaust ports.

ionizer spring-loaded outward. Figure 17c shows a better view of the exhaust ports on a mechanical sample. These exhaust ports have also been demonstrated, by immersing them in water and producing a flow through them. Note that the flow path can be captured, and ported as required.

Sacrificial materials

Sacrificial materials were mentioned in conjunction with the fabrication of the ionizer end piece. Sacrificial material techniques have broader value in microfluidics in general and in other microfluidic applications associated with the IMS. Previously, techniques have been employed that create cavities and then use uniaxial lamination or fine geometry such that cavities are not caved in.[8] The general technique as well as a discussion of sacrificial material is included in an excellent review.[9] Sacrificial materials have also been described for wick structures in internal volumes of heat spreaders.[6] This is similar to the principle used to fabricate fluidic channels in printed circuit boards.[10] Meso-scale techniques have even been described which rely on etching of sacrificial layers.

A fabrication technique for cavity and channel formation in LTCC has been employed using a sacrificial material that is removed cleanly during the burnout cycle of LTCC fabrication. The sacrificial material is patterned using a variety of approaches, and included during in the stackup during lamination. Here we describe the use of a low molecular weight polymer sheet that can be easily punched or laser cut to provide anchor lines for cavity perimeters, points of attachment, surface texture, and via fill. Our earliest prototypes involved patterns cut with a scissors. Figure 18 shows microfluidic routing that can include side ports on microsystem boards as well as surface ports that can be used in conjunction with soldered annular seals and interconnections.

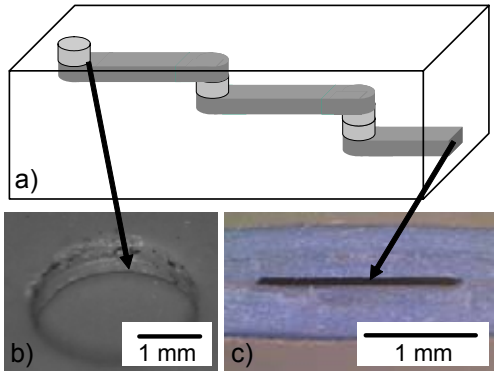

Figure 18. Microfluidic routing flexibility can mimic that in microelectronic boards.

Several demonstrations have been completed. One is the serpentine manifold shown in Figure 19. Figure 19a shows the channel as designed in sacrificial material. In a thin polymer of low molecular weight, a pattern can be generated as shown in Figure 19b. This piece has support ligaments that were removed prior to lamination. The lamination and firing produces the piece shown in Figure 19c, which was made into part of an in-line bubbler with 73 cm of channel 100 micrometers tall by 1.25mm wide for demonstration at a flow of 1 liter/minute. The structure was capable of supporting pressures of 0.14 Mpa (20psi).

Another demonstration is shown in Figure 20a where orthogonal flow channels have been constructed on two levels. This part was also immersed in water for demonstration, and the images below show operation of channels on left side, both sides, and right side, as desired. This technique can be used to independently address channels in microfluidics system board applications

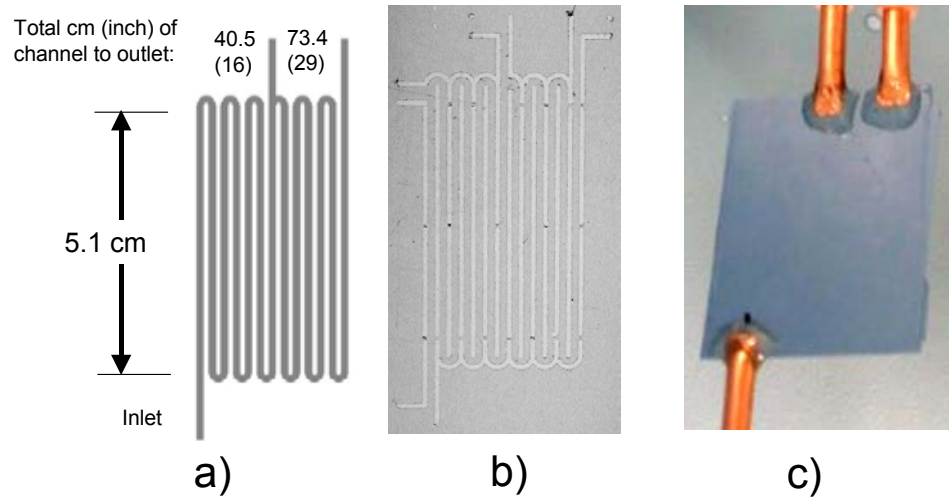

Figure 19. Serpentine manifold.

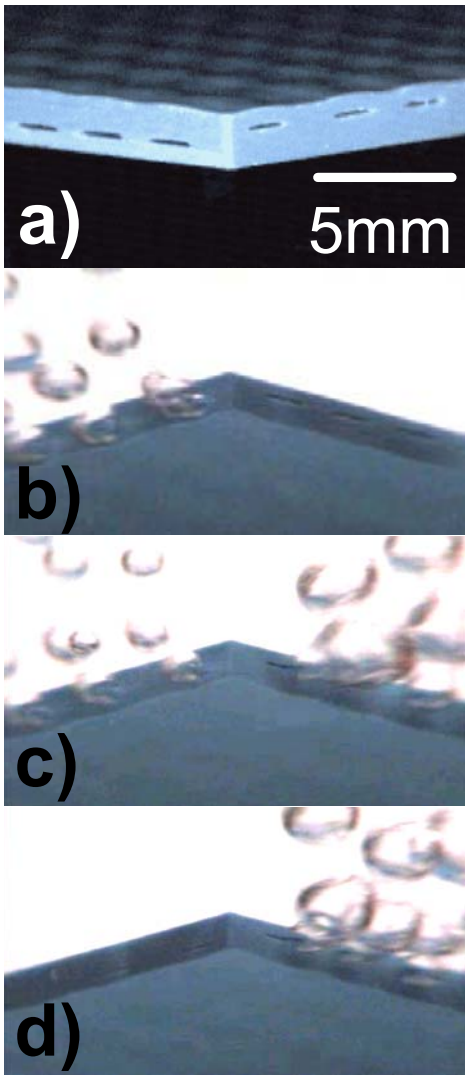

Figure 20. Orthogonal side ported channels on multiple levels in LTCC

Which we have also demonstrated pneumatically while immersed in a fluid. We have fabricated blind cavities, and have addressed microfluidic interconnection ports as small as 300 μm diameter.

TRANSPARENT WINDOWS

Earlier success with incorporating transparent windows into LTCC by cofiring[2] has been demonstrated on the IMS as shown in Figure 21.

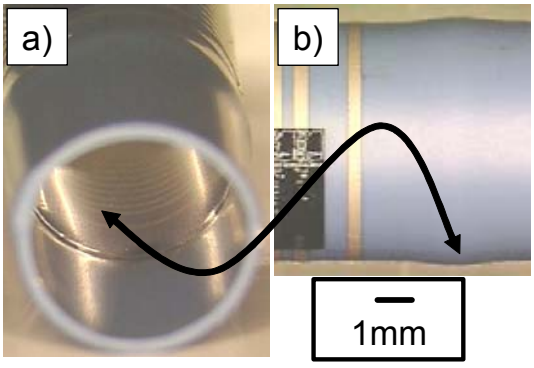

Figure 21. IMS transparent windows. a) Perspective view from end. b) Side view showing bulge where tube contacts window.

The interest in such a feature comes from the desire to use photo-ionization as a future replacement for the

radioactive source. In LTCC package and lid features, these windows have proven hermetic and a sample of 17 parts has survived 100 temperature cycles from –45°C to 155°C, with 5°C/minute ramps and 30 minute dwell times, without any negative effect on hermeticity. Implementation of such a window could take many forms, but one such demonstration is shown in Figure 21.

CONCLUSIONS

LTCC has been used to fabricate prototype micro-IMS devices with an inherent simplicity that reduces the parts count by more than 150, makes them easier to fabricate and ultimately produce in large quantities. The design improves function and makes the device more robust. A sacrificial material technique has proven useful where a microfluidic application required a mildly tortuous path. Additional innovations in transparent windows will extend the usefulness of the micro-IMS.

ACKNOWLEDGEMENTS

The authors wish would like to thank Kevin Linker of Sandia and Alan Drumheller of Ohmcraft, Inc. Numerous others in Sandia's Thin Film, Vacuum and Packaging Department, and in the LIGA Fabrication Department have made this work possible.

Sandia is a multiprogram laboratory operated by Sandia Corporation, a Lockheed Martin Company, for the United States Department of Energy under Contract DE-AC04-94AL85000.

REFERENCES

[1] S. Rohde and K. Peterson, Applying New LTCC/LIGA Construction Techniques in Realizing a Miniature Ion Mobility Spectrometer," IMAPS Advanced Technology Workshop on Packaging of MEMS and Related Micro Integrated Nano Systems, Denver, September 6-8, 2002.

[2] Peterson, K. A. Rhode, S. B., Tuner, T. S., Casias, A.L., "Novel Structures in Ceramic Interconnect Technology", IMAPS Ceramic Interconnect Technology Conference, Denver, CO, April 7-9, 2003.

[3] Peterson, K. A., Rohde, S. B., Pfeifer, K. B., Turner, T. S., "Novel LTCC Fabrication Techniques Applied to a rolled Ion Mobility Spectrometer," Abstract 1153, 204th Meeting of the Electrochemical Society, Orlando, Florida, October 12-16, 2003.

[4] Eiceman, G. E.; Karpas, Z.; *Ion Mobility Spectrometry*, CRC Press, Boca Raton, FL, 1994, pp 57-66.

[5] Plumlee, D.G, Tam, M, Dwivedi, P, Hill, H. H, Hartman, J. A, and Moll, A. J, "Ion Mobility Spectrometer Fabricated in LTCC", IMAPS Ceramic Interconnect Technology Conference, Denver, CO, April 7-9, 2003.

[6] Moll, A. J, Plumlee, D. G., "MEMS Devices in LTCC," Abstract 1161, 204th Meeting of the Electrochemical Society, Orlando, Florida, October 12-16, 2003.

[7] Pfeifer, K. B.; Sanchez, R. C.; International Journal of Ion Mobility Spectroscopy, 5 (2002) 3, 63-66.

[8] D.G. Plumlee, Y. Morales, B. Cheek, A.J. Paris, H.A. Ackler, W.B. Knowlton and A.J. Moll, "Pressure Sensors built in Low Temperature Co-Fired Ceramic Materials," Presented at IMAPS Advanced Technology Workshop on Packaging of MEMS and Releate Micro Integrated Nano Systems, September 6-8, 2002, Denver.

[9] H.H. Bau, S.G.K. Ananthasuresh, J.J. Santiago-Aviles, J. Zhong, M. Kim, M. Yi, P. Espinoza-Vallejos, L. Sola-Labuna, "Ceramic tape-based meso systems technology," DSC-Vol. 66, Micro-Electro-Mechanical Systems (MEMS), 1998, ASME, PP. 491-498.

[10] T. Merkel, M. Graeber, L. Pagel, "A new technology for fluidic microsystems based on PDB technology," Sensors and Actuators 77 (1999) 98-105.

Appendix I. Macro-Meso-Microsystems Integration in LTCC

Microsystem Integration with New Techniques in LTCC

K. A. Peterson, S. B. Rohde, C. A. Walker, K. D. Patel, T. S. Turner, C. D. Nordquist
Sandia National Laboratories
P.O.B. 5800, MS 0959
Albuquerque, NM 87185-0959

peterska@sandia.gov, sbrohde@sandia.gov, cawalke@sandia.gov, kdpatel@sandia.gov, tsturne@sandia.gov, cdnordq@sandia.gov

Abstract

Ceramic interconnect technology in general, and Low Temperature Cofired Ceramic (LTCC) technology in particular can meet many requirements for a broad range of critical microsystem elements on microsystem boards. LTCC is a technology of choice for its excellent material properties for high frequency circuits, nearly unlimited stacking capability, and form and fit versatility. Microsystem integration involves technologies as varied as integrated digital logic, RF, optics, microfluidics, a host of sensors and actuators, and chemical and physical analysis. A new suite of structures and techniques built around creating sacrificial volumes is described as an avenue toward integration of increased variety that would be expected in a complex microsystem. These volumes are not predefined in individual laminates, but can be created by deformation upon lamination. In addition to serving as microfluidic channels, these volumes can accommodate microelectronic and MEMS devices as well as thick film sensor materials in smart packages. Several limitations of shape previously imposed on LTCC system boards have been challenged.

Sandia is a multiprogram laboratory operated by Sandia Corporation, a Lockheed Martin Company, for the United States Department of Energy under contract DE-AC04-94AL85000.

Key Words: LTCC, microsystem, sacrificial, fugitive, channel, burnout, microfluidic, MEMS

Introduction

Hybrid integration of key elements has maintained a strong presence in microsystem technology because it enables proof-of-concept and accommodates variety in real applications. Low Temperature Cofired Ceramic (LTCC) technology can be a cornerstone of this capability. Microelectronic routing of electrical traces through available area on any layer has long been a feature of multilayered microelectronic board technologies. Recent development using sacrificial material makes this same routing versatility available for sealed and vented unfilled volumes (sacrificial volumes) in ceramic laminated boards for multiple purposes. We will highlight this suite of techniques and correlate it with applications in micro electro mechanical systems (MEMS) and microfluidic, RF, optical, and sensing capabilities in potential microsystem boards. We will directly apply LTCC structures to microfluidics, and suggest others that are still being enhanced with novel uses of sacrificial materials, such as high frequency, thermally isolated, and air core inductor applications for the thick film free-standing structures shown in Figure 1. Recent application of LTCC to a micro-total analysis system (Micro-TAS) including micro-high performance liquid chromatography (μ-HPLC) has demonstrated distinct performance advantages of LTCC.

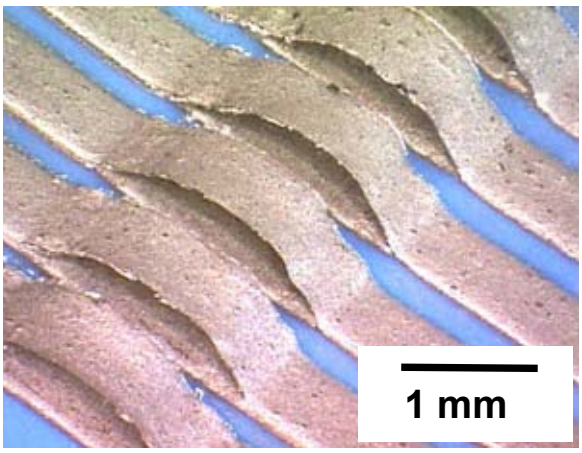

Figure 1. Thick film, free-standing conductor loops above thick film lines on LTCC were created using sacrificial materials.

Background

LTCC is a well-known commercial technology. An excellent review [1] highlights the process steps and describes techniques which we relate to our own use of sacrificial materials. Enclosed unfilled volumes have been envisioned in many areas of potential use with respect to LTCC, but conventional high pressure lamination poses problems for defining such volumes. Techniques have been employed that first create openings in unfired ceramic tapes and then use uniaxial lamination or fine geometries to prevent the collapse of the open volumes. [2] High pressure lamination of tape cast layers can be used in conjunction with a filler material, either in the form of a temporary insert [3], an insert that can be etched after firing [4], an insert that would disassociate during burnout and firing [4, 5], or an insert that could be poured, shaken or flowed out after firing [6]. In some cases, this insert is cast in-place [7]. In other instances, the insert is a discrete layer or stack matching the appropriate opening in a corresponding ceramic tape structure [8]. Low pressure lamination without an insert through the use of an adhesive has also been described [9].

Sacrificial Volumes

Each of the above descriptions, that uses a sacrificial (fugitive) material, has the point in-common that a cavity is first created and then filled with a close-fitting insert. We have demonstrated a technique whereby the sacrificial volume is formed during lamination by the deformation of the unfired ceramic tape around sacrificial materials and the resulting bonding of compatible areas without the use of a pre-existing cavity [10, 11]. We have accomplished this in several ways, with materials of various form and compliance. One such technique is shown in the sketch of Figure 2. In Figure 2a, the LTCC tape and sacrificial material are collated. The arrows indicate

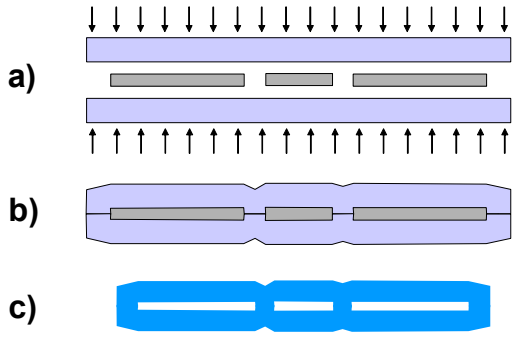

Figure 2. Cross-sectional sketch of one sacrificial volume technique. a) tape layers and sacrificial material are collated (arrows indicate lamination), b) laminated result, c) fired appearance.

that the stack will be laminated. Figure 2b shows the result after lamination with the LTCC tape bonded in sections between sacrificial material. Finally, in Figure 2c, the clean removal of the sacrificial material during burnout and firing leaves sacrificial volumes.

A sheet or tape material with an appropriate pattern is one of the forms we have used for sacrificial material. The existing LTCC techniques are adequate to define this material via punching, laser cutting, stenciling, or other techniques. When the material is non-compliant, the deformation leaves the imprint of the sacrificial material in the LTCC tape. When the material is compliant, and in some cases visco-elastic, the deformation can be shared between the sacrificial material and the ceramic tape, rounding corners and giving a net shape with appealing qualities. Certain dried thick films can be deformed to an extent with their critical properties intact, as shown in prior work [12]. An open view of this behavior is illustrated in Figure 3 where a trench has been impressed on an LTCC surface by laminating a carbon tape strip to the surface in

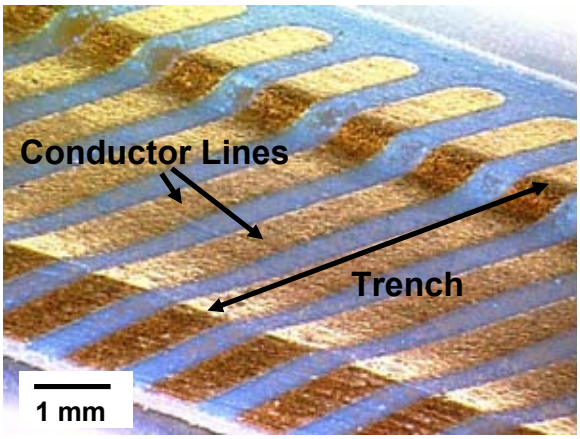

Figure 3. A cofired trench formed by laminating a strip of 200μm (0.008") thick sacrificial material to an unfired LTCC surface with dried thick film conductor lines (confocal optical image).

contact with a firm support. Thick film conductor lines running orthogonally across the trench are intact. By aligning LTCC with thick film electrodes and laminating them face to face with sacrificial material between them a hollow rectangular cylinder with internal electrodes has also been fabricated.

Materials that we have used as sacrificial materials in solid form include a low molecular weight sheet of a polymer (such as polypropylene), commercial carbon tape (TCS-CARB-1 by Harmonics, Inc. [13]), and

assorted other materials and shapes, including mandrels defined with stereolithographic techniques [5]. We have performed this work using commercial LTCC tapes—primarily DuPont 951 with limited (but successful) experience using DuPont 943. We have used a conventional firing profile with a burnout dwell at 450ºC and a firing dwell at 850ºC. As subsequent photographs will show the burnout and firing process is clean and functional but it has not been quantitatively studied. Further quantification should consider the effects of furnace environment, material melting, boiling, pyrolysis, combustion (exothermic effects), and condensation. [14]. One of the sacrificial materials we have encountered had a solvent effect on thick film layers upon melting.

Because the sacrificial volume is defined by the technique and the response of the sacrificial material, we have studied the range of possibilities for channel and wall shapes with a resolution pattern, shown in tape form in Figure 4. Figure 4a shows variation in the width of the channel from 110 μm to 625 μm with a constant laminated area width of 1.04mm. Figure 4b shows variation in the width of the laminated channel separator from 227 μm to 645 μm with a constant channel width of 1.25 mm. These

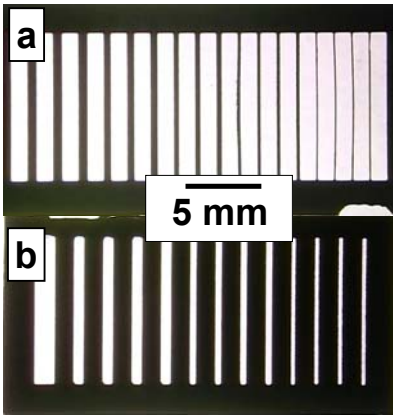

Figure 4. Resolution patterns for determination of feature size are shown as-punched in a 60μm (0.0015") carbon tape.

resolution patterns were defined by punching for both 38μm (0.0015") and 200μm (0.008") thick carbon tape. In general, lamination pressure of 20.7 MPa (3000 psi) yields good results for sacrificial material as thick as 100μm (0.004"). When the sacrificial material is 200μm (0.008") and thicker, the lamination at edges can be incomplete. This study is still underway as we have explored very high pressure lamination recently with good results (Figure 5). The effect of the normal isostatic lamination pressure with a 200μm (0.008") carbon tape is shown in Figure 5a. These channels are still functional for most microfluidic applications. Much higher pressures, such as 207 MPa (30,000psi), result in complete lamination at edges of very thick sacrificial material, as shown in Figure 5b. We have also employed localized high pressures. In thick sacrificial layers, such as the 200 μm (0.008") tape, lamination closure failures were observed when trying to laminate through open dimensions of 650 μm and below. Related work on unfilled channels in LTCC correlates well with these results [4].

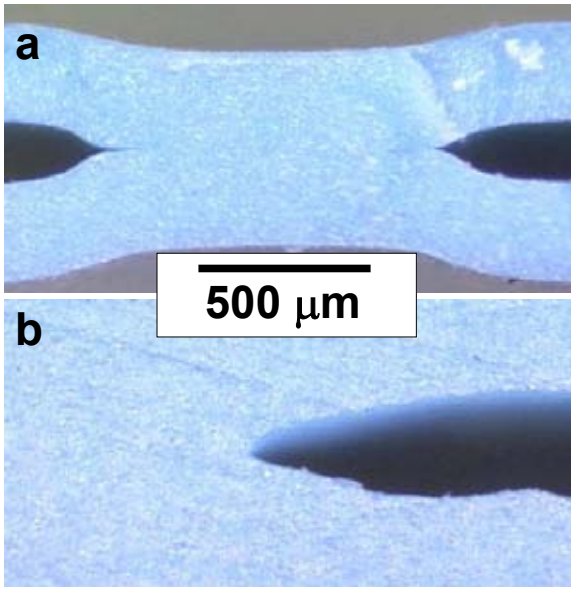

Figure 5. Increased lamination pressure effects complete lamination. a) 20.7 MPa (3000 psi), 200 μm carbon tape thickness. b) 207 MPa (30,000psi), 400 μm carbon tape thickness.

Another technique, not involving a solid form, patterns the sacrificial material to an LTCC surface. Using some techniques, the height of the sacrificial material may be bit-mapped to obtain complex shapes. Again, the existing infrastructure has been used in the form of screen printing, stenciling, dispensing, and direct-write techniques although others can be envisioned, including photoresist and dry deposition. Various materials have been used to pattern in this way including screen printable inks and the slurry from which a commercial carbon tape is cast (provided by Harmonics, Inc.). We have screen printed the slurry to an average thickness of 16 μm as shown in Figure 6. The dried film shows considerable texture, but it is on top of a plateau at 10 μm, leading us to believe these would laminate to

useful sacrificial volumes. We have also used a conventional 50 µm (0.002") stencil, as shown in Figure 7, but have used stencils as thick as 1.5 mm (0.060"). We are also using resolution patterns to study patterned application of sacrificial material.

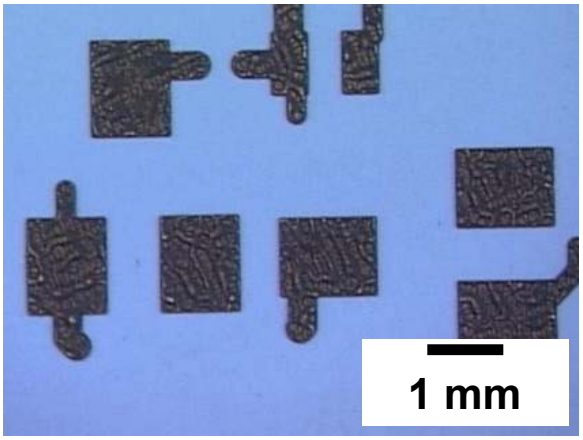

Figure 6. Screen printed carbon slurry shows considerable surface texture.

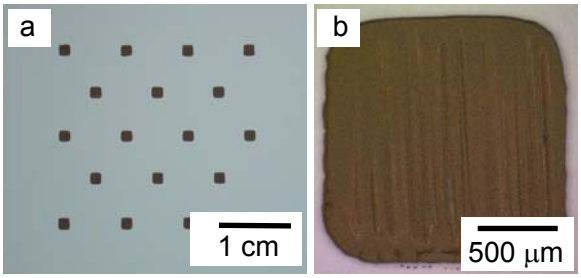

Figure 7. Stenciling of slurry using 50 µm (0.002") stencil in a test pattern.

The fluid definition holds the most promise for performance and versatility because the slumping and drying of a slurry or paste will feather out edges, and that can be used to advantage. Furthermore, this gives the ability to combine sacrificial material in the form of surface features, sacrificial material via fills, and even multilayering of sacrificial material for complex schemes that would permit side by side integration of thick film features and sacrificial volume structures as shown in Figure 8.

Microfluidics

The manifold of Figure 9 illustrates a simple use of a sacrificial volumes technique for a test manifold. The use of this technique prompts a reconsideration of the real requirements of microsystem boards. One example is that boards frequently don't need to be flat, but rather need to have flat areas. These flat areas would likely involve the attachment of discrete

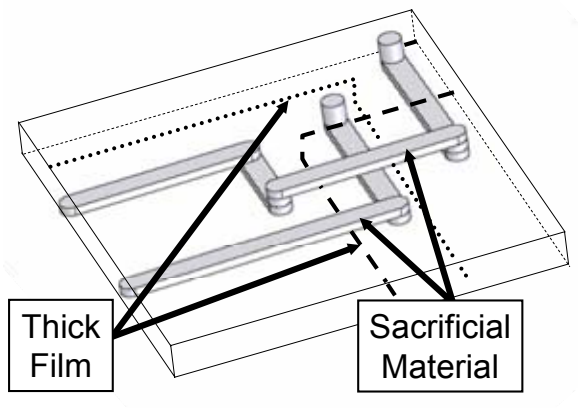

Figure 8. Combination of sacrificial volumes with thick film and LTCC infrastructure.

devices or sealing ports. In Figure 9a, where closely-spaced 300µm (0.012") diameter surface ports have not been protected against deformation on the die side of a microfluidic manifold, resulting in a funnel-shaped cross section. These ports match deep RIE-etched backside ports in a microfluidic device. The case of a textured board is seen Figure 9b, which shows the imprint of sacrificial material channels guiding flow to larger surface ports on the opposite side. In neither case have the ports or vias been filled with sacrificial material. A channel that is not closed and has not been damaged is as functional as a more conventional straight channel.

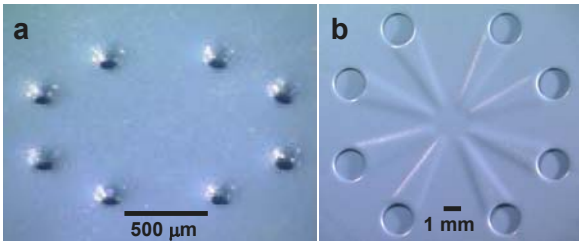

Figure 9. Test manifold for microfluidic device. a) microfluidic die side, b) farside.

It is further possible to have ports on each surface on flat areas without a requirement for the area between to be flat. We have made test structures with as many as 30 surface ports, 300µm (0.012") in diameter, in an area that is 3.8mm by 2.3 mm (0.150" by 0.090"). Figure 10 shows that it is possible to fill vias with sacrificial material for preservation of sidewall geometries and lamination to yield a flat surface at that pitch.

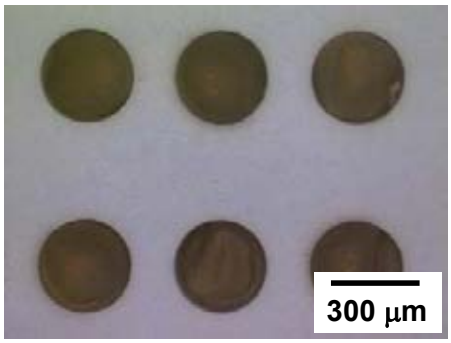

Figure 10. Filled microfluidic vias.

Another improvement being implemented is the routine use of seal rings that can be soldered to microfluidic devices or suitable packages, as shown in Figure 11. We anticipate that this type of package development will lead to complete fluidic grid array (FGA) packages, where soldered annular connections can provide fluidic, mechanical, and electrical interconnections to microsystem boards. The package type shown was pretinned with 63Sn/37Pb solder, cleaned, and attached to a simulated FGA board (another package) without the use of solder flux. The annular seal ring was qualitatively demonstrated to flow copious amounts of water without leakage at seals.

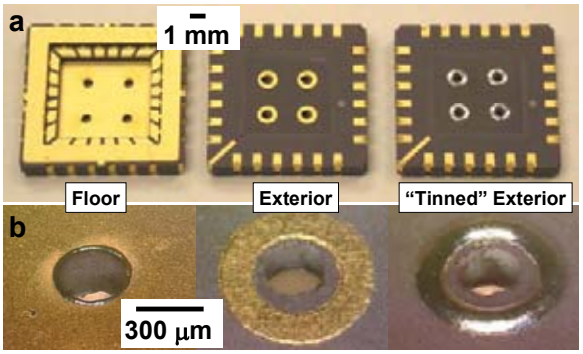

Figure 11. Experimental packages as fluidic grid arrays (FGA). The package is 1 cm (0.40") on a side, the hole diameter is 300µm (0.012").

Micro-total analysis systems--µHPLC

Typical microfluidic applications have been discussed that follow a literature trend of being low pressure devices involving about 21 kPa (3 psi) [15] to 0.7 MPa (100 psi) [16, 17, [18]]. In fact, the pressure that LTCC can support can be quite high. LTCC offers the ability to make structures that can withstand high pressures making µHPLC realistically possible. Therefore, an immediate interest was to demonstrate the pressure capability of an LTCC microchannel. The surface ports were permitted to be conical, and capillary tubing was adhesively attached directly to the microchannel ports. The nominal channel width was 300µm (0.012"), height was 250µm (0.010"), and length was 16.4mm (0.645"). The microchannel was successfully tested to 36.3 MPa (5260 psi) without failing the bond plane, bulk structure, or via holes. The test was limited to this maximum pressure due to the liquid pump's capability. These good results might be considered surprising because the channel cross section has not yet been optimized for maximum strength.

LTCC enables µHPLC structures to be made which are not possible in other materials such as glass or plastic. Ceramic materials can potentially correct some of the limitations of properties of glasses, not the least of which is pressure. Glass structures are useful up to a range of about 10.3 MPa (1500psi). Furthermore, glass structures require photolithographic definition by etching which is expensive and time-consuming. The ability to easily construct microchannels in this laminated structure is attractive from a producibility viewpoint.

The next step will be to improve the design of microchannels and to incorporate other necessary structures such as mixers, heaters, and connection schemes. One drawback to ceramics would be the inability to observe the function as in glass. Toward that end, a prior development of transparent windows is being combined with channel formation and sacrificial materials to investigate a sight-glass approach where needed. Figure 12 shows an initial approach at combining a sapphire window with a channel defined by a sacrificial volume approach. The incorporation of the window in LTCC structures is as described earlier [19], but in this structure a strip

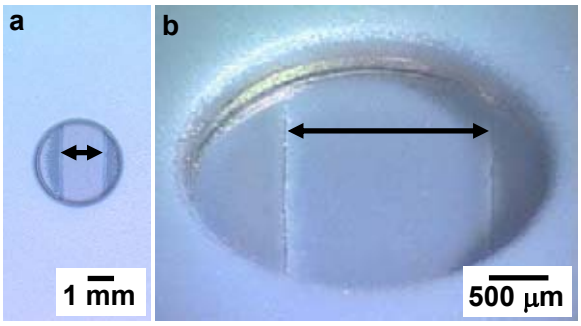

Figure 12. Microfluidic sacrificial channel in LTCC with sight glass. a) Top view, b) Tilted confocal view. Arrows indicate channel width.

of sacrificial material has been laminated against the layer bearing the window. This forms a channel in the LTCC that also runs along the inside surface of the window. These structures have passed helium leak detection with a leak rate less than 5X10-12 Atm cc/sec He. These structures have also been qualitatively checked with a syringe dispensing water with no apparent impediment to flow due to the channel. Fine beads can be introduced to the flow to illustrate the nature of the flow for calibration purposes. This structure will be subjected to higher pressure tests in the near future.

Other structures

In LTCC applications in the literature, a suspended thick film is supported by a bridge/layer of LTCC. In one instance, a thermally isolated bridge structure is used as a support for thick film elements of a thermal flow sensor [20]. In another, a microstrip structure is constructed with a void cavity over the thick film conductor line and beneath the bridge [21]. In such instances, new design possibilities would be presented if the bridge could be made negligibly small or non-existent. The sacrificial volume technique offers a mechanism to build freestanding structures for that purpose.

By applying structural material such as thick film to the sacrificial material, several new features are possible. The thick film is essentially applied to the surface of a material that will disappear. This surface may then be laminated to the surface of another material that will disappear. We have created air-bridges and meshes using this technique. Buckling of the thick film can either be controlled, or exploited. Figure 1 shows a demonstration structure formed by laminating a printed sacrificial material face down over another sacrificial material void.

This potentially useful structure will be considered in several possible designs. By analogy with several structures found in the literature, one use is for the fabrication of a lateral 3-dimensional spiral structures, such as solenoids, toroids, and transformers [22, 23, 24, 25]. Such a component could be self-assembled in a sacrificial volume within a microsystem board, where it would not consume external surface area and where it would be protected from damage. Because the inductor will have an air core instead of a dielectric core, it will have lower loss and parasitic capacitance, allowing usage at higher frequencies than typical spiral or embedded inductors.

In addition, this technique allows for the possibility of fabricating air-gap stripline structures. Lee reports a stripline structure in which the conductor line rests on a thick LTCC bridge [21]. The loss and dispersion of this type of stripline can be improved if the bridge were negligibly thin or removed altogether using this process, leaving a conductor suspended between two ground planes in an air volume. This will enable improved filters and delay elements in this technology. Through a design combination of vias and flip-chip devices, RF components can be connected in close proximity with the embedded and air cavity striplines, with large distributed and delay elements realized in the LTCC rather than on the more expensive chip components. This will improve the functionality of the microsystem, reduce costs, and eliminate a major source of loss as identified in [26]. Additionally, these structures may allow electrostatic modulation of the air gaps to achieve tuning in these structures, enabling tunable filters, phase shifters, and other networks to be realized directly in the LTCC structure.

We plan to evaluate this technology for the realization of these novel RF structures. Integrating these structures and components into the RF substrate may be a critical element in miniaturized RF systems, enabling specific RF functions in smaller volumes and reduced weights, or even enabling new performance previously unobtainable in small volumes.

Discussion

LTCC has been the topic of study for new applications. We have previously used the ability of LTCC to be shaped and formed to provide useful functional structures, such as a rolled IMS drift tube [11, 12, 16]. LTCC channels are no longer limited to the thinnest layer of LTCC tape that can be cast, nor the narrowest opening that can be punched. Extreme aspect ratios with small minimum dimensions, and large cavities of defined cross-section are possible. Definitions of thickness and width are challenged as structures can be pre-laminated and incorporated into a more comprehensive structure in various orientations. A compilation of a number of LTCC structures we have demonstrated in this or referenced work is shown in Table 1.

We are evaluating a silicon die capture mechanism for potential use in MEMS. A related concept has been mentioned in other literature as well [1]. There are classes of MEMS for which this can be useful. One is a released device with no contacting MEMS structures. Released SMM micro fluidic die have been raised to 1000°C with no loss of function [27]. Such die have been captured in a LTCC framework

with no severe effects. Work is continuing in this area.

Table 1. Compilation of several LTCC structures that have been demonstrated.

--Large reservoir (16 cm2 X 100 μm tall) with pillar support structures.
--Serpentine manifold, 66cm of channel, 100 μm tall, 1.27mm wide.
--Spiral channel on tube.
--Radial exhaust ports on ion mobility spectrometer (IMS) tube.
--Orthogonal channels on multiple (2) levels.
--Microfluidic side ports.
--Microfluidic surface ports.
--Microfluidic sight glass.
--HPLC column for high pressure. Width 300μm, height 250μm, length 16.35mm, withstood 5700psi.
--Microfluidic entry/exit on multiple (3) levels.
--Microfluidic channels for 35 valves/chip, 8 fanned out channels, accepts microfluidic package or chip.
--Air loop conductor capability.
--High aspect ratio hollow cylinder with internal electrodes.

LTCC will enable other MEMS applications. Wafer scale processing is essential to production. Packaging remains a problem area for MEMS. Surface micro-machined (SMM) MEMS frequently do not have packaging considerations in the on-chip area. LTCC can participate in a technique we term wafer-scale-"like"-packaging. This concept would use unreleased MEMS devices arrayed in a hybrid fashion on a carrier that can be processed. The submounts can be considered to be the final product. LTCC will not retain its properties through MEMS release etch involving hydrofluoric acid, so a mask for the release etchant would be one way to accomplish this [28].

We had experienced past success with low molecular weight polymer films as sacrificial materials. In general, we are very encouraged by our experience with the carbon tape and even the carbon slurry. However, true to the warning we received from Harmonics, Inc. when we requested the slurry, the rheology and drying properties are not optimum for routine use as a thick film substance. Although we remain interested in the slurry, we are anticipating a paste formulation designed for that purpose.

Conclusions

We have shown a sacrificial material technique and demonstrated early structures that can be fabricated in support of microsystems integration. Microfluidic applications for this technique are plentiful. We have also suggested new benefits from a capability to fabricate air-bridge structures in thick film materials. We are continuing to develop a complex combination of the sacrificial volume technique with microelectronic infrastructure of LTCC that will highlight additional performance advantages of LTCC. We are also quantifying useful channel sizes, operating pressures, environmental factors and stress concentration factors to material strength properties of LTCC.

Acknowledgements

The authors would like to thank Luke Fergusson of Harmonics, Inc., Richard Sanchez, Robert Stokes, and Bart Chavez of Sandia Laboratories for contributions that made this work possible. Optical confocal images were generated on a system developed for Sandia Laboratories by John Hickey of Cimarron Computer Engineering, Inc.

Sandia is a multiprogram laboratory operated by Sandia Corporation, a Lockheed Martin Company, for the United States Department of Energy's National Nuclear Security Administration under contract DE-AC04-94AL85000.

References

[1] M.R. Gongora-Rubio, P. Espinoza-Vallejos, L. Sola-Laguna, J.J. Santiago-Aviles, "Overview of low temperature co-fired ceramics tape technology for meso-system technology," Sensors and Actuators A 89 (2001) 222-241.
[2] D.G. Plumlee, Y. Morales, B. Cheek, A.J. Paris, H.A. Ackler, W.B. Knowlton and A.J. Moll, "Pressure Sensors built in Low Temperature Co-Fired Ceramic Materials," Presented at IMAPS Advanced Technology Workshop on Packaging of MEMS and Releate Micro Integrated Nano Systems, September 6-8, 2002, Denver.
[3] D.J. Miehls, F.J. Martin, R.G. Pond, P.S. Fleischner, "Method of fabricating a multilayer electrical circuit structure," U.S. Patent #5,249,355, October 5, 1993.
[4] P. Espinoza-Vallejos, J. Zhong, M. Gongora-Rubio, L. Sola-Laguna, J.J. Santiago-Aviles, "Meso (intermediate)-scale electromechanical systems for the measurement and control of sagging in LTCC structures," Mat. Res. Soc. Symp. Proc. Vol 518, pp. 73-79, 1998.
[5] W.K. Jones, Y. Liu, and M. Gao, "Micro heat pipes in low temperature cofire ceramic (LTCC) substrates," IEEE Trans. Comp. Packaging

Technologies, Vol. 26, No. 1, March 2003, pp. 110-115.
[6] J.D. Cawley, A.H.Heuer, W.S. Newman, "Method for constructing three dimensional bodies from laminations," U.S. Patent # 5,779,833, July 14, 1998 .
[7] E.A. Trickett, R.C. Assmus, "Ceramic monolithic structure having an internal cavity containte therein and a method of preparing the same," U.S. Patent # 4,806,295, February 21, 1989.
[8] J.H. Alexander, "Method of making ceramic article with cavity using LTCC tape," U.S. Patent #5,601,673, February 11, 1997 .
[9] Burdon, J.W., Huang, R.F., Wilcox, D. and Naclerio, N.J., "Method for fabricating a multilayered structure and the structures formed by the method," U.S. Patent # 6,592,696, July 15, 2003.
[10] Patent pending.
[11] Peterson, K. A. Rhode, S. B., Turner, T. S., Casias, A.L., "Novel Structures in Ceramic Interconnect Technology", IMAPS Ceramic Interconnect Technology Conference, Denver, CO, April 7-9, 2003.
[12] S.B. Rohde and K.A. Peterson, "Applying new LTCC/LIGA construction techniques in realizing a miniature ion mobility spectrometer," presented at IMAPS 2002 – 35th annual symposium on microelectronics, Denver, CO, September, 2002.
[13] Harmonics website: http://www.users.qwest.net /~hmnx/CarbonTape _description.pdf
[14] P. Ferkul, K.R. Sacksteder, P.S. Greenberg, D.L. Dietrich, H.D. Ross, J.S. T'ien, R.A. Altenkirch, L. Tang, M.Bundy, and M. Delichatsios, "Combustion experiments on the MIR space station," Microgravity News, http://spaceresearch.hamptonu.edu/NASAMir /mir-combustion/background.html
[15] O. Hohlfeld and R. Werthschutzky, "Miniature hermetically sealed housing for pressure sensors," Mechatronics 12 (2002) 1201-1212.
[16] Peterson, K. A., Rohde, S. B., Pfeifer, K. B., Turner, T. S., "Novel LTCC Fabrication Techniques Applied to a rolled Ion Mobility Spectrometer," Abstract 1153, Proceedings of the 204th Meeting of the Electrochemical Society, Orlando, Florida, October 12-16, 2003.
[17] D.W. Matson, P.M Martin, W.D. Bennet, D.C. Stewart, and C.C. Bonham, "Laminated ceramic components for micro fluidic applications," Proceedings of the SPIE conference on microfluidic devices and systems II, SPIE Vol 3877, (1999), pp. 95-100.
[18] K. Saxena, G. Wang, S. Ang, A. Elshabini, and F. Barlow, "LTCC based MEMS impingement coolers," Proceedings of the 2003 Ceramic Interconnect Technology Conference, 211-216.
[19] K. A. Peterson and R. D. Watson, "Multilayered Microelectronic Device Package with an Integral Window," U.S. Patent 6,538,312.
[20] Gongora-Rubio, M; Sola-Laguna, LM; Moffett, PJ; Santiago-Aviles, JJ, "The utilization of low temperature co-fired ceramics (LTCC-ML) technology for meso-scale EMS, a simple thermistor based flow sensor," SENSORS AND ACTUATORS A-PHYSICAL; MAR 30 1999; v.73, no.3, p.215-221.
[21] Y.C. Lee, K.C. Eun, C.S. Park, "A new low-loss microstrip structure on LTCC substrate, IEICE Transactions on Electronics, May 2003, vol. E86-C, no. 5, p. 867-9.
[22] O. Dezuari, E. Belloy, S.E. Gilbert, M.A.M. Gijs, "High inductance planar transformers," Sensors and Actuators A (Physical); 1 April 2000; vol.A81, no.1-3, p.355-8
[23] N. Chomnawang and J.B. Lee, "On-chip 3D air core microinductor for high-frequency applications using deformation of sacrificial polymer," Proceedings of the SPIE - The International Society for Optical Engineering; 2001; vol.4334, p.54-62
[24] J.B.Yoon; B.I. Kim; Y.S. Choi; E.Yoon, "3-D construction of monolithic passive components for RF and microwave ICs using thick-metal surface micromachining technology," IEEE Transactions on Microwave Theory and Techniques; Jan. 2003; vol.51, no.1, pt.2, p.279-88.
[25] Y.J. Kim and M.G. Allen, "Surface micromachined solenoid inductors for high frequency applications," IEEE transactions on components, packaging, and manufacturing technology, part C, vol. 21, no. 1, January 1998, pp. 26-33.
[26] Y. Huang and K.L. Wu, "A broad-band LTCC integrated transition of laminated waveguide to air-filled waveguide for millimeter-wave applications," IEEE Transactions on Microwave Theory and Techniques; May 2003; vol.51, no.5, p.1613-17
[27] Paul Galambos, Sandia National Laboratories, Personal communication.
[28] Patent Pending.

Appendix II. Macro-Meso-Microsystems Integration in LTCC

Novel Microsystem Applications with New Techniques in LTCC

K. A. Peterson, K. D. Patel, C. K. Ho, S. B. Rohde, C .D. Nordquist, C.A. Walker, B.D. Wroblewski, M. Okandan
Sandia National Laboratories
P.O.B. 5800, MS 0959
Albuquerque, NM 87185-0959

peterska@sandia.gov, kdpatel@sandia.gov, ckho@sandia.gov, sbrohde@sandia.gov, cdnordq@sandia.gov, cawalke@sandia.gov, bwroble@sandia.gov, mokanda@sandia.gov

Abstract

Low Temperature Cofired Ceramic (LTCC) enables development and testing of critical elements on microsystem boards as well as non-microelectronic meso-scale applications. We describe silicon-based MEMS packaging and LTCC meso-scale applications. Micro fluidic interposers permit rapid testing of varied silicon designs. The application of LTCC to micro-high performance liquid chromatography (μ-HPLC) demonstrates performance advantages at very high pressures. At intermediate pressures a ceramic thermal cell lyser has lysed bacteria spores without damaging the proteins. The stability and sensitivity of LTCC/chemiresistor smart channels are comparable to the performance of silicon-based chemiresistors. A variant of the use of sacrificial volume materials (SVM) has created channels, suspended thick films, cavities, and techniques for pressure and flow sensing. We report on inductors, diaphragms, cantilevers, antennae, switch structures and thermal sensors suspended in air. The development of 'functional-as-released' moving parts has resulted in wheels, impellers, tethered plates and related new LTCC mechanical roles for actuation and sensing. High-temperature metal-to-LTCC joining has been developed with metal thin films for the strong, hermetic interfaces necessary for pins, leads, and tubes.

Sandia is a multiprogram laboratory operated by Sandia Corporation, a Lockheed Martin Company for the United States Department of Energy's National Nuclear Security Administration under contract DE-AC04-94AL85000.

Key Words: LTCC, microsystem, sacrificial, channel, microfluidic

Introduction

We will demonstrate widely varied LTCC applications to microsystems and meso-scale devices. The mere testing of silicon microfluidic chips has been complicated due to nonstandard designs in a rapidly expanding research environment. To alleviate such a problem we have developed practical solutions like the interposer/manifold/socket combination shown in Figure 1. LTCC tubes--rolled and highly stacked--have practical uses, including smart channels, drift tubes, chemical and thermal reaction chambers, inductors, and heated fluidic headers. They can be used as chemical separators, coolers, or other applications with longitudinal or radial channels that spiral or serpentine. As with microfluidic boards, the serpentine can be in-plane or out of plane with the tape layers. Suspended thick films permit more sensitive thermal sensing and anemometry, as well as enabling components like air- core inductors, raised planar inductors, antennae, and electrical switch and micro fluidic valve applications. Micro total analysis systems (μTAS) including microstructures, and

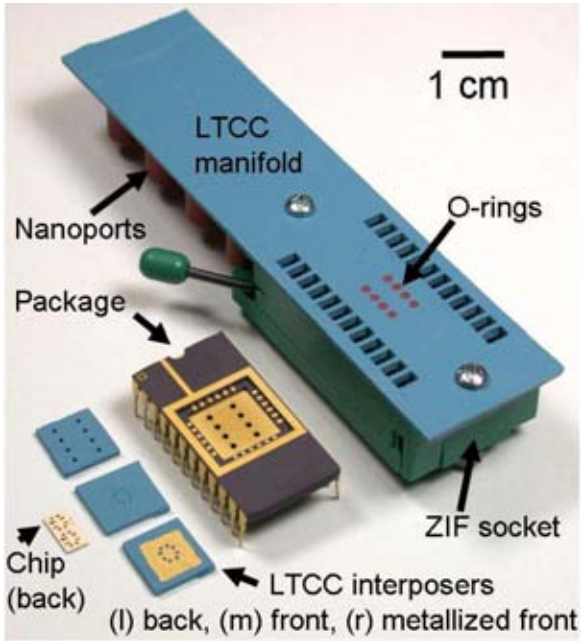

Figure 1. LTCC microfluidic test system.

micro high performance liquid chromatography (μHPLC) at pressures greater than 35 MPa (5000 psi) offer new miniature analytical capabilities. LTCC lids and channels with windows from 3 mm diameter to the size of an optical fiber (125 μm) permit new optical capabilities. A cell lyser has been shown to lyse biological species without damaging the proteins. Coarse and fine manifolds are simple and have repeatedly turned out functional prototypes on the first try. The requirement for planar systems has been eliminated in the case of Bourdon-tube and other types of pressure sensors and manifolds. Microfluidic O-ring seals and interfaces to a range of commercial connectors have simplified connections to the outside world. The demonstrated ability to braze strong joints for pins, tubes, and custom connectors will be useful in several disciplines. Much of the current work involves the use of sacrificial volume materials (SVM) in new and traditional ways. Commercial ceramic setter sheet has been added to our suite of SVMs, and these suggest the need for an inert-substance fill such as a setter paste for the attainment of micrometer-scale thicknesses. This new approach has enabled meso-scale 'functional-as-released' moving parts including wheels, impellers, shutters, cantilevers, pressure diaphragms, tethered plates, shuttles (pistons), and others. A freely spinning wheel/impeller is shown in Figure 2a, and a suspended spring-tethered plate is shown in Figure 2b.

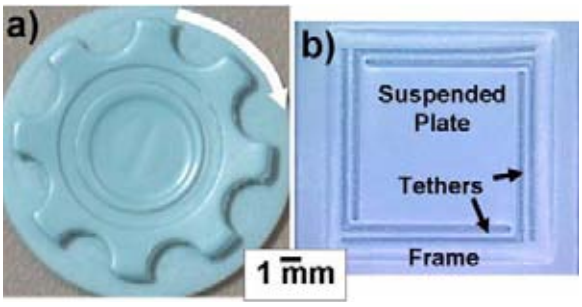

Figure 2. (a) Freely rotating 'functional-as-released' wheel. (b) Suspended square plate tethered to outer frame.

Background

Low Temperature Cofired Ceramic (LTCC) technology has an increasingly important role in enabling microsystem elements and their integration, just as hybrid microcircuits integrated monolithic silicon with a mix of technologies for special performance for many years. Modular hybrid microelectronics thrived due to performance that was superior to wafer-scale-integration. The term multichip module (MCM) was descriptive of a changing emphasis. First popularized by the fine feature size afforded by deposited thin film technology (MCM-D), they soon included ceramic (MCM-C) due to the reinvention of hybrid microcircuit technology using LTCC, in particular. Performance improvements were realized, particularly for high frequency and high current applications. LTCC also permitted a large cross-section of captive and commercial sources to use cofired ceramics. Prototyping in LTCC even accelerated design cycles for ultimate production in high temperature cofired ceramics (HTCC). An approach based on laminated printed circuit technology (MCM-L) also developed fine patterning capability to complement its high conductivity metals and inexpensive, low dielectric constant polymers. Several recent requirements for inert materials in extreme environments favor ceramics. Technologies that multiplex between use of polymers, deposited films, ceramic, and other materials and methods succeed when they are solution-oriented.

Integrated microsystems have now gone through some of the same phases as their microelectronic predecessors. An initial emphasis on minimum feature size in microelectromechanical systems (MEMS) is shifting to solution-oriented trade-offs considering ultimate packaged system size. Between these two scales lies the opportunity to add value with meso-scale functions. Well-known commercial entities successfully integrate surface micromachined (SMM) MEMS on the same chip with silicon integrated circuits (ICs). However, a large contingent remains interested in hybridizing the unique capabilities of microelectronic, microelectro-mechanical, microfluidic, radio frequency (RF), and optical functions while providing an interface to the outside world. LTCC provides solutions for these applications, many of which are still developing, including functions associated with health, detection of toxic or illicit materials, and security.

LTCC is a well-established commercial technology based on processing of unfired glass-ceramic tape. Processing steps are covered in detail in a comprehensive review [1]. In applications of LTCC to microsystems, it is important to understand the material properties of the available constituents (tapes, thick films, and auxiliary products). These materials, which are continuously being improved, determine the kinds of structures that can be made. These structures are, in turn, made by various methods. There is an enduring drive to look at technical needs and evaluate whether structures and methods used in other disciplines would be improved by LTCC. Some of the material properties (i.e., low

thermal conductivity) that are a detriment in some applications can benefit others. A variety of devices and systems result from these materials, structures, and methods. Then come some hard questions on the selection of optimum materials for manufacturing, as some of these devices and systems critically depend upon the unique capabilities of LTCC, while others only contain LTCC.

Although the available technologies that can be used in the manufacture of systems are continually evolving, there will always be a premium on features that are completely integral, cofirable, and 'functional-as-fired' in LTCC. The LTCC device as defined requires little additional assembly. However, the benefit of this approach must be weighed with the advantages of assembling a system of individual components that are each optimized for their intended function. As such, the complete integration of cofired systems is a work-in-progress, and a great deal of admirable work in the literature has enhanced the acceptance of LTCC in microsystems.

Materials and properties

The suite of tape and thick film compositions, functions, and application techniques to LTCC is ever-increasing. Studies have helped to quantify the chemical, structural, and mechanical properties of LTCC. [2] Particular attention is being given to materials interactions [3] and mechanical behavior during firing, [4, 5] as well as reliability implications, including failure analysis, [6] as LTCC finds new applications as mechanical structures. Characterization of thick films in general includes applications for ceramic humidity and multifunctional sensors on alumina, [7, 8] thermistors on alumina and fired LTCC, [9, 10] and piezoresistors on various substrates. [11,12,13,14,15] Most of the work we report here uses DuPont's 951 line of LTCC tapes and DuPont thick film compositions. Carbon-loaded tape and fluids and inert loaded setter tapes from Harmonics, Inc. are also used. [16]

Structures

Cavities have been used since the inception of LTCC, and interest in enclosed unfilled volumes (channels, chambers, etc.) was anticipated. In fact, microfluidic applications are given their own section below. LTCC unsupported bridges have been used to carry thick film structures for rapid thermal response [17], coils [18]and for an air core microstrip. [19] Suspended thick films have been fabricated that would enhance both of these applications. [20] Thick film diaphragms have also been demonstrated, [20, 21] as have thick conductor heat-spreading columns and tapes in cooling channels. [22]

Devices

There are several examples in the literature where a hybrid approach has been used to integrate microsystems in LTCC, [1] as with valves and windows in a microfluidic LTCC board, [23] and silicon or ceramic membranes in an LTCC valve. [24] Partially sintered membranes and bodies were joined with a glass frit for an all-ceramic pressure transducer. [25] Other distinctive devices include rolled tubes formed prior to firing (ion mobility spectrometer (IMS) drift tube), [26], stacked thick-walled IMS drift tubes, [27] micro heat pipes, [28] and micro-nozzles. [29]

Methods

LTCC tapes can be perforated and deformed. Thick film materials can be screen-printed, stenciled, dry-transferred, or written directly on surfaces and into vias. When collated, laminated and cofired, monolithic microsystem structures are the product. Collating can include unusual approaches such as rolling or fixturing for viscoplastic forming.

Our interest in novel capabilities of LTCC predated our work in rolled tape techniques, for cavity lids with three-dimensional relief. Whether by laminating complex layer stacks, [30, 31] deforming prior to firing, [26] slumping during firing, [32] or use of thick film loading, [4] the 3-D capability of LTCC has been appealing for a long time.

Shaping of LTCC

Shaping of LTCC has been used in designs such as the rolled ion mobility spectrometer drift tube reported elsewhere (Figure 3a). [33] This device

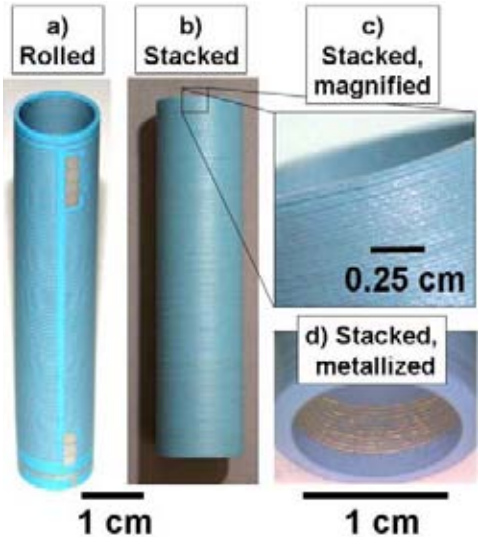

Figure 3. Fired LTCC tubes:. (a) Rolled, (b-c) Stacked, (d) Metallized and stacked.

included an embedded heater and surface cofired resistor networks (we have recently added thick film thermistors to the device). Tubes have been rolled on a 1.43 cm (0.563") mandrel to a layer count of 17 using 250 μm (0.010") tape layers. Firing was performed with the tube standing on-end using our normal temperature profile. Two orthogonal cross-sections revealed no apparent defects.

As a demonstration, a device of similar wall thickness was fabricated by stacking, as cracking had temporarily stalled previous efforts to build a stacked drift tube. The tube shown in Figure 3b was stacked to a layer count of 300 using 250 μm (0.010") tape. Stacking of washers maximized the availability of air to inner volumes during burnout and firing. All stacked parts made in this way were hermetic. Metallization on the face of the washer connected external traces to internal traces, whether they consisted of a thick film conductor on-edge or on the inner bore surface of alternate washers (Figure 3d). All such interior electrodes were electrically continuous to the exterior. Lamination was performed in either 20.7 MPa (3,000 psi) or in 207 MPa (30,000 psi) isostatic laminators. The inner bore, which was laminated to a mandrel, was quite smooth. The outer surface, which was wrapped in a buffer, could be smoothed, if required. The availability of tapes as thin as 50 μm (0.002") means the electrode size and separation could be very small. This was not necessary in the current drift tube design. The quality of the internal electrodes for face-metallized washers was degraded by tape edge deformation at the mandrel, and would have been improved by reaming before firing. [27]

Another rolled tube application to replace an inert ceramic feed tube for a gas sample has been prototyped. The existing alumina tube had been fitted with a discrete heater and temperature sensor that were quite bulky. An LTCC tube was fabricated with a buried gold thick film heater and a surface thick film thermistor (Figure 4). This tube was light weight and functional, actually melting the soft solder joints on its first trial. The smallest diameter mandrel used for this tube approach was about 2 mm diameter, and the fired outer diameter is 3 mm.

Smart Channels

Feasibility demonstrations for smart channels were fabricated from rolled LTCC tubes. As with the rolled IMS, the electrodes on the concave surface were rolled into contact with the electrodes on the convex surface, which were electrically terminated on the exterior of the tube with solderable thick film pads.

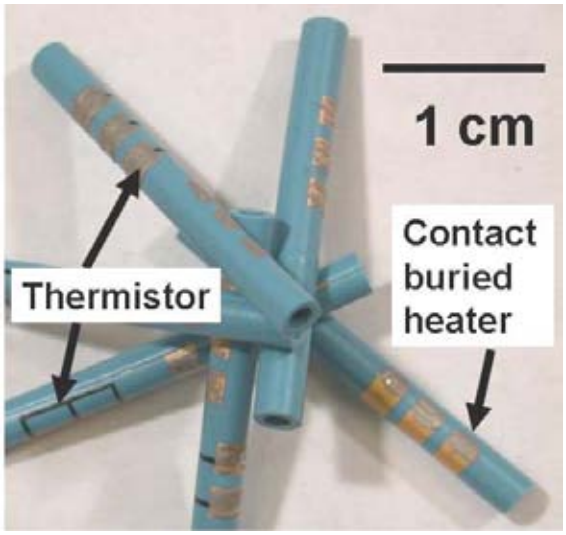

Figure 4. Miniature heated tubes with thermistors simplify point-of-use heating.

The smart channel integrates several sensors using the LTCC as a common substrate for: (1) a chemical sensor, (2) temperature sensors and (3) a flow sensor. The tube has provisions for internal surface thermistors, precision thick film electrodes for the sensing medium, and a small multipurpose heater embedded in the tube wall. Figure 5 shows the rolled LTCC tube, with electrodes both on the exterior and interior surfaces, during testing.

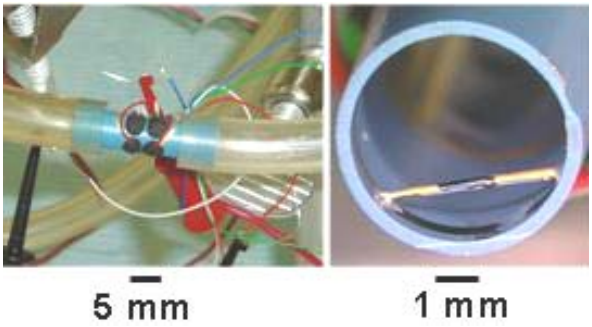

Figure 5. (a) Measuring chemical concentration, air flow, and temperature through the LTCC chemiresistor smart channel with integrated anemometry, (b) Suspended thermistor assembly.

Chemical Sensing

A chemical sensor (chemiresistor) was fabricated by depositing a conductive polymer "ink" across a pair of electrodes along the interior of the LTCC tube. In the current method, the "ink" was deposited inside the tube in the desired location using a micropipette. Volatile organic compounds can absorb into the polymers, causing them to swell and change in electrical resistance. The change in resistance is

proportional to the concentration, so these devices can be calibrated. The unique aspect of this device is that the sensors are integrated within the channel/tube, eliminating the need for extensive plumbing to introduce the fluid sample to the sensors. The location of electrodes at the end of the tube was ideal for applying the polymer.

The ends of the LTCC smart channel were connected to 6 mm (0.25") Tygon tubing, and dry air, trichloroethylene (TCE), and m-xylene gas were passed through the tube at known concentrations. A noise/stability analysis showed that the LTCC chemiresistor exhibited noise that was comparable (or lower) to conventional chemiresistors made from a silicon substrate. Results also showed that the LTCC chemiresistor responded well when poly (ethylene-vinyl acetate) (PEVA) was exposed to cycles of TCE and m-xylene (Figure 6). The response was approximately linear up to 1000 ppm of TCE and 100 ppm of m-xylene. A new design will increase the number of electrode pairs for the chemiresistors so several polymers can be simultaneously evaluated for discrimination of different chemicals.

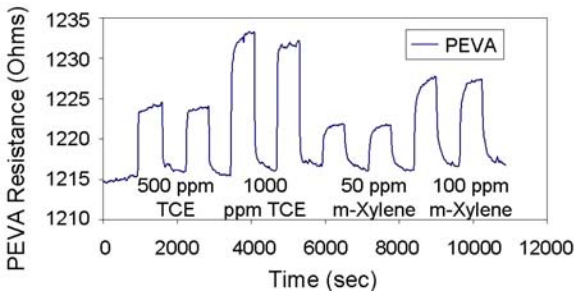

Figure 6. Response of the LTCC chemiresistor to different concentrations of TCE and m-xylene.

Flow and Temperature Sensing

Thermistors were fabricated and co-fired in the LTCC smart channel to provide temperature sensing and anemometry (Figure 5). Heating elements were also integrated with the smart channel to allow temperature control for the chemiresistors and for the flow measurement. The thermistors in the LTCC smart channel were first calibrated in an oven to yield a resistance/temperature coefficient. Air was then passed through the channel at different flow rates, and the thermistor temperatures were recorded while the heating element was maintained at a constant temperature. The thermistors were positioned at several locations in the channel to monitor the spatial temperature distribution. Preliminary results showed that flow rates above one hundred milliliters per minute could be measured with thermistors printed on the inner surface. We anticipate that with suspended thermistor structures (Figure 5b) the sensitivity can be significantly increased.

Sacrificial volume materials (SVMs)

Enclosed unfilled volumes have been formed by a number of different techniques. [1] Frequently, channels are left open and closed later with a cover—transparent if desired. They can be formed in an unfired ceramic surface, firing, and joining to a second surface Openings can be made through all or part of the full thickness of unfired tape layers by machining, punching, solvent jetting, laser ablation, stamping [34] or other. These volumes can be preserved in high pressure lamination using uniaxial pressing, fine geometries, [35] or selective protection during isostatic lamination (used by authors). Sagging in firing has been studied and thick film overlayers were used for shape compensation during firing. [4] Increasing the thickness of overlying unfired tape can also mitigate the closing of these volumes during firing. Low pressure lamination with an adhesive has also been used. [36, 37]

Another technique for preserving enclosed unfilled volumes involves a temporary insert, [38] as might be used in for component cavities. Cracking has been seen to result from differences in density following lamination [28] and friction against an insert or fixture can result in such density differences.

Enclosed unfilled volumes can also be protected by inserts that are etched away after firing, [4, 21] or an insert that would disassociate during burnout and firing. [4, 28] In some cases, this insert is cast in-place. [39] In most other instances, the insert is a discrete layer or stack matching the appropriate opening in a corresponding ceramic tape structure [40]. Another insert has been described that could be poured, shaken or flowed out after firing. [41] We and others have referred to these volumes as sacrificial and to the materials used to make them as SVM. The term 'fugitive phase' is also used in the literature for a subset of these.

While SVMs are not new, as referenced above, they have greatly enhanced the versatility and manufacturability of specialty LTCC applications. We previously described our use of SVMs in detail. [20] A distinct feature of one aspect of our use of SVM is that we don't require a pre-existing volume, but rather form the volume upon lamination according to the placement of the SVM. This technique is integrable with the existing infrastructure in industry which can regard SVM as a unique thick film or tape material.

We have used a variety of materials as SVM including polymer sheets and fluids, and commercial carbon-loaded tapes and pastes. We will also describe our use of inert loaded setter material in this paper. [16] A combined thermogravimetric (TGA) / differential scanning calorimetry (DSC) curve is shown in Figure 7 for a 2 mm diameter button of the carbon tape enclosed in 3 mm diameter LTCC tape wraps. Temperature is plotted versus time, as the light line, for a steady heating rate burnout and firing process (3ºC/min). The heavy dotted line—the calorimetry curve—indicates measured heat flow. Sample weight is shown as the heavy solid line. Both curves show the enclosed carbon-filled SVM 'burnout' in a range around 650ºC.

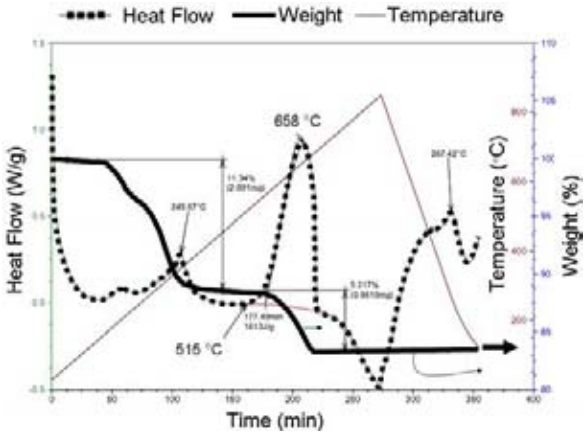

Figure 7. Thermogravimetric / differential scanning calorimetry analysis shows weight loss and exotherms associated with burnout and firing.

Figure 8a illustrates the use of SVM tape or fluid-defined layer, including its use as a substrate level for other thick film materials. This ability to print to a material of various thicknesses that is essentially going to disappear is very useful. It compares with dry-transfer of thick film we have performed in our lab and with thin film lamination described by others. [42] Plugs or thick film via fills, that are dielectric, conductor or other, as shown in Figure 8a, become z-axis supports. Use of SVM in conjunction with unfired ceramic tape is illustrated in Figure 8b. SVM tape, fluid, and other forms can be incorporated by a large number of techniques summarized in prior work [20]. It can be vanishingly thin (<< 1 μm) or remarkably thick (>>1 mm) as dictated by the particular application. Just as vias can be filled with SVM in Figure 8b the ability to route SVM anywhere on a layer or between layers complements its addition to the suite of available thick film materials. Several structures from Figure 8 are listed in Table 1. Features i and ii can be laminated to other areas

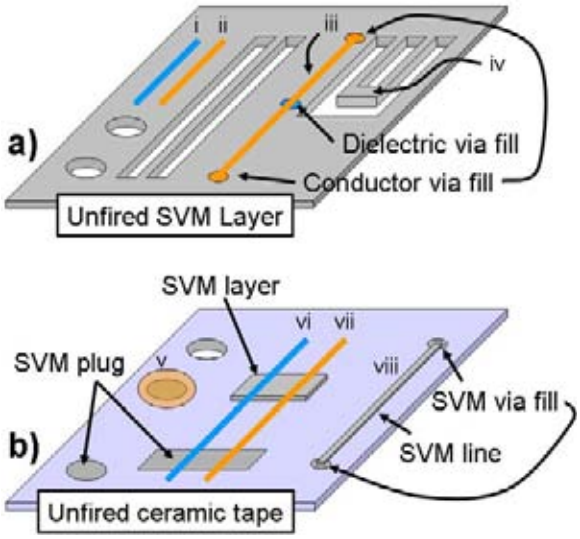

Figure 8. (a) SVM layer with thick film lines on top, (b) Ceramic tape with thick film and SVM lines on top, and cutouts/vias filled with SVM.

Table 1. Explanation of features in Figure 8.

Feature	Description
i	Thick film dielectric line on SVM.
ii	Thick film conductor line on SVM.
iii	Conductor on conductor vias with center support that is dielectric.
iv	Sacrificial volume area surrounded by open area for unfired tape bonding.
v	Conductor bridging SVM plug on ceramic tape to form diaphragm on firing.
vi	Thick film dielectric line crossing SVM layer to form bridge suspended above substrate and crossing SVM plug to form bridge across gap in tape layer.
vii	Thick film conductor line crossing SVM layer to form bridge suspended above substrate and crossing SVM plug to form bridge across gap in tape layer.
viii	SVM line on top of ceramic tape layer and on top of SVM via fill to form fluidic channel when laminated to another ceramic tape and fired.

shown on SVM or on LTCC tape. Feature iii is a raised conductor with conductive and/or insulating supports. Other structures shown in Figure 8a can be laminated as well. An example of such a method is shown in Figure 9, where feature iv, an SVM-defined serpentine channel, has been incorporated into a tube wall. A related simple shape has been discussed in the literature and suggested for use as cooling channels. [32]

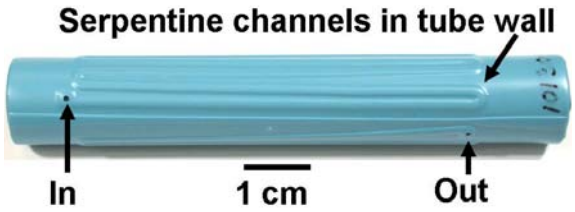

Figure 9. Serpentine channel defined by SVM with surface ports in the wall of a rolled tube.

Feature v shows thick film diaphragms supported over the tape openings by SVM plugs or via fill. Such diaphragms are shown in Figure 10. The rings in Figure 10a show a carbonaceous contamination associated with burnout and firing that has yet to be eliminated completely.

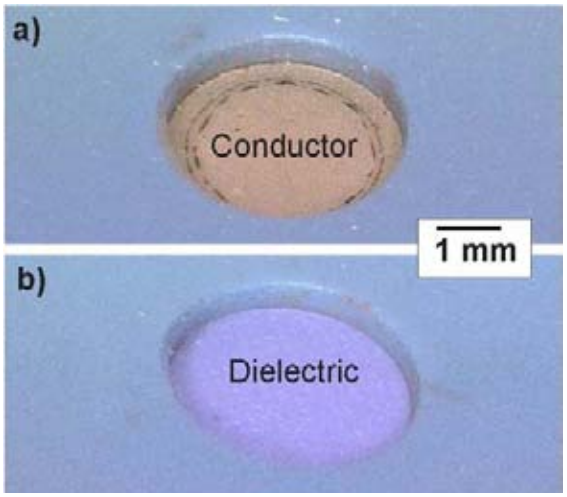

Figure 10. Thick film diaphragms have been fabricated using both conductor and dielectric.

Features vi and vii in Figure 8b show thick film lines that can be raised above the substrate or suspended over an opening. Feature viii shows one way to create a microfluidic channel with inter-level access.

Microfluidic channels

Microfluidic channels have been formed by the methods referenced above. Even in conventional board thicknesses, uses for both very large and very small channels are found (Figure 11). Miniaturization is recognized as key to future analytical chemistry and life sciences success. An excellent review of micromixers discusses miniature channels in silicon, polymers, glass, and metals. [43] Revolutionary results are now possible in laminated cofired ceramics. Surface considerations will receive special attention, particularly with respect to texture 44] and inertness. Recently, the suggestion of low-level Pb contamination in electrolytes by LTCC and conductors in certain applications [45] reinforces the expectation that coatings such as parylene, particularly for some biological applications, may play an important role. Another possibility might be atomic layer deposition (ALD) of materials like aluminum oxide that can coat aspect ratios approaching 10^4 under some circumstances. [46]

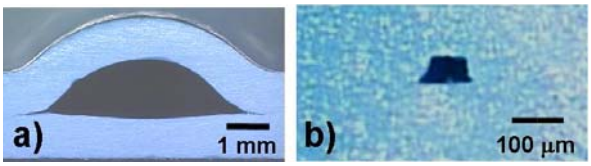

Figure 11. (a) Fired large channel formed by deforming ceramic tape around SVM during lamination. (b) Fired small channel punched through tape layer and laminated to top and bottom tape layer with protection over the channel.

Filling with an SVM has preserved vias and ports under a variety of lamination techniques. The device shown in Figure 12a is an example of a larger scale manifold for a valve component, mounted using through-holes. Ports were protected by SVM and fabrication succeeded on the first try.

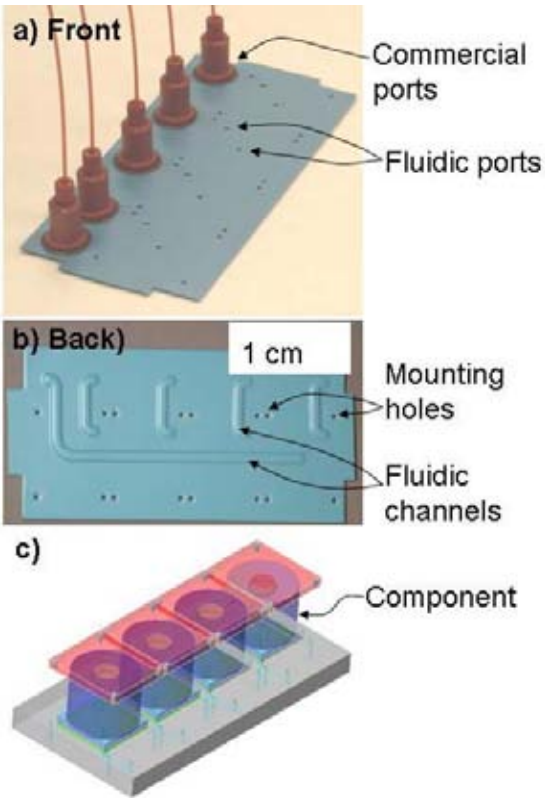

Figure 12. (a) Front of mesovalve manifold with standard connectors. (b) Back of manifold showing contoured channels formed by SVM lamination. (c) Mounted component sketch.

We made no attempt to limit backside topography associated with the sacrificial channel formation because it was not a requirement for this device. The manifold was required to effect no more than a 3.5 Pa (0.5 psi) pressure rise at a flow of 0.2 liter/min. Figure 12 shows the device ported to commercial fluid ports. Figure 12b shows the backside of the device with the topography evident. Figure 12c shows the design sketch including the component.

Integration / interposers for silicon microfluidics

MEMS is an area of intense activity with new designs coming out every day. Packaging has frequently been an afterthought, particularly in a research environment. Unfortunately, simple tests on devices sometimes present challenges. Just as packages provide microelectronic fan out, we have previously used discrete electrical interposers to interconnect MEMS devices such as high density mirror arrays. Now, electro-microfluidic interposers are also needed. In SMM silicon microfluidics, the most common microfluidic access is through the backside of the silicon using deep reactive ion etching (RIE) to define ports. Frequently, the features at the front of the chip dictate the minimum wall thickness between ports at the back of the chip.

The use of a disposable microfluidic/microelectronic interposer eases the fast acquisition of test data on new designs. One technique we have used was illustrated in Figure 1. This is a ceramic version that builds one earlier work on an electro-microfluidic dual in-line package (EMDIP™). [47, 48] It involves a standard package that can be easily connected in a commercial 'zero insertion force' socket including provision for microfluidic connections—in this case a low-profile LTCC manifold with O-ring glands (far right). This results in leak-tight connections up to greater than 200 kPa (30 psi). These ports have not yet been tested to failure. Ports on the standard package are adapted to the customized ports on the silicon device by a microfluidic interposer (Figure 13). Devices are attached to the front side with an appropriate method. Currently, depending on the application, epoxies, medical grade silicones, soft solders, Au/Si eutectic die attach and field-assisted bonding are used. The interposer can be fabricated with electrical traces and, ultimately, replace the package altogether. The LTCC manifold can be thin to be placed atop the socket or thicker to replace the top layer of the socket. The outside world connections are large, so the end of the manifold is large. Leadless chip carriers (LCC), pin grid arrays (PGA), fluidic grid arrays (FGA), and custom packages and sockets also lend themselves to this type of fixture. One stroke of a cam could connect the part mechanically, electrically, and fluidically for testing and that end of the manifold becomes much smaller. Also under consideration are miniature ports resembling ribbon cable for microfluidics.

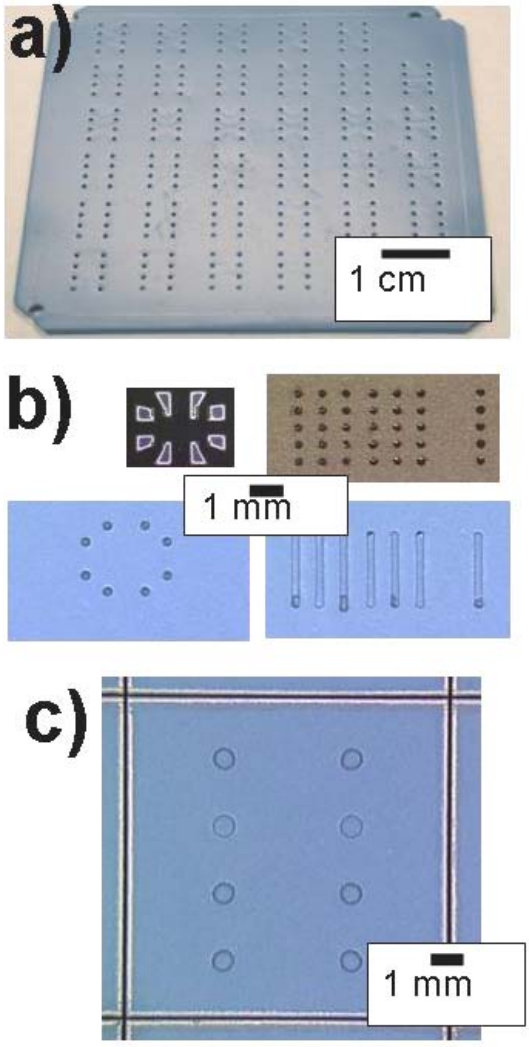

Figure 13. a) Interposer array, b) Silicon access holes (above) and mating interposer holes (below), c) Laser-scribed interposer.

Figure 13a shows a standard footprint hole array on the back of an interposer. Figure 13b shows the deep RIE fluidic ports on two silicon parts just above their mating interposers. Figure 13c shows the magnified back of an interposer, laser scribed and ready to singulate, whereupon it will fit closely onto the package floor without any special demand for alignment. The backside flatness is adequate for holes at this scale. The interposer array in Figure 13a was specified, defined, cofired, and singulated within 24 hours. Interposers as thick as 1.5 mm (0.060") have been used but interposers thinner than 300 mm (0.012") would work with a lower profile for most

applications. Figure 14 (a and b) shows an earlier manifold for 16 fluidic ports. Manifolds demonstrated previously, [49] similar to that shown in Figure 14c, may be replaced by LTCC.

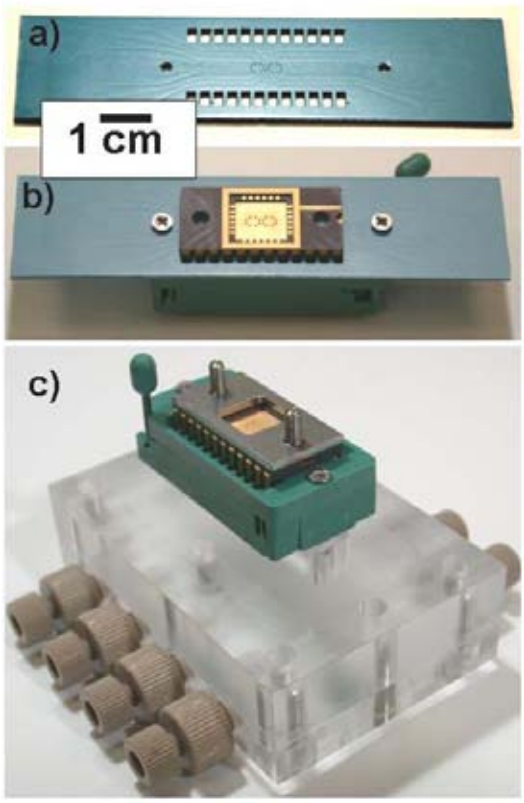

Figure 14. Testing is facilitated by an LTCC manifold that takes the place of a manifold block.

Miniaturization is still lost, however, when a 0.3 cm square MEMS chip is packaged in a 1.5 cm X 3 cm (or larger) package. Packages shown in Figure 15 are leading to the development of complete fluidic grid arrays (FGA) in multiple materials. We have successfully sealed FGAs with soldered annular seal rings that were prepared using flux, cleaned, and finally joined without flux. We have also investigated soldering in environments that obviate the need for flux—especially for high temperature solder.

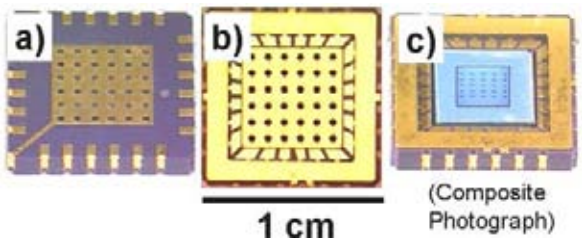

Figure 15. Fluidic grid array precursor a) back b)front c)composite photograph with interposer.

Applications in the near future will populate microfluidic system boards with a high silicon-to-board ratio, reminiscent of MCMs. Meanwhile, the first high density applications may involve "parts farms" in order to generate large amounts of reliability information in a compact manner. This would expand on an approach used in the past for MEMS. [50] A candidate would be an interposer, used for mechanical/fluidic testing of silicon devices that are placed in a harsh environment (Figure 16).

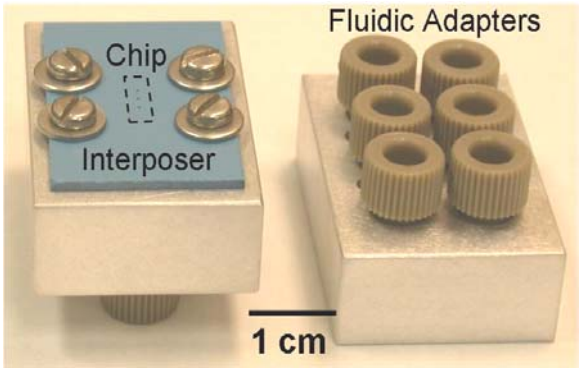

Figure 16. Alternate interposer used in harsh environment test.

Ports

Many microfluidic prototypes have had a glass capillary tube glued into place for fluidic connection. We have developed structures that are compatible with commercial connectors and have used various types, including adhesively attached surface ports that mate to a range of fittings. We have also used O-ring glands in a top layer of a microfluidic board for connections which will be re-used frequently, such as the test fixture shown in Figure 1.

It is further possible to active braze or direct braze metals with compatible thermal coefficients of expansion to LTCC devices. Test specimens using American Society for Testing and Materials (ASTM) F19 tensile buttons and LTCC interlayers with thin film metals have been successfully joined at temperatures up to 750ºC with strengths approaching 55 MPa (8000 psi). It is anticipated that reducing the brazed joint area to capillary tubing sizes will produce even greater joint strengths substantially reducing the surface area currently required for high strength interconnections. Parts sealed with the newly developed process pass helium leak testing with leak rates less than $5.0X10^{-10}$ atm-cc/min He. The direct incorporation of metals into LTCC structures during cofiring is also being evaluated by us and by others. [29] An environment that will properly cofire the LTCC without irretrievably degrading the metal is of interest.

μ-HPLC

Channels in LTCC have been made on a scale with those used for typical glass devices that have been chemically wet-etched (50 μm X 100 μm). The pumping hardware for such a system is shown in Figure 17. Early experiments have been performed

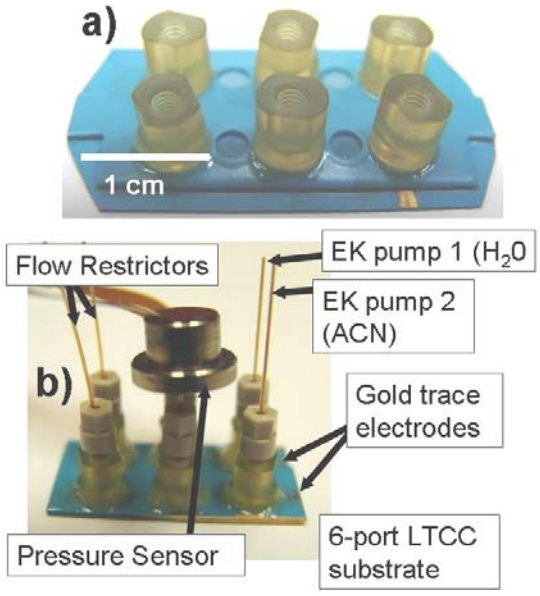

Figure 17. Micro HPLC fluid pumping apparatus

where an electrode in the leading port is used to complete electrical connections for a capillary-based electrokinetic micropump. Two parallel channels are shown for introduction of two different solvents (water and acetonitrile (ACN)). The center taps of each channel permit the pressure to be measured, followed by a fluid outlet port. Channels in μHPLC samples have been pressurized higher than 35 MPa (5000 psi) for electrokinetic pumping combined with μHPLC in an LTCC board for μTAS.

Cofired transparent windows have been incorporated with microfluidic channels for observation of fluid flow and mixing. [20] Early large windows (3 mm diameter) leaked at about 0.69 MPa (100 psi), but work continues to improve the integrity of the seal between the window and the substrate at high pressure, including design considerations. For example, we have succeeded with sealing viewing ports into LTCC as small as an optical fiber (125 μm diameter). These also pass helium leak testing with no detectible leak. We previously had sealed optical fibers into wall sections of LTCC structures for optical applications. Optical fibers have also been cofired into zero-shrinkage LTCC in the literature. [51]

Cell Lyser

A new application to take advantage of LTCC properties for biological systems is a compact version of a rapid cell lyser and solubilizer. Channels were formed with LTCC features that readily accepted a glued-on surface port. The channel was surrounded by heaters on layers above and below. The ability to heat and apply pressure to the channel was used to successfully lyse robust spores of *Bacillus Subtilius*. An example of one of the heater configurations is shown in Figure 18a.

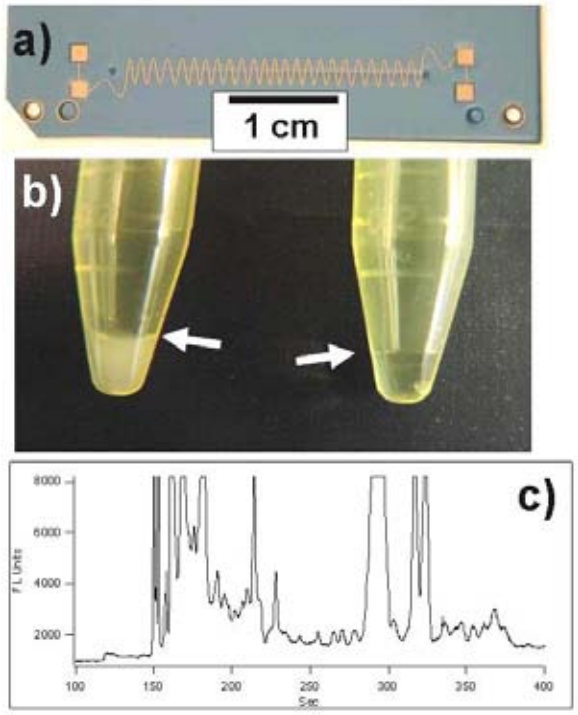

Figure 18. a) LTCC cell lyser with integrated heater traces. b) Processed spores through the lyser at room temperature (left) and at 180degrees C (right). c) Separation of solubilized proteins by molecular weight after lysing spores with the thermal lyser.

The vial tips shown in Figure 18b have captured the output of the cell lyser operating at room temperature and at 180ºC. The difference in turbidity suggests that the spores have been successfully lysed. The plot in Figure 18c demonstrates that the spore contents have been successfully solubilized and the proteins, still intact, can be separated with conventional analytical techniques. [52, 53]

Suspended thick films

The technique for making thick film air bridges has previously been described to make structures like those shown in Figure 19. Features like i and ii in

Figure 8a can be laminated transversely to a feature like the SVM layer in Figure 8b to cofire structures like the conductor in Figure 19a or the dielectric in Figure 19b. The usefulness of these suspended thick films can be enhanced in certain applications by making the bridge a cantilevered structure that would result in a lower mass as shown in Figure 20.

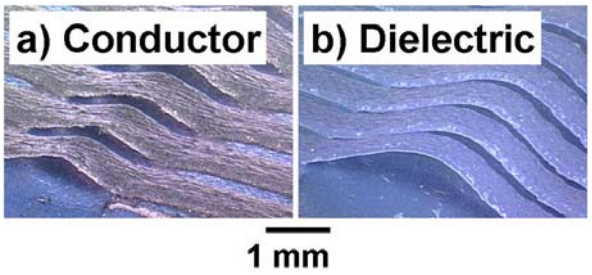

Figure 19. Suspended thick film bridges using a) thick film conductor (b) thick film dielectric.

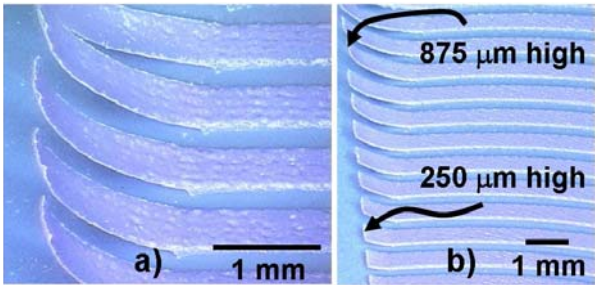

Figure 20. Cantilevered dielectric thick films.

Inductors

The use of suspended thick films to realize inductors as shown in Figure 21 may allow inductors with performance superior to planar spiral inductors. The technique will allow inductors with reduced inter-turn capacitance and series resistance, allowing higher Q and self-resonant frequencies. A similar approach was described using wirebonding, [54] but the high series resistance due to the small wire cross-section limits the overall Q of the structure. Because the inductance of the structure is proportional to the cross-sectional area of the loops, maximizing the loop height above the substrates is critical. An example of fabricated inductors with 'through' and 'open' test structures is shown in Figure 21b. However, the inductance of the structure was only about 1 nH (compared to the expected 4 nH) due to the small height of the loops above the substrate, which also increased the inter-turn parasitic capacitance. Increasing the bridge height to improve the loop cross-section and lower the parasitic capacitance is expected to improve the overall

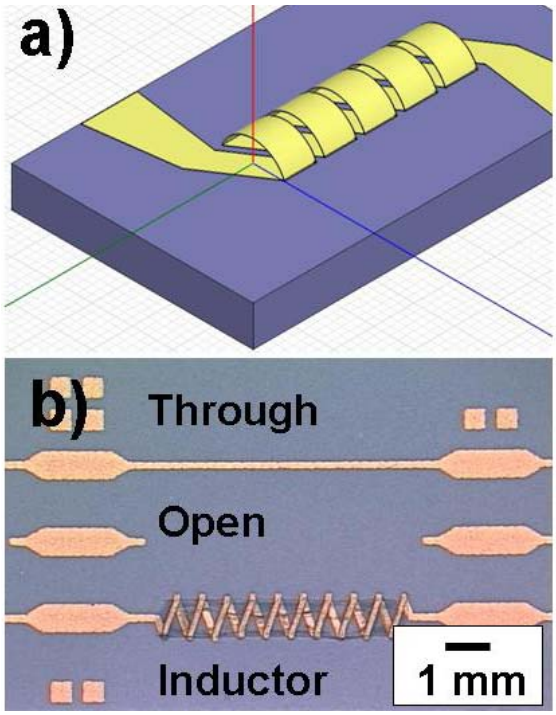

Figure 21. Air core inductors fabricated using SVM with LTCC.

inductor performance to the point where it is a viable alternative to lossy planar inductor structures. Simulation to determine the optimum dimensions for these types of structures is ongoing, but preliminary simulations indicate inductances of several nH with Q's over 200 may be possible for these structures at frequencies up to a few GHz. Additionally, these inductors may allow the insertion of a ferrite material into the core, increasing the inductance of the component and allowing for components such as integrated transformers.

Because Q of an inductor generally increases with cross-sectional area, the approaches used to demonstrate LTCC tubes can also be used to realize high-inductance air-core inductors with thick film conductors. One such example demonstrated inductance of 17 μH with a peak Q of 49 at 23 MHz and a self-resonant frequency over 40 MHz, which was the upper frequency limit of the test equipment. The hollow core of the tube will also allow the insertion of ferrite material, allowing extremely large inductors and transformers with better reproducibility than the typical wire-wound components.

Antennae

Suspended thick film material may be used to realize integrated antennae on LTCC substrates. Generally, integrated antennae have poor performance due to the high dielectric constant and loss of the dielectric

substrate, but the ability to suspend traces above the substrate should allow antenna designs with improved efficiency, directivity, and gain. A simple 3D electromagnetic simulator model of one such antenna is shown in Figure 22a. The antenna uses a coplanar launch and a simple balun to feed a 6 GHz dipole antenna suspended above the substrate. While initial simulations of this design only shows slight improvement over antennae fabricated directly on the substrate, further optimization of this and other antenna designs should benefit from the ability to suspend the metal thick films above the substrate. Antennae have been fabricated using thick film raised above the surface of the substrate as shown in Figure 22b-d. This prototype was assembled for the purpose of measurements and is not co-fired yet. Planar coils may also be improved by elevating them off the substrate. As with a planar coil, this structure may resort to having periodic dielectric supports made of LTCC.

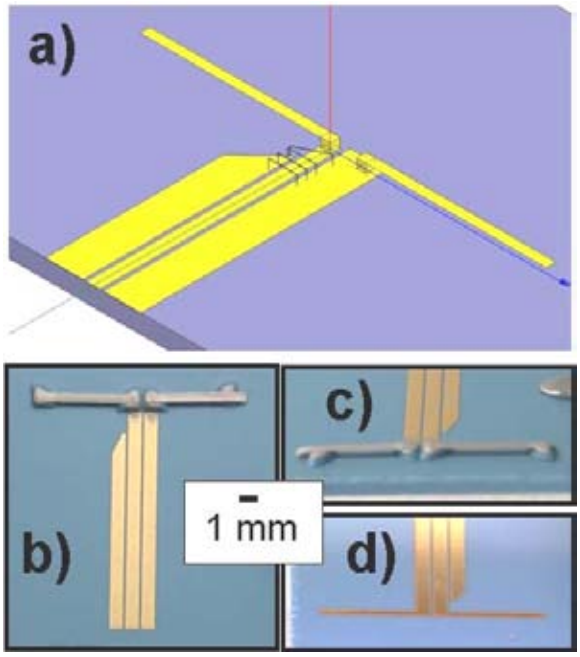

Figure 22. Suspended thick film antennae a) as-designed, b) top view, c) tilted view with thick film raised 250μm from surface, d) antenna fired on surface for comparison.

Cavity Resonators

A potential application of internal sacrificial volumes is cavity resonators similar to those realized previously in silicon and other technologies [55]. These internal cavities may allow the realization of high-frequency filters and resonant structures with Q values previously unobtainable on LTCC materials. These cavities offer the potential for Q's of several hundred at frequencies of 10 GHz and higher. Additionally, these cavities will be inside the ceramic, leaving the ceramic surfaces for surface mount components and other large items. Process development for the realization of these structures is ongoing.

Thermistors

Prior work in the literature identified commercial thermistors that had very good properties. [9, 10] The behavior of these thermistors was even found to be better on fired LTCC than on alumina, and evaluation of cofiring was recommended. We worked with the same thermistors, examining printing conditions and their effect on performance on fired LTCC. Because several of our applications involved immediate integration, such as anemometry in complex locations in proximity to heaters that would furthermore be air bridges, we cofired these thermistor compositions with satisfactory results. As reported, the values were variable but the performance was quite good for prototypes and proof of concept. Other thermistor devices have been made for flow sensing, such as the device shown in Figure 23, currently being tested. Here, the thermistors and heaters are located along a flow channel on the external surface.

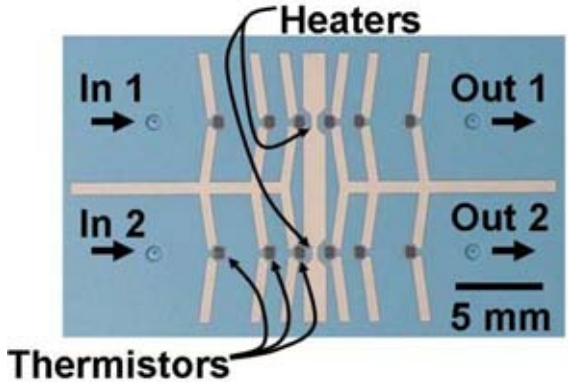

Figure 23. Surface thermistors on a flow sensor.

Thermistor in channels

It was mentioned that the use of channels and SVMs has expanded the number of compositions that can be considered for cofiring. Several materials would survive cofiring on a surface exposed to air during firing, but will not survive if buried and enclosed in the matrix of the body of a part. The use of a cavity permits non-buried thermistors to be considered for incorporation. A unique set of circumstances exists in a case like this. It can be desirable to have the fluid move through the channel without a great amount of heat being diverted. One would also like to have a thermal measurement without electrodes

being directly exposed to the working fluid. Thick film resistors are insulating on their surfaces. This makes an ideal situation for placing a thermistor in a channel. If, for instance, the thermistor crosses the channel, the amount of the buried resistor can be reduced to be an insignificant amount. At the same time, the cofirable electrodes can be buried in the matrix. Channels have been made in this way and appear to work as desired. A schematic for the technique is shown in Figure 24.

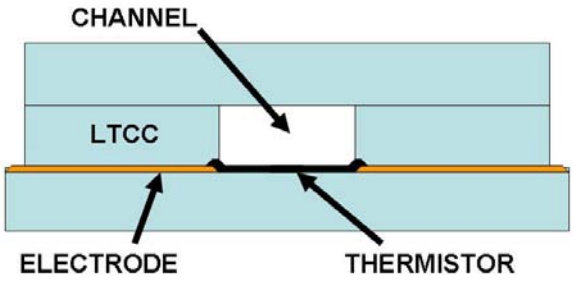

Figure 24. Thermistor on interior surface of a microfluidic channel.

This device has been tested in conjunction with the heater shown in Figure 4 to detect air flow as shown in Figure 25. The resistance for both the thick film heater and the thermistor are plotted. Both plots suggest useful applications as flow indicators.

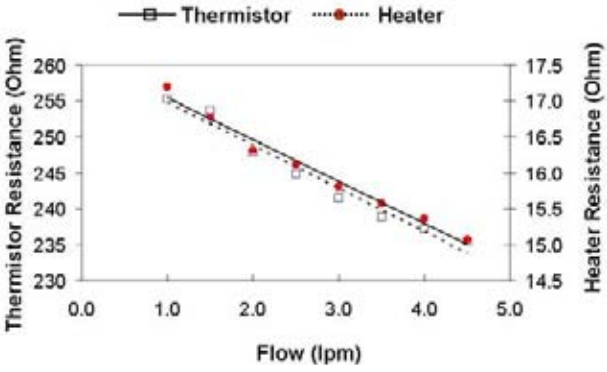

Figure 25. Flow calibration for gold thick film heater and thermistor.

Thermistors on suspended thick films

Figure 26 shows an air bridge test part where 0.5 mm wide resistors were applied to cofired dielectric bridges in geometries that varied from 1.5 squares to 8 squares. These parts showed remarkable results, such as registering a 1 degree Celsius temperature rise under illumination from a flashlight, and 0.1 degree Celsius sensitivity. Using a rotating optical shutter, the time constant of these thermistor bridges was determined to be 0.5 seconds.

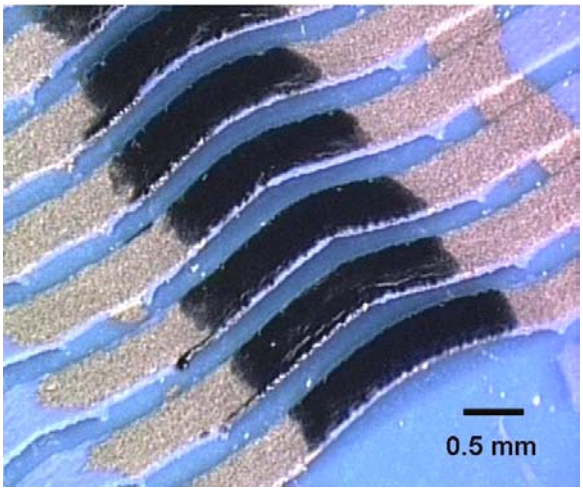

Figure 26. Thermistors on suspended thick film bridges.

These materials have also been cofired on thick film bridges with good results. Our yields need to improve but the performance of the devices is good. In order to succeed with cofired thermistors, we have needed to support the glassy thermistor portion structurally. While they survive when printed directly onto the LTCC surface, they would droop and become discontinuous in mid-air. We have supported the thermistor on a dielectric bridge, concentrating on having a small thermistor with electrical leads no more massive than they have to be. Because the conductor can support itself, we have also used suspended metal traces that overlap a small dielectric patch that serves as a platform for the thermistor and lets it overlap the conductor for proper electrical termination.

We have also cofired structures in the z-axis by sandwiching thick film thermistor between the tips of thick film metal lines. These devices result in very low resistances, but they are thermally responsive. They also can serve as heaters. When the heater is off it can be used to indicate a cooling rate proportional to flow rate in its surroundings. A similar structure has also been used in an application for an array of vertical load sensors, using the piezoresistive properties of the thick film resistor. [56] Because anemometry may involve thermistors in close proximity to heaters, we have considered the SVM technique for construction of heaters and thermistors in layers with a small gap between them.

Setter tape as a sacrificial material

We previously alluded to a technique for preserving shapes that seemed impractical at the time. We have adopted a variant of that approach to further refine devices that can be made where sagging during firing would otherwise prevent them.

By treating a commercial setter tape from Harmonics Inc. as a sacrificial material, and copying from surface micromachined (SMM) MEMS manufacture geometrical techniques for achieving minimum spacing smaller than the stated minimum feature size we have been able to create 'functional-as-released' moving parts. 'functional-as-released' in this context means that aside from removing the sacrificial material, no additional assembly is required. Alignment of features is performed prior to lamination, just as alignment of mask layers would be performed on an SMM MEMS device. Release consists of blowing the setter particles out of the structure, either with compressed gas or some other particular working fluid for the device.

The technique we are using is to place a material in contact with the desired layers that prevents tape bonding but then occupies the space during firing. An expansive thin layer that would sag upon firing is restrained from doing so. Deformation during lamination can be used to tighten the tolerance on a hub for a wheel. The concept for a simple wheel is shown in Figure 27. The deformation of the unfired setter tape has repeatedly resisted perforation so that it does not fuse to the other layers of tape, say at a corner. A space is defined that permits the hub for the wheel fuse to the substrate, but keeps the wheel from sticking to the hub or to the substrate. The top setter could also be an unfilled SVM in certain cases.

One factor to be considered is the large differential shrinkage between the setter layer (1%) and the LTCC layer (12-15%). Although it becomes a loose powder, trapping the material in certain ways can gives rise to problems seen in laminated object manufacturing. [57] This problem can be mitigated by using the supporting material in a pattern, such as support posts or rings, or coated with carbon SVM.

Structures including the one shown in Figure 2a were driven pneumatically in a manifold that directs jets of air at the structure perimeter--also constructed from LTCC. While these structures are just over 1 cm in diameter, they served to prove the concept. A useful size range for such devices was likely to be 1-3 mm. Figure 28 shows a second attempt resulting in a freely spinning, 'functional-as-released' 3 mm diameter impeller. The tape setter materials suggest a use for inert filler materials such as pastes in order to reduce minimum spaces to microns where needed.

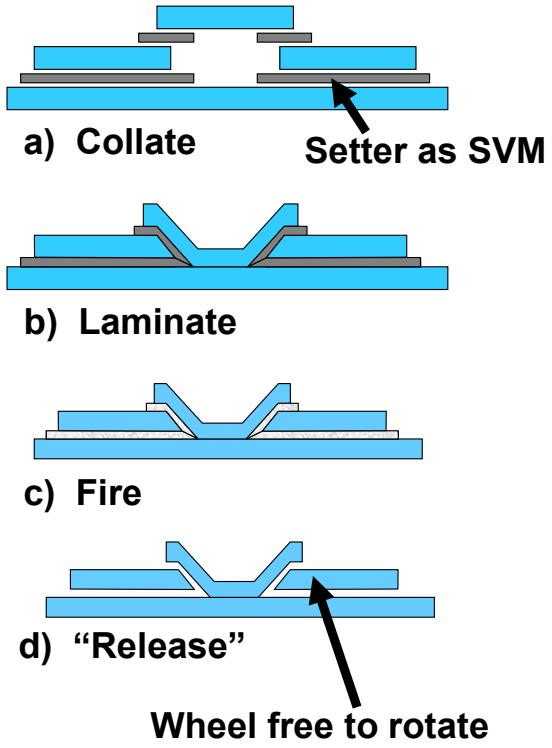

Figure 27. Simplified illustration of 'functional-as-released' LTCC wheel.

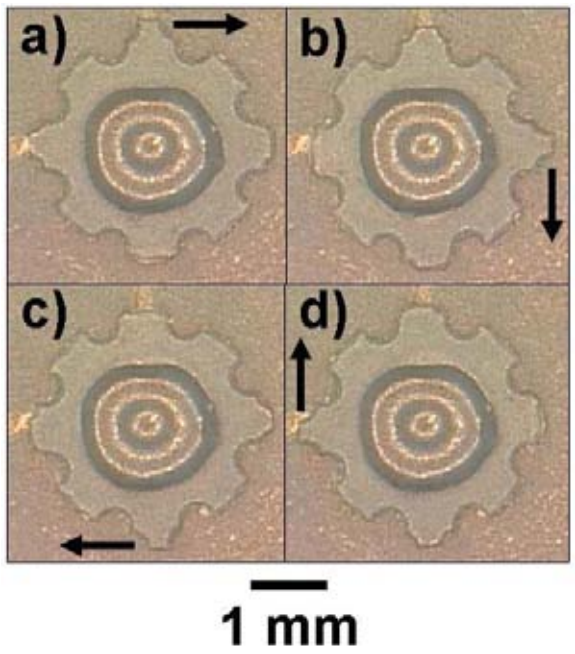

Figure 28. A 3 mm 'functional-as-released" freely rotating wheel is parked at four positions around one revolution.

Capacitance sensing

Measurement of variable parallel plate capacitance as a mechanism for obtaining response is obvious in existing pressure sensors, accelerometers, and other devices. Several sensor types could be constructed in LTCC using this approach. A related example of such a product is the floating accelerometer plate shown in Figure 2b. This plate is held to the surrounding frame by tethers, a technique copied from oscillators, comb drives, and other silicon SMM MEMS parts. Just as the wheels are free and can be rotated, the suspended plate in Figure 2b is free and can be deflected up or downward by probing. The device in Figure 2b is a prototype without metallization.

A device was fabricated, consisting of a metallized cofired parallel plate, 1 cm in diameter, suspended on an LTCC tether in proximity to its metallized base as shown in Figure 29. Metallized "functional-as-released" parts have some technical issues. For parallel plate devices, to raise the capacitance one would like small separations and large metallized areas. These patterned metallized areas increase metal loading and may result in differential shrinkage and warpage. One would like thin conductive layers to avoid having to use a mesh pattern as have been used in ground planes. Techniques already mentioned that would put a thin coating of the thick film or a dry transferred thin film would meet this need.

Figure 29. Suspended structure: Cantilevered capacitor plate (12mm diameter).

We looked at capacitance at various spacings on a cantilever/tether device as shown in Figure 30. The parallel plate capacitance as calculated is shown in the solid line. Four data points were measured using shims, and that curve fit is also shown. The ability to both actuate and measure capacitive response suggests several devices that can be made.

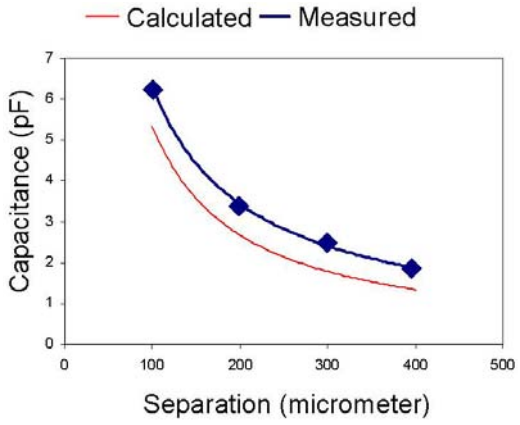

Figure 30. Capacitance variation with gap spacing for metallized ceramic plates.

Strain gage pressure sensors

We have encountered applications with very different pressure requirements from 750 Pa (a few inches of water) to greater than 35 MPa (5000 psi). Pressure sensors are integral parts of many silicon microfluidic MEMS, and would be a key addition to LTCC boards. Pressure sensors have been fabricated using cavities and membranes with an SVM technique using the carbon and the setter material. Such a device is shown superimposed on a plot of the voltage output Figure 31. This pressure sensor is also a hybrid type, using a commercial foil diaphragm strain gage that comprises a Wheatstone bridge, with two elements in tension and two in compression. The 1mm (0.040") thick LTCC base serves as the diaphragm of this 12 mm diameter device. This device survived repeated excursions to 0.69 MPa (100 psi). We also tested a diaphragm of 100 µm (0.004") thick LTCC and saw a comparable voltage span and stability whereas maximum stress would

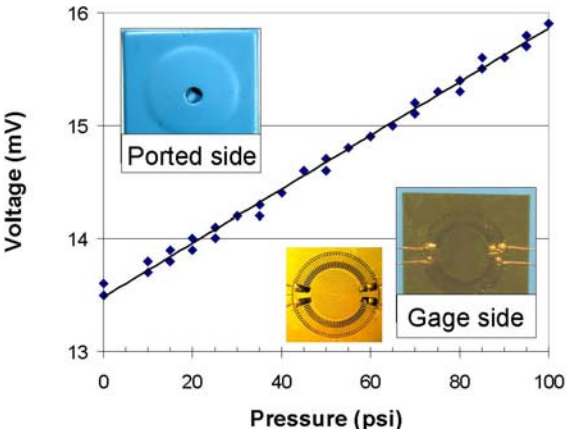

Figure 31. Pressure readouts from an LTCC diaphragm indicate a useful pressure sensor.

be expected to be about 15 times higher, neglecting the glue and the gage. Quantitative calculations of membrane stress have not yet been performed. These sensors could be miniaturized by directly printing piezoresistive compositions in patterns appropriate to the device. Thick film piezo resistors have been reported with gage factors almost an order of magnitude higher than can be obtained purely with geometrical effects. [11] Because these structures are not limited to planar geometries, we have also investigated curved channels that can change their shapes and sense pressure operating as miniature Bourdon tube devices. We continue to work with strain indicators to produce pressure sensors that work over wide ranges of pressure.

Electrostatic Actuation

Vertical actuation of cantilevered LTCC structures can be accomplished by electrostatic operation. We have electrostatically actuated fragile LTCC cantilevers normal to the plane of the substrate. We have yet to achieve anything as useful as a comb drive or other actuator (electrostatic, thermal, electromagnetic). The deformation of layers during firing and as affected by thick film loading is more a factor here than in other applications, due to the small, uniform gaps required. All aspects leading to the net shape of the structures need additional work.

We have also deflected freestanding thick film beams into contact with their activation pads as shown in Figure 32. We have also deflected these structures

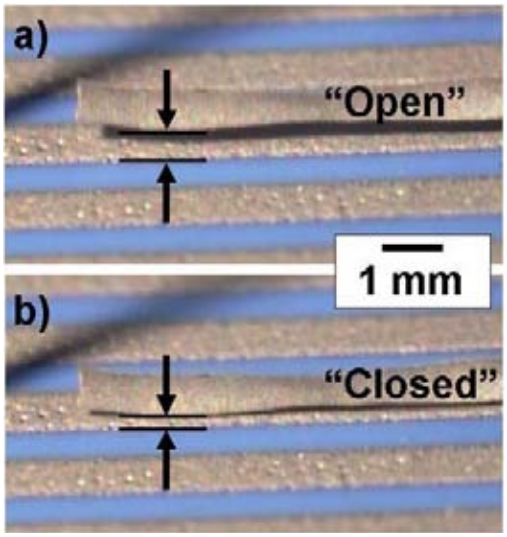

Figure 32. Suspended thick film conductors actuated vertically.

into contact with a third line but have not yet shown activation of a switch. This thick film was as-fired without any other surface preparation.

Conclusions

New techniques in LTCC technology continue to expand the integration of microsystems including connections to the outside world. These range from functionalizing existing silicon microfluidics to enabling meso-scale devices using new techniques. LTCC meso scale devices bridge the size gap between the micro and macro worlds, and add real value in new functions. We fabricated smart channel prototypes using polymer chemiresistors that are responsive and offer promise for embedding these functions in smaller integral channels. Analytical functions such as μHPLC can be miniaturized using LTCC. Biological cell lysing using an LTCC device has been demonstrated. Large manifolds that need to be more inert than polymers are simple to fabricate in LTCC. RF components with improved performance such as inductors, antennae, and perhaps even switches are being developed. Raised bridges of low mass that are integral with the LTCC board provide several capabilities, including rapid thermal measurements for flow measurement. LTCC as a membrane has been used to obtain pressure measurements. Finally, 'functional-as-released' moving mechanical structures have been demonstrated and continue to be developed.

Acknowledgements

The authors would like to thank Timothy Turner, Richard Sanchez, Dennis DeSmet, and Tom Massis of Sandia National Laboratories for contributions that made this work possible. The authors further wish to thank Luke Fergusson of Harmonics, Inc.

Sandia is a multiprogram laboratory operated by Sandia Corporation, a Lockheed Martin Company for the United States Department of Energy's National Nuclear Security Administration under contract DE-AC04-94AL85000.

References

1 MR Gongora-Rubio, P Espinoza-Vallejos, L Sola-Laguna, JJ Santiago-Aviles, "Overview of low temperature co-fired ceramics tape technology for meso-system technology," Sensors and Actuators A 89 (2001) 222-241.

2 WK Jones, Y Liu, B Larsen, P Wang, and M Zampino, "Chemical, Structural and Mechanical Properties of the LTCC Tapes," Proc. Int. Symp. Microelect., IMAPS, Boston, (2000) 469–473.

3 KG Ewsuk, CB DiAntonio, F Uribe, SL Monroe, "Materials and process control technology for LTCC microelectronics packaging," Proc. Cer. Intercon. Tech. Conf., IMAPS, Denver, (2004) 1-6.
4 P Espinoza-Vallejos, J Zhong, M Gongora-Rubio, L Sola-Laguna, JJ Santiago-Aviles, "Meso (intermediate)-scale electromechanical systems for the measurement and control of sagging in LTCC structures," Mat. Res. Soc. Symp. Proc. 518, 1998, 73-79.
5 M Wagner, A Roosen, A Stiegelschmitt, D Schwanke, F Bechthold, "Optical dilatometer for in-situ measurements of warpage effects during firing of LTCC multi layer structures, Proc. Int. Symp. Microelect., IMAPS, Washington, (2002) 71-75.
6 H Dannheim, U Schmid, A Roosen, "Lifetime prediction for mechanically stressed low temperature co-fired ceramics," J. Eur. Cer. Soc. v24 no.8 (2004) 2187-92.
7 LJ Golonka, BW Licznerski, K Nitsch, H Teterycz, "Thick-film humidity sensors," Meas. Sci. Technol. 8 (1997) 92-98.
8 W Qu, R Green, M Austin, "Development of multi-functional sensors in thick-film and thin-film technology," Meas. Sci. Technol. 11 (2000) 1111-1118.
9 M Hrovat, D Belavic, Z Samardzija, "Temperature sensors made by combinations of some standard thick film materials," J. Mat. Sci. Lett. 19 (2000) 651-655.
10 H Birol, T Maeder, C Jacq, P Ryser, "Effects of firing conditions on thick-film PTC thermistor characteristics in LTCC Technology," Proc. Ceram Interconnect Tech. Conf., IMAPS, Denver, (2004) 106-109.
11 M Hrovat, D Belavic, S Samardzija, "Characterisation of thick film resistor series for strain sensors," J. Eur. Ceram. Soc. 21 (2001) 2001-2004.
12 D Belavic, M Hrova, S Bencan, W Smetana, H Homolka, R Reicher, L Golonka, A Dziedzic, J Kita, "Investigations of thick-film resistors on different substrates for strain-gage applications," Proc Int. Symp. Microelec., (2002) 441-446.
13 M Hrovat, D. Belavic, A. Bencan, J. Bernard, J. Hole, J. Cilensek, W Smetana, H. Homolka, R. Reicher, L. Golonka, A. Dziedzic, J. Kita, "Thick-film resistors on various substrates as sensing elements for strain gauge applications," Sensors and Actuators A 107 (2003) 261-272.
14 M Hrovat, J Holc, S Drnovsek, D Belavic, J Bernard, M Kosed, L Golonka, A Dziedzic, J Kita, "Characterization of PZT thick films fired on LTCC substrates," J. Mat. Sci. Lett., 22 (2003), 1193-1195.
15 J Juuti, A Lozinski, S Leppavuori, "LTCC compatible PLZT thick-films for piezoelectric devices," Sensors and Actuators A, 110, (2004) 361-364.
16 Harmonics, Inc. website:
http://www.users.qwest.net/~hmnx/
17 M Gongora-Rubio, LM Sola-Laguna, PJ Moffett, JJ Santiago-Aviles, "The utilization of low temperature co-fired ceramics (LTCC-ML) technology for meso-scale EMS, a simple thermistor based flow sensor," Sensors and Actuators A; v73 no3 (1999) 215-221.
18 M Gongora-Rubio, L Sola-Laguna, JJ Santiago-Aviles, M Smith, "Integrated LTCC Coils for Multiple Applications in Meso-Electromechanical Systems," Proc. of IMECE99:MEMS, (1999) 189-194.
19 YC Lee, KC Eun, CS Park, "A new low-loss microstrip structure on LTCC substrate," IEICE Trans. Elect. 2003, vE86-C no. 5, p. 867-9.
20 KA Peterson, SB Rohde, CA Walker, KD Patel, TS Turner, CD Nordquist, "Microsystem integration with new techniques in LTCC," Proc. Ceram. Intercon. Tech. Conf., IMAPS, Denver, (2004) 19-26.
21 CB Sippola, CH Ahn, "A ceramic sealed cavity with screen printed ceramic diaphragm," Proc. Ceram. Intercon. Tech. Conf., IMAPS, Denver, (2004) pp. 179-182.
22 H Adluru, MA Zampino, Y Liu, WK Jones, "Embedded heat exchanger in LTCC substrate," Proc.
Cer. Intercon. Tech. Conf., IMAPS (2003) 205-210.
23 L Rebenklau, KJ Wolter, S Howitz, "Realization of hybrid microfluidic systems using standard LTCC process," Proc. Elect. Comp. and Tech. Conf, (2000) 1696-1700.
24 M Gongora-Rubio, L Sola-Laguna, M Smith, JJ Santiago-Aviles, "A meso-scale electro-magnetically actuated normally closed valve realized on LTCC tapes, Proc. SPIE, Conf. on microfluidic dev. and syst. II, Santa Clara, V3877 (1999) 230-239.
25 H Lynch, J Park, PA Espinoza-Vallejos, JJ Santiago-Aviles, L Sola-Laguna, "Meso-scale pressure transducers utilizing low temperature co-fired ceramic tapes, Mat. Res. Soc. Symp. Proc. v546, (1999) 177-182.
26 SB Rohde, KA Peterson, "Applying new LTCC/ LIGA construction techniques in realizing a miniature ion mobility spectrometer," presented IMAPS 35th ann. Symp. on microelect., Denver, Sept., 2002.
27 DG Plumlee, M Tam, P Dwivedi, H Hill, JA Hartman, AJ Moll, "Ion Mobility Spectrometer (IMS) Fabricated in Low Temperature Cofire Ceramic (LTCC)", Proc. IMAPS Ceram. Intercon. Tech. Conf., 2003, pp.240-245.
28 WK Jones, Y Liu, M Gao, "Micro heat pipes in low temperature cofire ceramic (LTCC) substrates," IEEE Trans. Comp. Pack. Tech., v26 No1 (2003) 110-115.
29 D Plumlee, J Steciak, A Moll, "Development of a monopropellant micro-nozzle and ion mobility

spectrometer in LTCC," Proc. Ceram. Intercon. Tech. Conf., IMAPS, Denver, (2004) pp. 115-120.
30 BB Mathewson, WS Newman, AH Heuer, JD Cawley, "Automated Fabrication of Ceramic Components from Tape-Cast Ceramic," Proc. Solid Freeform Fab. Symp. Austin, (1995) 253-260.
31 JD Cawley, AH Heuer, WS Newman, BB Mathewson, "Computer-Aided Manufacturing of Laminated Engineering Materials," Am. Cer. Soc. Bull., v75 No5, May (1996) 75-79.
32 J Li, GK Ananthasuresh, "Three-dimensional low-temperature co-fired ceramic shells for miniature systems applications," J. Micromech. Microeng.; v12 no. 3 (2002) 198-203.
33 KA Peterson, SB Rohde, KB Pfeifer, TS Turner, "Novel LTCC fabrication techniques applied to a rolled ion mobility spectrometer," Electrochem. Soc. Series; v2003 no.27 156-171.
34 JG Lee, HW Shin, ED Case, P Kwon, "The fabrication of smooth, sub-millimeter open channels and internal channels in ceramics and ceramic composites without machining," J. Mat. Sci. Lett.; 2001, v20 no.2 (2001) 107-9.
35 DG Plumlee, Y Morales, B Cheek, AJ Paris, HA Ackler, WB Knowlton, AJ Moll, "Pressure Sensors built in Low Temperature Co-Fired Ceramic Materials," Presented at IMAPS ATW Packaging of MEMS and Releate Micro Integrated Nano Systems, September 6-8, 2002, Denver.
36 JW Burdon, RF Huang, R.F., D Wilcox, NJ Naclerio, "Method for fabricating a multilayered structure and the structures formed by the method," U.S. Patent # 6,592,696, July 15, 2003.
37 A. Roosen, "Cold Low Pressure Lamination of LTCC's," Proc. SPIE – Int. Soc. Optic. Eng. (2002) v4931 (2002) 45-50.
38 DJ Miehls, FJ Martin, RG Pond, PS Fleischner, "Method of fabricating a multilayer electrical circuit structure," U.S. Patent #5,249,355, October 5, 1993.
39 EA Trickett, RC Assmus, "Ceramic monolithic structure having an internal cavity contained therein and a method of preparing the same," U.S. Patent # 4,806,295, February 21, 1989.
40 JH Alexander, "Method of making ceramic article with cavity using LTCC tape," U.S. Patent #5,601,673, February 11, 1997 .
41 JD Cawley, AH Heuer, WS Newman, "Method for constructing three dimensional bodies from laminations," U.S. Patent # 5,779,833, July 14, 1998 .
[42] J Van Tassel, CA Randall, "Potential for integration of electrophoretic deposition into electronic device manufacture; demonstrations using silver/palladium, J. Mat. Sci. 39 (2004) 867-879.
43 NT Nguyen and Z Wu, "Micromixers—a review," J. Micromech. Microeng. 15 (2005) R1-R6.
44 DJ Draeger, ED Case, "Engineering the surface texture and shape of channels in ceramic substrates," Mat. Sci. Eng. B97, (2003) 94-105.
45 MR Gongora-Rubio, MBA Fontes, Z Mendes da Rocha, EM Richter, L. Angnes, "LTCC manifold for heavy metal detection system in biomedical and environmental fluids," Sensors and Actuators B 103 (2004) 468-473.
46 JW Elam, D Routkevitch, PP Mardilovich, SM George, "Conformal coating on ultrahigh-aspect-ratio nanopores of anodic alumina by atomic layer deposition," Chem. Mater. 2003, 15, 3507-3517.
47 Benavides, GL, Galambos, PC, "Electro-microfluidic packaging," SAND2002-1941, unlimited release, June 2002, Sandia National Laboratories (http://www.ntis.gov/ordering.htm).
48 GL Benavides, PC Galambos, JA Emerson, KA Peterson, RK Giunta, DL Zamora, RD Watson, "Packaging of electro-microfluidic devices," US Patent No. 6,548,895, April 15, 2003.
49 P Galambos G Benavides, M Okandan, D Hetherington, "Precision alignment packaging for microsystems with multiple fluid connections," Proc: ASME IMECE, Nov. 11-16 (2001) New York, 1-8.
50 DM Tanner, NF Smith, DJ Bowman WP Eaton, KA Peterson, "First reliability test of a surface micromachined microengine using SHIMMeR," Proc SPIE 1997;3224 14.
51 E Amaya, "Designing with Heralock™ 2000 self-constrained LTCC tape," Technical Presentations, IMAPS ATW: Ceramic Applic. Microwave and Photonic Packaging, Providence, RI, May 2-3, 2002.
52 Patent pending.
53 K Patel, K Hukari, K Peterson, "Low-temperature cofired ceramic substrate technology for microfluidic systems: development of a high-temperature ceramic lyser for solubilizing spores," Conf. MicroScale BioSeparations Feb 13-17th 2005 New Orleans, LA.
54 SJ Kim, YG Lee, SK Yun, HY Lee, "Realization of High-Q Inductors using Wirebonding Technology", Proc. AP-ASIC, (1999) 13-16
55 L Harle LPB Katehi, "A horizontally integrated micromachined filter," IEEE MTT-S Digest, (2004) 437-440.
56 D Belavic, M Hrovat, M Pavlin, "Vertical thick-film resistors as load sensors," J. Eur. Ceram. Society 21 (2001) 1989-1992.
57 BY Ang, CK Chua, ZH Du, "Study of trapped material in rapid prototyping parts," Int. J. Adv. Manuf. Technol. (2000) 16:120-130.

Appendix 3. Macro-Meso-Microsystems Integration in LTCC

LTCC Microsystems and Microsystem Packaging and Integration Applications

K.A. Peterson, K.D. Patel, C.K. Ho, B.R. Rohrer, C.D. Nordquist, B.D. Wroblewski, K.B. Pfeifer
Sandia National Laboratories
P.O.B. 5800, MS 0959
Albuquerque, NM 87185-0959
Phone 505-845-8549
Email: peterska@sandia.gov

Abstract

Low Temperature Cofired Ceramic (LTCC) has proven to be an enabling medium for microsystem technologies, because of its desirable electrical, physical, and chemical properties coupled with its capability for rapid prototyping and scalable manufacturing of components. LTCC is viewed as an extension of hybrid microcircuits, and in that function it enables development, testing, and deployment of silicon microsystems. However, its versatility has allowed it to succeed as a microsystem medium in its own right, with applications in non-microelectronic meso-scale devices and in a range of sensor devices. Applications include silicon microfluidic 'chip-and-wire' systems and fluid grid array (FGA)/microfluidic multichip modules using embedded channels in LTCC, and cofired electro-mechanical systems with moving parts. Both the microfluidic and mechanical system applications are enabled by sacrificial volume materials (SVM), which serve to create and maintain cavities and separation gaps during the lamination and cofiring process. SVMs consisting of thermally fugitive or partially inert materials are easily incorporated. Screeding is an incorporation technique we describe that improves uniformity and eliminates processing steps. Recognizing the premium on devices that are cofired rather than assembled, we report on functional-as-released and functional-as-fired moving parts, including an impeller that has been exercised over thirty million cycles, and a cofired pressure sensor that requires only pressure source and electrical connections. Additional applications for cofired transparent windows, some as small as an optical fiber, are also described. The applications described help pave the way for widespread application of LTCC to biomedical, control, analysis, characterization, and radio frequency (RF) functions for macro-meso-microsystems.

Key Words: LTCC, microsystem, sacrificial, channel, microfluidic, pressure sensor, tube

1. Introduction

Microsystems present a vast array of capabilities, including electrical, radio-frequency electrical, optical, fluidic, and electro-mechanical phenomena, often implemented in what are known as micro-electro-mechanical systems (MEMS). Many of these systems involve silicon devices, many of which are fabricated by surface micromachining (SMM) techniques on layers that are stacked within several microns of the surface. They enable biological and life science analyses, optical switching and beam modification, wireless communication, and many developing applications. Frequently, the advantage is lost if they are not integrated in a way that preserves miniaturization. Low temperature cofired ceramic (LTCC) can meet many integration needs while bringing well-known advantages including high conductivity electrical traces, low dissipation factor dielectrics, inherent manufacturability, high temperature operation, chemical inertness, and versatility in integrating multiple interrelated devices in a variety of critical proximities, orientations, and environments. This integration can be accomplished with superior performance at a reasonable cost. Literature documents the appeal to ceramic sensor and system applications (macro-, meso-, and micro-). [1,2] In this paper we will discuss processing techniques we have used to generate new structures. These include the use of various sacrificial volume materials (SVM) to create moving parts, sensor cavities, microfluidic channels and suspended thick films, and the use of novel forming and fabrication techniques to obtain structures such as rolled tubes. We will then give examples of these structures in several applications where LTCC has been essential to microsystems and meso-scale-sensors. By tailoring processes to meet specific program needs, LTCC can interface to microsystem components at their tiny scale and present them in usable form to the outside world.

2. Background

LTCC is a well-known commercial technology based upon flexible tapes composed of glass and ceramic particles held together by an organic binder that can accommodate thick film and other traces as well as machining or deformation operations. Most of our work is done with various DuPont tapes (951C2, PX, AT, and 943). The tapes are collated, laminated, and then fired on a prescribed temperature profile to accomplish sintering to a monolithic piece. More specific details are addressed in a comprehensive review. [1]

LTCC technology continues to advance from its roots in thick film hybrid microcircuit technology. One of the most significant reasons for which it was established was to address the need for a single thickness of dielectric (resulting from a tape layer) to be sufficient to eliminate pinholes between layers that required multiple printed dielectric layers with thick film. Additionally, the serial nature of thick film hybrid microcircuits meant that technical difficulties on upper layers negated the value added to the lower layers, which were usually built up in laborious print-dry-fire cycles. Multiple prints of a dielectric paste worsened cumulative planarization problems for upper layers. Finally, attempts to cofire thick film dielectric and conductor layers produced undesirable interactions that do not occur using LTCC. Starting with embedded resistors and proceeding to other integral structures, the capability of LTCC is rapidly advancing.

More applications are using enclosed unfilled volumes in designs for sensors, microfluidic manifolds, actuators, and other microsystem applications. Different types of SVMs permit more unconventional structures to be built. The sacrificial elimination of these materials from the assembly may involve cofiring of completely thermally fugitive materials, or removal of inert-loaded materials following firing. They can also be used to transfer features to the unfired ceramic tape. These features may be conductors, resistors, or many other structures. An example of printing conductor lines to a SVM tape is shown in Figure 1. The ability to print to a material that essentially disappears enables one to make suspended thick film structures or micro tensile bars from thick films (see Figure 1b).

Volume-preserving techniques that are removable prior to firing consist of mandrels, inserts, forms, 'lost wax,' and others. Dry-transfer of thick films, or lamination of thin films can even be accomplished for additional capabilities such as fine features. [3] Thermally fugitive materials can affect the finished product according to their behavior with respect to compliance, thermal expansion, softening, melting, boiling, condensation, pyrolysis, sublimation, exothermic and endothermic reactions, combustion, delamination, and shrinkage.

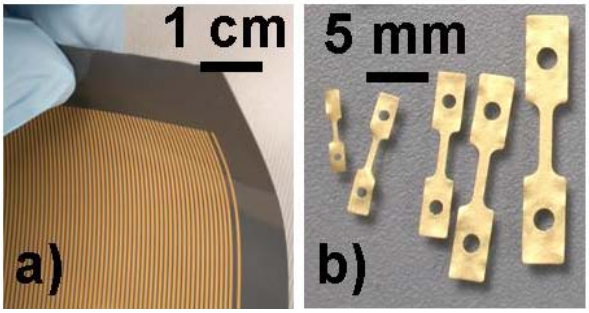

Figure 1. a) Features (in this case, thick film conductors) are printed on an SVM tape which disappears during firing. b) Thick film tensile test samples remain intact after SVM is fired.

3. Processes

One of the processes we have used does not seek to avoid latent damage in the form of deformation of unfired tapes, but turns it into a feature. Cases where one surface is permitted to have texture in the form of mounds over channels are very simple to fabricate. Latent damage need not be considered a defect if it is healed in lamination and cofiring. In fact, the most significant discontinuity—two completely unattached surfaces—is routinely overcome as the most basic principle of this multilayer technology. These separate layers must be successfully laminated and sintered to provide function and avoid extreme stress concentrators. Successful lamination and firing of deformed areas can be trivial by comparison.

3.1. Lamination Practices

Largely due to the ease of use, most of our lamination is performed in an isostatic laminator at 20.7 MPa (3000 psi) and 68°C. In an isostatic laminator, parts are typically laminated by the isostatic application of pressure on a free surface, protected by a flexible membrane on one side of the part and a rigid form on the other side of the part. Standard practice is to 'vacuum-bag' a part along with any required mandrels or forms for protection against the aqueous hydraulic fluid. Different designs have different lamination requirements. We have laminated certain parts with no rigid form at all (the pressure acts on both sides simultaneously). However, rigid plates can be used on both sides of the part to essentially convert the isostatic pressure into uniaxial force on the part. For instance, punched, unprotected open volumes in tape are susceptible to crushing. Lamination with a top plate

above a channel can preserve walls and overall surface flatness but, because material around surface microfluidic ports is free to translate laterally, the lamination pressure in such an area can be less than desired. Lamination without a top plate can result in rounding of surface port edges by deformation, which is not always detrimental and can, in fact, be exploited as a feature. Variations in lamination pressure are reported to have resulted in density variations which, in turn, can lead to variations in shrinkage tolerance and cracking from nonuniformities in stress. Sideways extrusion of perimeter material during lamination is mitigated when there is no top plate and the pressure also acts on the perimeter of the part. An example of this is sketched in Figure 2.

Partial area protection during lamination with a top plate that does not extend to the perimeter of the part combines the best aspects of two lamination techniques. This perimeter may be a cut-off zone or may remain as a functional part of the sample. In some cases, the top plate is small and covers only a small portion of the part. Imprints can be designed to be benign. Overlying LTCC layers have also been used to preserve channels when slight topography is not considered to be a flaw. When the overlying material is of sufficient thickness, it can act as a plate in protecting a small channel.

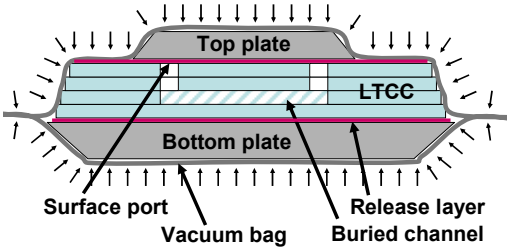

Figure 2. Partial protection of unfilled channels and ports allows isostatic pressure to mitigate lateral extrusion during lamination.

3.2. SVMs

Presently, the goal of using SVMs as an addition to the suite of materials used in familiar thick film and dielectric tape techniques is being realized to create enclosed unfilled volumes for channels and cavities. Not only can these materials be printed, they can be written directly, stenciled, screeded, and applied in a variety of ways. We have also obtained setter pastes and mixed pastes which consist of a carbon paste mixed with a setter paste. [4] Several prototypes have been fabricated by serial lamination for proof of concept when individual filled layers were hard to handle without damage. Yet only when individual tape layers can be handled with filled microfluidic channels does the technique take full advantage of existing practice and avoid the prior inefficiencies of fabrication associated with serial processing.

Channels can be incorporated by standard punching and laminating. They can also be punched into tape layers which are then filled with SVM. Another technique is to pattern SVM by a variety of techniques and permit the lamination step to deform the tapes to a net shape which is functional and easy to make. Figure 3a shows an example of closely spaced channels fabricated by filling pre-punched features. Figure 3b shows a comparable result fabricated by laminating intact tape layers between staggered arrays of SVM channels. The resulting

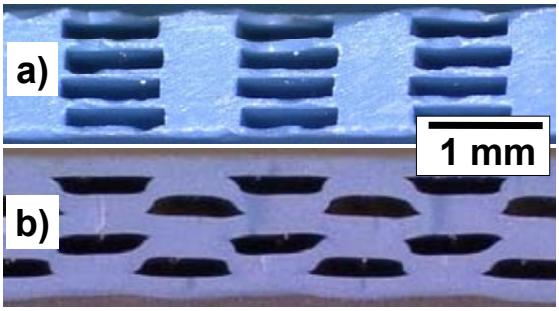

Figure 3. a) Channels that are predefined (punched) and SVM-filled prior to lamination are compared to b) channels formed by patterned SVM during lamination.

wall shape in the latter case indicates a sharing of deformation between the SVM and the ceramic tape. The use of SVM permits large arrays of channels to be fabricated, as in the case of Figure 4a, where a 7.62 cm (3") long, densely-channeled structure with an electrode in each channel has been fabricated in a round cross section for a high flow fluid analysis device. Figure 4b shows a magnified view.

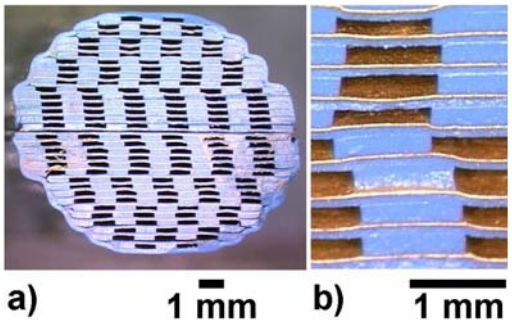

Figure 4. a) A dense array of channels in a circular cylinder prototype includes an electrode running the length of every channel. b) A close-up view shows the manually-aligned channels and walls.

Finally, it is possible to increase the amount of fluid processed by removing the walls altogether as shown in the device of Figure 5. Figure 5a shows the densely-electroded surface which occurs on the 'floor' and 'ceiling' of every channel. The close-up view in Figure 5b shows these traces as well as the test points that are exposed by sawing multiple parts from a 6.63 cm (2.61") square blank (7.6 cm (3") unfired dimension) in which they are fabricated. Each channel is nominally 11.4 mm (0.45") wide, 250 μm (0.010") tall and runs the entire length of the part. Initial prototypes were interconnected using these emergent electrode ends to provide a single series circuit of electrodes running through all channels in the device.

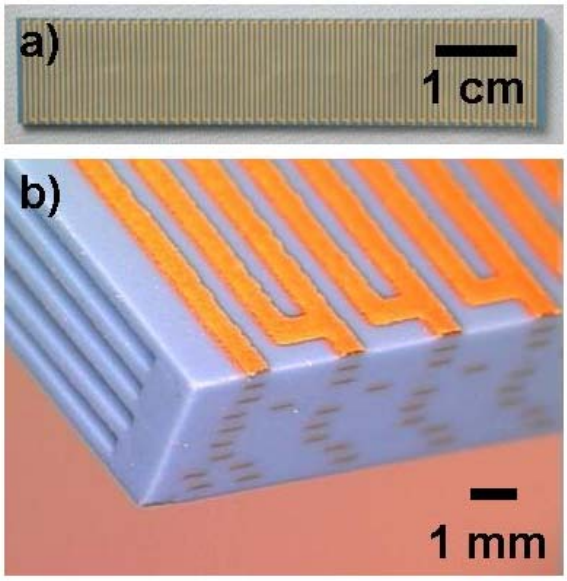

Figure 5. The device shown in Figure 4 is further improved by increasing the electrode surface area and removing the intermediate channel walls. a) A serpentine electrode pattern on a finished part is shown. B) The test points for electrodes are visible on the side following sawing to size.

A commercial setter sheet that turns to powder upon burnout has been used to maintain separation between surfaces where the influence of gravity during firing would have otherwise resulted in sagging floors.

3.3. Application by Screeding

Conductive via-fill for interlayer connections is commonly performed using a stencil and a vacuum 'hold-down' through a porous plate and a porous release material. The vacuum doubles as a mechanism to assist the filling of vine vias with paste. Microfluidic vias and channels can be filled in much the same way. Increasingly, tape layers are available that can be perforated with a punchable backing still in-place. We use a tape with a punchable backing as a form and a blade or squeegee to fill vias and channels with SVM paste. We refer to this as screeding. This reduces the number of processing steps by using the punchable backing as the artwork/stencil layer itself rather than peeling it off and using a screen or stencil. This is particularly useful when microfluidic channel vias are larger than microelectronic vias because microfluidic ports and channels are filled with a SVM to a wet height equal to the thickness of the tape and the backing. The thickness of the backing helps add thickness in view of the shrinkage of the carbon paste (Harmonics Paste-CARB-1 High Viscosity) [4] upon drying. Multiple screeding passes may also be used.

An example of screeding of open ports in LTCC for a microfluidic pattern to match the backside of a silicon microfluidic die is shown in Figure 6. The streaking shown atop the vendor's polymer backing in Figure 6a is an artifact of the squeegee and the fine size of the carbon particles. This is analogous to the smear that remains on a thick film screen or stencil under certain circumstances. The same properties make cleanup of the paste more challenging than with other thick film pastes but this is an acceptable inconvenience.

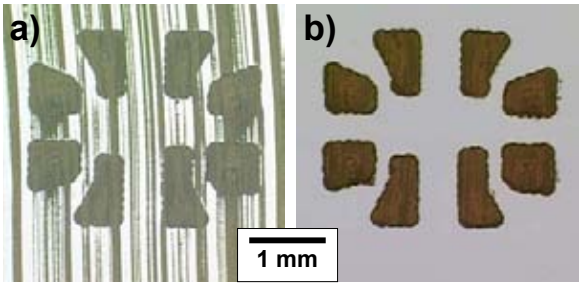

Figure 6. Screeding carbon paste onto unfired tape masked by a punchable backing is shown a) with backing intact and b) with backing removed.

The structure in Figure 6b results when this backing is peeled off. The slight bleeding of carbon between backing and tape, shown at edges in Figure 6b, arises from separation of the backing from the tape at the deformed edge of a punched perforation. We have experimented with re-lamination of these layers, but prefer to use squeegee pressure to seal the backing to the tape. The bleeding can largely be eliminated as shown in the more complicated screeded device of Figure 7. Punching with the backing facing the punch, rather than the die, is also helpful in minimizing the separation. In addition, screeding ceramic tape on a polymer film release layer backing that is stretched and held in tension until carbon paste dries has significantly enhanced yield and handling

durability of filled channels. This permits the release layer to detach itself from the tape in a shear mode. While long channels can be filled successfully, the tape handling results are better when a channel on a single layer can be stitched to run instead between two available layers with overlapping segment ends. This avoids long slits in the tape and tethers the smaller open areas to reduce its tendency to deform or break in handling. This channel geometry is more than tolerable for many applications and actually ideal for others such as micromixers. [5]

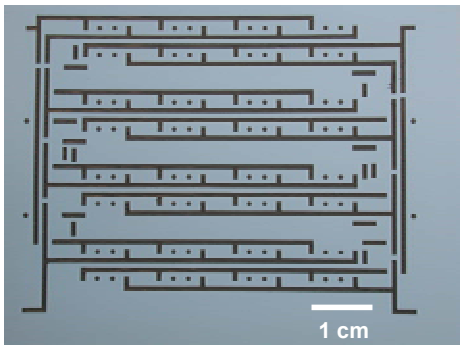

Figure 7. Screeding is used for a microfluidic module to preserve channels during lamination.

4. Applications

4.1. Pneumatic Chip and Wire 'Postage Stamp'

Surface micromachined (SMM) fluidic microelectromechanical systems (MEMS) valves provide fluidic control at low flow rates and are orders of magnitude smaller than solenoid-actuated valves. While the valves themselves are most easily controlled in a binary fashion, arraying a number of them allows more graded control and a higher maximum flow rate. A demonstrative board was fabricated to establish a capability to address SMM polysilicon valves having polysilicon actuators.

The access to the electrically-addressed, thermally actuated valves within the silicon is through deep reactive ion etched (DRIE, also known as Bosch-etched) ports of 200 μm (0.008") diameter on approximately 1 mm (0.040") centers. The 3 mm (0.129") by 6 mm (0.236") MEMS chip contains 11 such features and the demonstration is capable of addressing two of these on a board of dimension 20.4 mm (0.80") X 16.4 mm (0.65"). With LTCC, the ability to properly route each of the 32 traces to control 16 valves is easily integrated with the ability to route proper pneumatic input / output lines on the backside of the die. Figure 8 shows an example of such a device. One blind cavity is provided in the LTCC behind a pressure sensor based on a Wheatstone Bridge on the silicon MEMS die. Two other cavities are routed to independent valves, both pressurized from the back, controlling the output port that is common to the front-side of the die. This completed board is shown in Figure 8a with MEMS die attached and in Figure 8b as fabricated in seven layers. Two tubes are simply glued into ports in the side of the board that are revealed when the part is singulated from the others. Thick film signal lines are visible at the bottom of certain ports in Figure 8b. This was done to reduce the layer count and simplify fabrication. Although these electrodes are not required to be exposed, they do no harm since these are pneumatic channels.

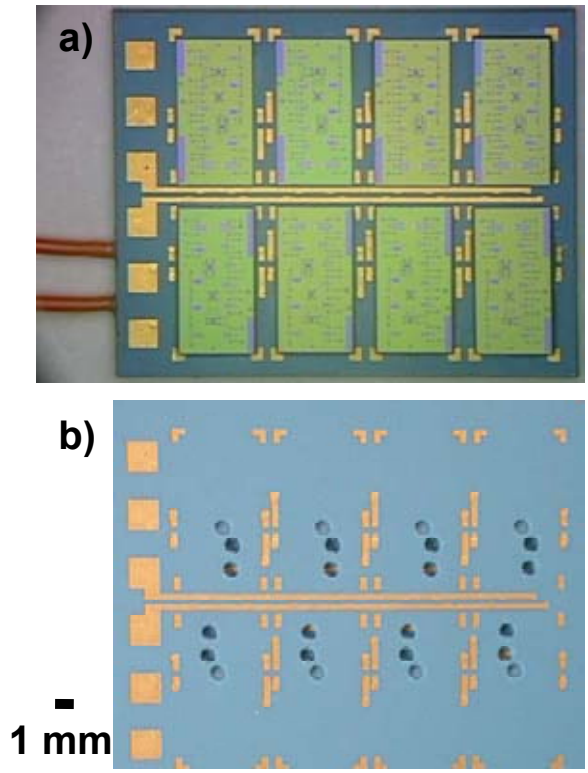

Figure 8. a) Silicon SMM electro-microfluidic die are mounted to a 'chip and wire' microfluidic LTCC board. b) The LTCC board is shown as-fabricated and cut to size.

As with other such devices, the die attach process is critical. A perfect microfluidic board is useless without die attach that provides continuity and isolation for the MEMS die. At times the feature spacing on the front side design of the MEMS die is translated to the backside, resulting in closely spaced ports, increasing the necessity for a continuous adhesive layer between the die and the LTCC to prevent leakage between the ports. Die attach issues can be illustrated with glass 'dummy die.' Figure 9a shows a die attach defect (air pocket at left) that

results in extra dead volume on a port connected to one of the channels. Figure 9b shows a similar defect on the blind cavity that is connected to the pressure sensor on the die (far right). Figure 9c shows die attach that establishes microfluidic continuity and isolation. Figure 9d shows another complex die attachment where the minimum wall is just 178 μm (0.007") wide. These fine wall areas have been sealed for proper function. Other techniques, including field-assisted bonding, eutectic bonding, or inorganic adhesives could also be considered.

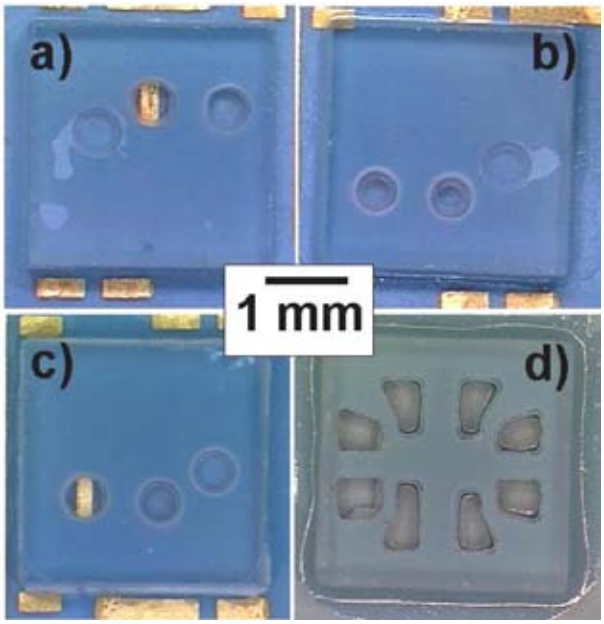

Figure 9. Adhesive attach of glass 'dummy die' helps to characterize fluidic continuity and isolation. Air pocket flaws are shown in a) and b). Microfluidic die attach shown in c) and d) is adequate for proper function.

4.2. Modular Microfluidic Fluid Grid Array

Interposers have been used in a lab environment where a large variety of silicon microfluidic research designs is available. An interposer can quickly adapt microfluidic and microelectronic connections for testing in a standard package. We have fabricated several thin microfluidic manifolds to work in conjunction with a zero-insertion force (ZIF) socket for a standard dual in-line package (DIP) that has been customized with eight standard through-holes. O-rings in glands fabricated in the LTCC board withstand 689 kPa (100 psi) without any problem. The maximum use pressure and ultimate pressure limit of this seal have yet to be determined. This microfluidic manifold has also been made more producible by screeding and stitching channels together on multiple layers. The "parts farm" we referred to in earlier work has been prototyped using combinations of interposers with fluidic grid array (FGA) patterns as shown in Figure 10. Interposers have been designed with annular soldered thick film seal rings that provide mechanical, electrical, and fluidic connections. These interposers have eight annular ports at the ends of four distinct microfluidic channels. Interposers about 1 cm on a side and 635 μm

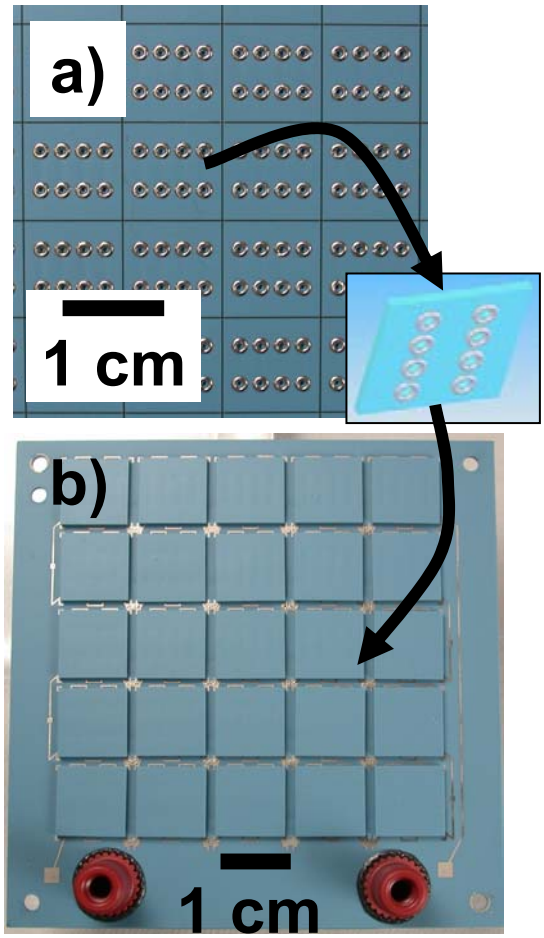

Figure 10. a) Interposers with 4 internal channels are 'tinned' with solder before laser-scribing. b) Interposers are mounted to a board containing a microfluidic continuity loop and an electrical continuity loop.

(0.025") thick are shown in Figure 10a following solder printing and reflowing to the underlying thick film trace. These parts were laser scribed following solder reflow. Laser scribing allows singulation of individual interposers for subsequent mounting to the microfluidic board. Figure 10b shows a 635 μm (0.025") thick microfluidic board fabricated with buried channels as shown in Figure 7. The channels are 762 μm (0.030") wide and the walls are

also 762 μm (0.030") wide. This size has been selected because it is easy to do, but much smaller dimensions are possible.

This part has been fabricated both with and without sacrificial material inserts, but the surface deformation that occurs without inserts is eliminated by screeding. Screeding is useful because it fills the channels and puts the sacrificial material in contact with the channel side wall. The solder used in this case was a 63Sn/37Pb solder applied by screen printing. Following reflow, the flux can be thoroughly cleaned. When both board and interposers are soldered and cleaned, it is straightforward to place the components using a simple laser-machined template. The template keeps the loose part from 'walking' too far, and when the solder is molten it pulls the component back to the center of the opening in the frame array. This board also has an electrical continuity loop that requires that every joint make electrical contact for the loop to be good. Although all continuity loops have tested good, test points also exist in the margins between interposers. This board had two joints that leak but the balance of the part was good on the first try. Work is proceeding on improving the process of making the joints.

The board shown in Figure 11 is more complicated and capable. It contains eight input ports, each one of which addresses only a single port position on each interposer. It was also fabricated using screeding and multiple layer channel stitching and was made using internal layers shown in Figure 7. With this capability to uniquely address

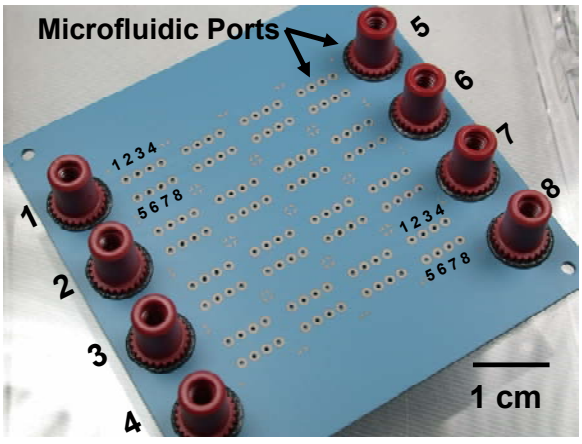

Figure 11. A maze of internal channels in a thin LTCC board connects specific macro ports to their associated microfluidic surface ports.

each port, the board is still only 1 mm (0.040") thick, and the restriction in an attached MEMS device would still be the dominant restriction. This mounting technique can also be used for a modular approach to a system which would include gas and fluid handling, pressure sensors, smart channels, silicon MEMS, RF modules, chemical separators, microelectronics and more.

A device was fractured in order to examine the joint. The image in Figure 12 shows that the joint was made with a stand-off distance sufficient to help mitigate future temperature cycling. Solder will not be the appropriate medium for all applications, but is functional for many tests.

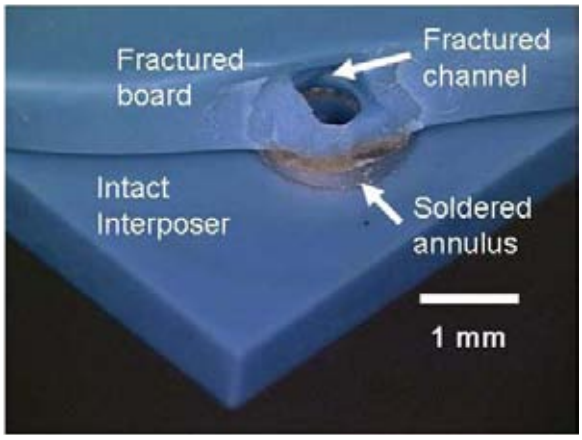

Figure 12. An assembled microfluidic board was fractured to reveal one of eight joints that connect it to a modular microfluidic interposer.

4.3. Windowed channels

Many microfluidic applications would benefit from the convenience, flexibility and properties of LTCC, but also have requirements for transparency. We have addressed this with windowed channels. We have previously highlighted cofired windowed channels made by using SVM. In Figure 13 we show three channels that have been punched in LTCC. Figure 13a shows a crossed channel in the center layer of 5 total layers. The channels were punched and the 3 mm (0.125") diameter 250 μm (0.010") thick sapphire window was collated into place. A matching hole in the layer on either side of the channel captures this window, and the outermost layer of tape is undersized slightly—also to capture the window. Isostatic lamination was performed from both sides simultaneously. The nibbled appearance of the channels was somewhat coarse on this prototype, and was exaggerated by lamination. Each leg of the channel is connected to a glued-on pressure port. Each of these devices is free of leaks, and Figure 13b shows a time exposure of a fluid solution with fluorescent beads moving through the upper two channels without affecting the lower two. Figure 13c shows a single sided device, with channels that do not cross the seam between the

window and the tape but are routed to the interior within the perimeter of the window. Finally, Figure 13d shows a device with a window on each side which was fabricated by screeding a carbon SVM paste into the punched channels and ports. Windows such as these will appeal to those applications where glass circuits have been used to perform optical analysis using dyes or fluorescence counting.

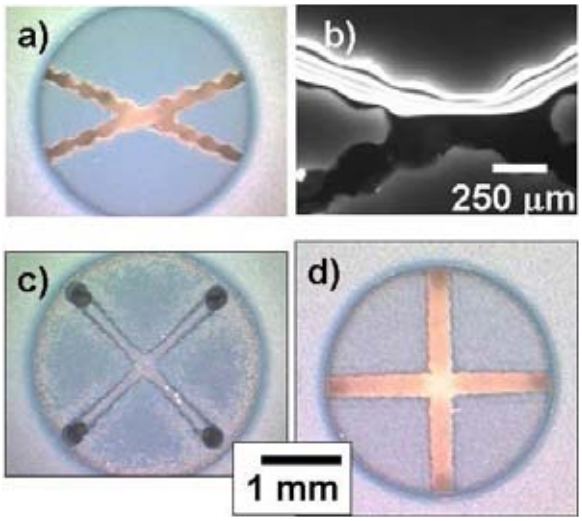

Figure 13. a) A cross-channel layer of LTCC, sandwiched between sapphire windows, is used for b) a time-exposure photograph of fluorescent particles in a flowing fluid. c) A single window covers channels that are routed to the interior of the board. d) An LTCC cross-channel, windowed on both surfaces, was fabricated using SVM.

4.4. Moving Parts

Previous work has highlighted techniques for making moving parts. A key component of this capability is the use of a commercial inert-loaded SVM tape to maintain separation between elements that can not be permitted to attach to one another (Harmonics CPL-AL-1, SPS-2ZR-1). Furthermore, these layers can be coated with carbon SVM in order to avoid imprinting the texture of the setter tape and powdered setter into the glass-ceramic tape. We have also obtained alumina setter paste, and carbon loaded alumina setter paste for thin, fluid-dispensed application, in addition to alumina setter sheets loaded with carbon [4]. One of the structures we previously reported was cantilevered thick film electrical switch structures. Removal of the setter from these experimental parts was as easy as tilting the substrate.

Another of the structures that we have fabricated is the impeller represented in Figure 14a. While smaller impellers have been fabricated, this one was operated in a simple LTCC pneumatic manifold where 34.5 kPa (5 psi) supplied 6 lpm flow to rotate the wheel. This relatively high flow rate was in part due to the fact that the manifold outlet at the wheel was open to the atmosphere. Operating at a speed of only 190 rpm, this wheel accumulated a total of 30 million revolutions before a pneumatic line shut-down dictated that it be sacrificed for SEM examination. A cross-sectional view of the fractured wheel's inner bearing surface is shown at left in Figure 14b. The bearing surface at the right in Figure 14b is shown facing forward in the fractured wheel of Figure 14c. The bright appearance of this edge is due not only to orientation to the electron detector, but to charging due to the debris shown. It is quite possible that this constitutes wear debris. More examination is needed to determine what amount of this debris is due to wear and what is due to fabrication in proximity to the inert powder. There are no circumferential wear tracks on the bearing surfaces of the wheel or the hub, and there was no performance degradation observed. These observations consisted of visual determinations of uniformity and speed. Figure 14d shows a comparable bearing surface for an impeller that has not been rotated.

Because the multi-purpose manifold was not attached, there were two brief mishaps during the course of the rotation where the manifold became slightly misaligned, and that situation was corrected. Work is ongoing to determine the durability of such a wheel. Work also continues in order to miniaturize the wheels further and to assess the effects of dimensional tolerance.

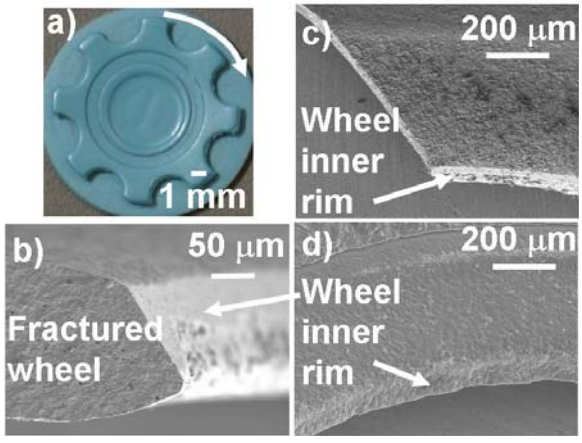

Figure 14. a) A cofired freely-rotating impeller (optical image) has been operated pneumatically. b) An SEM cross-sectional image of the fractured wheel after 30 million revolutions reveals debris. c) Debris is also visible on another view of the same bearing surface (SEM photo). d) A comparable bearing surface that has seen no revolutions shows less debris (SEM photo).

4.5. Cofired Pressure Sensor

A cofired enclosed volume with a membrane suitable for deflection by pressure has been equipped with a thick film diaphragm strain gage which makes a Wheatstone Bridge configuration. Except for the addition of the thick film (DuPont 5739) this is the same type of cavity previously reported for use with commercial foil strain gauges. Since the glue joint is frequently the failure location for such strain gauges, an important failure mode may be averted by thick film gauges. The pattern has been adapted from others already commercially available (Omega SG-13/200-DG11). [6] On a properly sized diaphragm, two resistive legs are in tension and two are in compression. The cavity has been created a number of ways, but the thick films are conventionally screen printed to about 10 μm (0.0004") thickness. Figure 15a shows a schematic of a collation technique for fabrication of a sensor with a single membrane

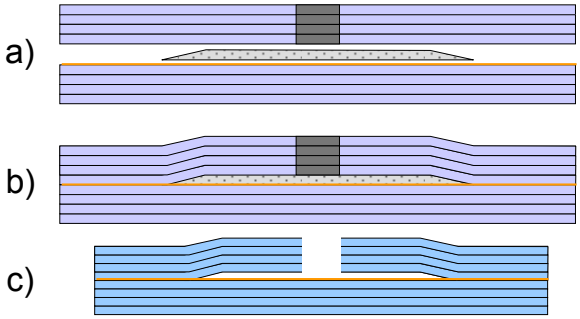

Figure 15. Fabrication sequence for a cofired pressure sensor. a) Collation of membrane layers including a thick film strain gage and an SVM. b) Formation of a cavity during lamination. c) Cofiring and elimination of SVM material result in a pressure chamber adjacent to the membrane.

opposite the side with a pressure port. A thick film strain gage is printed and included at the floor level of the sensor. As indicated in Figure 15a, many of our membranes have been fabricated from multiple layers, although we have also made single level membranes. Over this, SVMs are used to create a cavity upon lamination. Carbon (Harmonics TCS-CARB-1) and inert material loaded tape (Harmonics CPL-AL-1, SPS-2ZR-1), as well as composite compositions and structures, have been used for the volume definition during lamination shown in Figure 15b. The unfired tape is laminated to seal the device at the perimeter, and the port remains open. Hermetic thick film traces emerge from the cavity for external lead attachment. Upon firing and removal of any setter material as indicated in Figure 15c, a pressure sensor is completed. When a setter SVM layer is used, it is blown out as a powder after firing. The addition of a pressure port and electrical leads equips this cofired structure to sense pressure. The thick film bridge circuitry and a commercial power source and readout were used to collect data. [6] Figure 16 shows meter counts from an early suite of

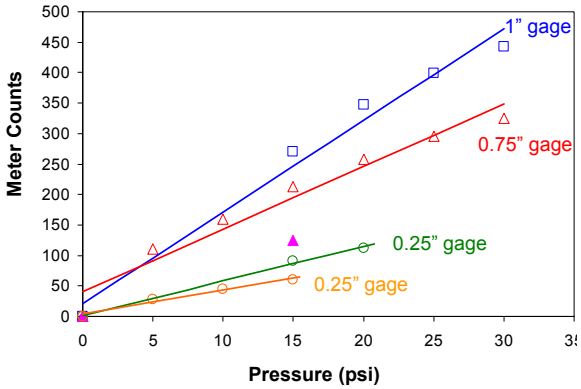

Figure 16. Data from multiple sizes of the earliest cofired pressure sensors indicate a response.

devices, ranging from 25.4 mm (1") diameter to 6.35 mm (0.25") diameter. A straight line has been fitted to the first rising pressure curve data.

In hindsight, these devices were crudely ported, and excessive fitting size and excessive glue interfered with diaphragm motion and led to hysteresis and instability. The 25.4 mm (1") diameter part was tested to failure at 276 kPa (40 psi), and the cofired strain gauge on the floor of the cavity, only visible after fracture, is shown in Figure 17a. The ultimate pressure depends upon diameter and thickness, and membrane diameters of 19 mm (0.75") have been used up to 689 kPa (100 psi). Upon proof of concept, we obtained ports that interfere less with the diaphragm deflection. We also used SVM channels to access these chambers from a remote port (Figure 17b), which is more likely for incorporating pressure sensors into boards.

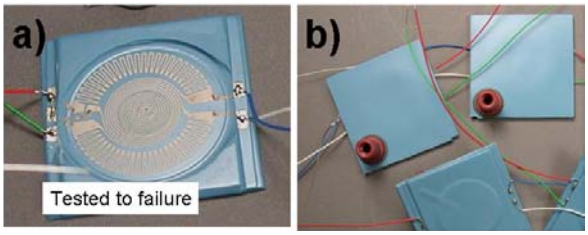

Figure 17. a) A thick film conductor strain gage pattern is visible on the diaphragm of a cofired pressure sensor following testing to failure. b) Ports attached to channels adjacent to the sensor membrane are less disruptive to the chamber.

Presently, the resistance of metallic thick film paths is only changing 0.01% at maximum test pressure. The plot in Figure 18 was constructed by fitting a straight line to points generated during several pressure cycle measurements on a 19 mm (0.75") diameter sensor. The resistance values of the

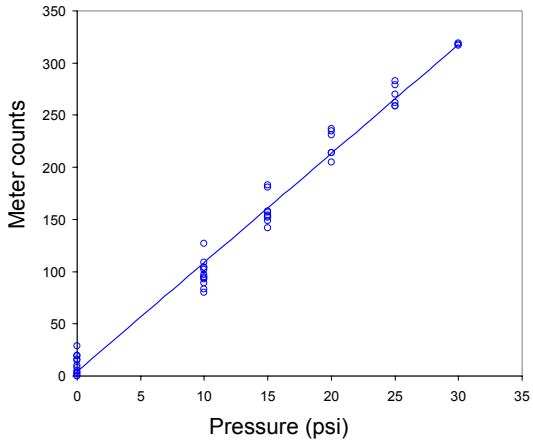

Figure 18. Several hysteresis loops' data plotted as a scatter plot with a linear fit.

four legs of the bridge were between 56 and 70 ohms. The output voltage of the bridge at 30psi was 14.8 mV. In order to obtain a measurable output, a significant current driven by 7.5-10 V dc was used. It caused heating of the structure to about 60°C. The temperature of the commercial foil gage, operated at the same voltage, rose to 40°C (200 ohm resistance per leg).

Thick films have been both printed on the surface of the membrane and embedded into inner layers of membranes. Work is proceeding on the use of a piezoresistive thick film (DuPont 3554) on the membrane layer as shown in Figure 19a. In addition, piezoelectric networks buried and cofired into diaphragms have shown response when subjected to loading on a vacuum plate. Figure 19b shows the imprint on the surface of one such embedded device.

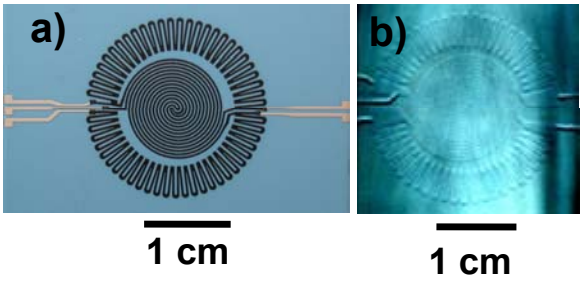

Figure 19. a) Piezoresistive strain gages printed in cofired pressure sensors and b) buried in cofired membranes (oblique lighting) respond to pressure.

Other LTCC pressure sensors have been summarized and reported with surface and buried piezoresistive elements. [7] Cantilevered strip resistors cofired on LTCC do respond in the anticipated fashion. Such a sample was subjected to flexing that put the cofired piezoresistor film in tension and compression, changing the resistance by a substantial amount, as shown in Figure 20. The microstrain has not yet been quantified for these parts. Cofired piezoresistive sensors have been fabricated and will be characterized.

A differential pressure sensor structure, with ported access to both sides of a membrane, has also been constructed as shown by a cross-section in Figure 21. The surface piezoresistors also respond to mechanical force applied to the surface as also described elsewhere. [8]

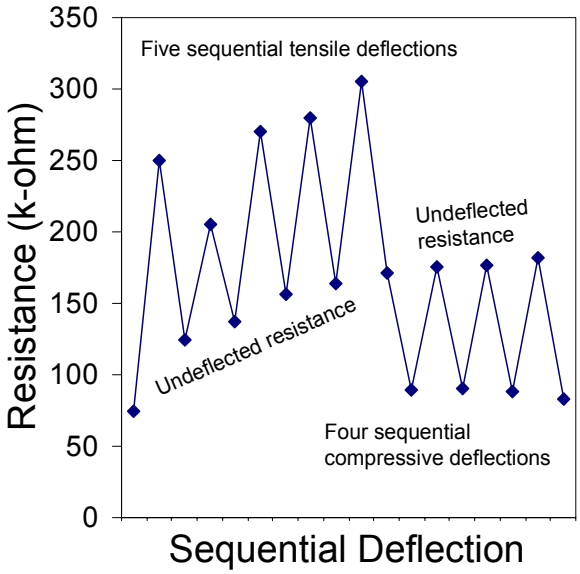

Figure 20. Sequential tensile and compressive deflection of cofired piezoelectric resistors on LTCC strips shows promising response.

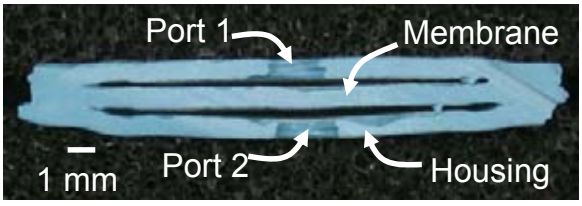

Figure 21. A prototype differential pressure sensor was cross-sectioned to show its structure.

4.6. RF Components

The sacrificial layer will enable the fabrication of patch antennas elevated above the

substrate, which may increase the efficiency, directivity, or other radiation parameters over those of a simple patch antenna. This approach has been described for microfabricated antennas [9, 10], but not for low-cost LTCC antennas. We are currently completing a design study based on the square microstrip patch antenna model shown in Figure 22. The 5 mm (0.2") x 7.62 mm (0.3") patch will be suspended between 250 µm (0.01)" and 1.27 mm (0.05") above the substrate to achieve the best antenna properties. This technology can also be used to realize more complex antennas such as planar-inverted F antennas (PIFA) or other compact antennas for direct fabrication on the LTCC substrate with high efficiency.

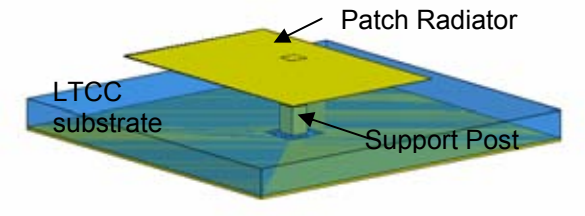

Figure 22. Three-dimensional model of the elevated microstrip patch antenna.

The sacrificial layer technology can also be used to fabricate high-Q cavity resonators to realize narrowband low-loss filters embedded in the LTCC substrate similar to those reported in silicon and other technologies [11]. These high-Q cavities should have Q-factors as high as 400, compared with 100 for a typical microstrip resonator. Fabrication challenges for these components include removing the sacrificial material from the enclosed cavities, maintaining the dimensional integrity of the cavity, and mitigation of cracking of the cavity at corners.

Another key RF element enabled by this sacrificial volume technology is the inverted microstrip, shown schematically in Figure 23. Compared to the traditional microstrip or coplanar waveguides, inverted microstrip will have a lower loss and lower dispersion because most of the electrical field is supported by air rather than in the dielectric, allowing a wider metal trace for a given impedance and reduced dielectric loss. This will enable lower-loss and higher-frequency distributed circuits such as filters and couplers than can be realized in baseline LTCC technology without the sacrificial layers.

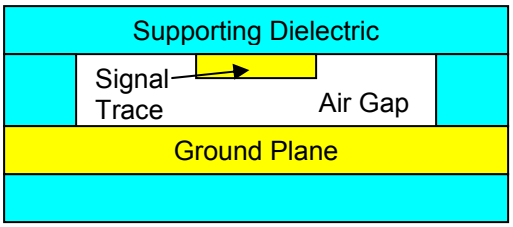

Figure 23. Cross-sectional conceptual view of inverted microstrip using sacrificial material in LTCC.

4.7. Rolled Structures

We have previously demonstrated rolled structures that can incorporate internal, external, and buried functional features. [12,13] These rolled structures perform reliably with enhanced functionality. At this point we have rolled hundreds of tubular structures, supporting applications such as micro ion mobility spectrometer (µIMS) drift tubes [14], smart channel prototypes [15], compact heater/sensors, and accessories to optical fiber devices, as shown in Figure 24.

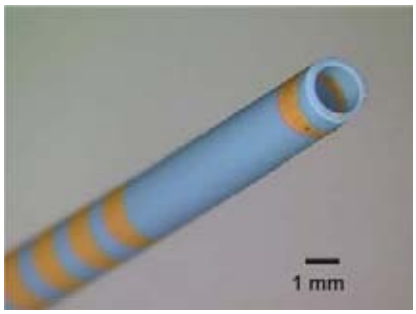

Figure 24. Fine tubes have been fabricated for optical fiber applications.

4.7.1. Micro Ion Mobility Spectrometer (µIMS)

An ion mobility spectrometer functions by ionizing chemical species and using an applied electric field to move the ionized species in a counter flowing gas, thus measuring the species' charge to collision cross section ratio. The tube consists of a series of rings which establish an electrical field (potential gradient) along the inside of the tube. A µIMS drift tube is shown in Figure 25.

Also visible are the resistors on the exterior of the tube which comprise the voltage dividers. There are 86 interior electrodes connected to a reference voltage divider and a main voltage divider (consisting of a total of 162 cofired thick film resistors). The rings not connected to the voltage divider are connected to other components or are

present to provide consistent metal loading. Although these resistors are on the curved surface of the tube, they were laser trimmed to a nominal precision of 1%.

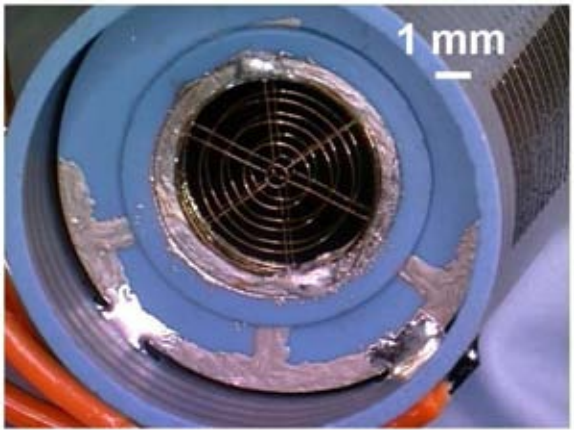

Figure 25. An LTCC washer with soldered LIGA grids is soldered to interior electrodes of an LTCC μIMS drift tube.

This rolled tube is printed, dried, rolled, and fired and becomes a single piece. The LIGA grids which make up the gating structure have been soldered to an LTCC washer which is in turn soldered to internal electrodes in the bore of the μIMS (see Figure 25). The image of the grids in Figure 25 is not blurred; rather, there are two grids 0.75 mm (0.030") apart. One side of the washer is attached electrically to one grid and its corresponding electrode while the other side of the washer is attached to the second grid and the next electrode in the chain. Thus, each washer is held in the tube by four solder joints which are mechanically and electrically critical--two on each side of the washer. The rolled LTCC drift tube has improved the μIMS device performance due to its hermeticity, inertness, high temperature operation (100°C) and manufacturability. For example, in a conventional stacked IMS there are many places where chemical species can be trapped for indeterminate periods of time resulting in spreading of the pulse and a slow chemical recovery of the tube to a transient chemical concentration change. We have observed significant improvement in the time response of the tube to chemical changes. We believe this improvement is due to the uniformity and smooth nature of the inside of the tube as compared to the conventional "stacked" construction approach. The tube can also be heated above 100°C to effect cleaning, as there are no organic materials remaining in the construct of the drift tube after assembly.

This approach to the development of IMS drift tubes has led to better performance of the tube from a chemical response perspective and a simpler manufacturing scheme. Previously, we have reported on IMS "stacked" tubes (Version 1, 6 mm inner diameter) that require 109 individual parts to implement including 55 handmade electrical connections to a circuit board. This rolled technique reduces that part count to 7 with less than 10 electrical connections depending on the specific configuration. [16,17]

Conclusions

We have discussed processing techniques we have used to accomplish particular structures. These include the use of various sacrificial volume materials (SVM) to create structures such as moving parts, sensor cavities, microfluidic channels, and suspended thick films. We have also used forming and fabrication techniques to obtain structures such as rolled tubes. We have given examples of these structures in several applications where LTCC has been essential to microsystems and meso-scale-sensors. By tailoring processes to meet specific program needs, LTCC can meet microsystem components at their tiny scale and present them in usable form to the outside world. We have shown this for highly-electroded (closely spaced) high flow fluid analysis, microfluidic chip and wire manifolds, and interposer manifolds that are ideal for testing silicon MEMS die. We have shown promising early results for cofired, scalable pressure sensors. Windows in microfluidic circuits will greatly increase the acceptability in life sciences analytical applications. Radio frequency applications such as patch antennas and inverted microstrip are feasible in view of success with high aspect ratio channels. Finally, rolled tubes are reaching maturity and are ready for commercialization for devices such as the rolled IMS drift tube.

5. Acknowledgements

The authors would like to thank Timothy Turner, Richard Sanchez, Dennis De Smet, Conrad James, and Gary Zender for technical contributions that made this work possible.

References

[1] M.R. Gongora-Rubio, P. Espinoza-Vallejos, L. Sola-Laguna, J.J. Santiago-Aviles, "Overview of low temperature co-fired ceramics tape technology for meso-system technology," Sensors and Actuators A 89 (2001) 222-241.

[2[L.J. Golonka, “New application of LTCC technology,” Proc. 28th Int. Spring Seminar on Electronics Technology, (2005) 148-152.
[3] J Van Tassel, CA Randall, “Potential for integration of electrophoretic deposition into electronic device manufacture; demonstrations using silver/palladium, J. Mat. Sci. 39 (2004) 867-879.
[4] http://www.harmonicsmaterials.com/
[5] G. Ostromecki, T. Zawada, L.J. Golonka, “Fluidic micromixer made in LTCC technology—preliminary results,” Proc. 28th Int. Spring Seminar on Electronics Technology, (2005) 352-357.
[6] Omega Engineering, “The Pressure Strain and Force Handbook,” pp.E17-E30.
[7] L.J. Golonka, A. Dziedzic, H. Roguszczak, S. Tankiewicz, and D. Terech, “Novel technological and constructional solutions of pressure sensors made in LTCC technology,” Proceedings of SPIE -- Volume 4516, Optoelectronic and Electronic Sensors IV, Jerzy Fraczek, Editor, August 2001, pp. 10-14.
[8] D Belavic, M Hrovat, M Pavlin, “Vertical thick-film resistors as load sensors,” J. Eur. Ceram. Society 21 (2001) 1989-1992.
[9] B. Pan, Y. Yoon, J. Papapolymerou, M. M. Tentzeris, M. G. Allen, "A High Performance Surface-Micromachined Elevated Patch Antenna," *IEEE AP-S Mtg. Digest*, vol. 1B, pp. 397-400, July 2005.
[10] Y. H. Cho, S.-T. Kahng, W. Chou, M.-L. Ha, C. Pyo, Y.-S. Kwon, “A frequency agile floating-patch MEMS antenna for 42 GHz application,” *IEEE AP-S Mtg. Digest*, vol. 1A, pp. 512-515, July 2005.
[11] L. Harle and L. P. B. Katehi, “A Silicon Micromachined Four-Pole Linear Phase Filter,” *IEEE Trans. Microwave Theory Tech,* vol. 52, no. 6, pp. 1598-1607, June 2004.
[12] SB Rohde, KA Peterson, “Applying new LTCC/ LIGA construction techniques in realizing a miniature ion mobility spectrometer,” presented IMAPS 35th ann. Symp. on microelect., Denver, Sept., 2002.
[13] KA Peterson, SB Rohde, KB Pfeifer, TS Turner, “Novel LTCC fabrication techniques applied to a rolled ion mobility spectrometer,” Electrochem. Soc. Series; v2003 no.27 156-171.
[14] K. B. Pfeifer, A. N. Rumpf; *Anal. Chem*., **77**, 16, 2005, 5215-5220.
[15] K.A. Peterson, K.D. Patel, C.K. Ho, S.B. Rohde, C.D. Nordquist, C.A. Walker, B.D. Wroblewski, M. Okandan, “Novel Microsystem Applications with New Techniques in LTCC,” September 2005 - Vol. 2 Issue 5 Page 345-363.
[16] K. B. Pfeifer, R. C. Sanchez, *IJIMS*, **5,** 3, 2002, pp 63-66.
[17] K. B. Pfeifer, S. B. Rohde, K. A. Peterson, A. N. Rumpf, *13th Int. Conference on Ion Mobility Spectrometry,* July 25, 2004, Gatlinburg, TN, USA.

Appendix 4. Macro-Meso-Microsystems Integration in LTCC

Development of LTCC Smart Channels for Integrated Chemical, Temperature, and Flow Sensing

Clifford K. Ho, Kenneth A. Peterson, Lucas K. McGrath, and Timothy S. Turner
Sandia National Laboratories
P.O. Box 5800
Albuquerque, NM 87185-0735
Phone: (505) 844-2384; Fax: (505) 844-7354
E-mail: ckho@sandia.gov

Abstract

This paper describes the development of "smart" channels that can be used simultaneously as a fluid channel and as an integrated chemical, temperature, and flow sensor. The uniqueness of this device lies in the fabrication and processing of low-temperature co-fired ceramic (LTCC) materials that act as the common substrate for both the sensors and the channel itself. Devices developed in this study have employed rolled LTCC tubes, but grooves or other channel shapes can be fabricated depending on the application requirements. The chemical transducer is fabricated by depositing a conductive polymer "ink" across a pair of electrodes that acts as a chemical resistor (chemiresistor) within the rolled LTCC tube. Volatile organic compounds passing through the tube are absorbed into the polymers, causing the polymers to reversibly swell and change in electrical resistance. The change in resistance is calibrated to the chemical concentration. Multiple chemiresistors have been integrated into a single smart channel to provide chemical discrimination through the use of different polymers. A heating element is embedded in the rolled tube to maintain a constant temperature in the vicinity of the chemical sensors. Thick-film thermistor lines are printed to monitor the temperature near the chemical sensor and at upstream locations to monitor the incoming ambient flow. The thermistors and heating element are used together as a thermal anemometer to measure the flow rate through the tube. Configurations using both surface-printed and suspended thermistors have been evaluated.

Keywords: LTCC, smart channels, anemometry, thermistor, chemiresistor

1.0 Introduction

Microsensor systems are often comprised of multiple components assembled onto a common platform. The individual components are fabricated separately and later assembled and connected. Assembly of individual sensor components can be complicated, and fluidic interconnects (e.g., for chemical or flow sensors) can occupy significant amounts of space. In this paper, we describe the development of "smart" channels that minimize post-fabrication assembly and interconnects. The smart channel can be simultaneously used as both a fluid channel and an integrated chemical, temperature, and flow sensor.

Low-temperature co-fired ceramic (LTCC) is used as the common substrate for both the channel and sensors. In contrast, emerging micro-analytical systems have typically utilized individual components fabricated from silicon that are later assembled and mounted onto a common platform with fluidic interconnects [1]. LTCC has several features that make it attractive in the use of integrated sensing and flow, including its ease of fabrication for a variety of shapes such as tubes and channels and its ability to integrate electronic components. A thorough description of LTCC materials and potential applications can be found in [2].

This paper begins with a description of the fabrication of LTCC smart channels. The design and testing of channels in the shape of tubes is presented here, but flat channels are also being investigated [3]. Testing and calibration of the integrated temperature, flow, and chemical sensors are then described in the remaining sections.

2.0 Design and Fabrication of LTCC "Smart" Channels

2.1 Background

Complex LTCC substrates can be fabricated with cavities for many microelectronic multichip module implementations, and these are typically used as boards and devices which are planar. The starting substrates are pliable unfired sheets of glass-ceramic

doctor-bladed tapes (DuPont 951AT). Perforations can be made in these tapes for vias and cavities and thick film materials can be screen-printed onto these tapes. These thick films may define circuit features or fill vias for interlayer connectivity. Following the drying of thick films, the tapes are inspected, collated, and laminated together, by a variety of techniques, to form a monolithic structure. Following that, the structure is cofired. Cofiring refers to the simultaneous firing of the substrate, various conductors, and any resistors or other structures that are included in the design. It is also possible to add thick films after cofiring and then refire the part to attain additional functions. Certain non-planar applications have also been enabled by LTCC. These include the rolling of a drift tube for an ion-mobility spectrometer and non-planar microfluidic devices [4].

2.2 Design

The smart channel was designed so that it could be rolled into a tube from a planar LTCC sheet. The internal electrical structures would be accessible from the outside for connectivity after the sheet was rolled. Thermistors, a heater, and chemical sensor (chemiresistor) electrodes were included on one side (the interior) of the sheet, and additional leads were added to the other side (exterior) to provide connectivity with the internal leads (Figure 1).

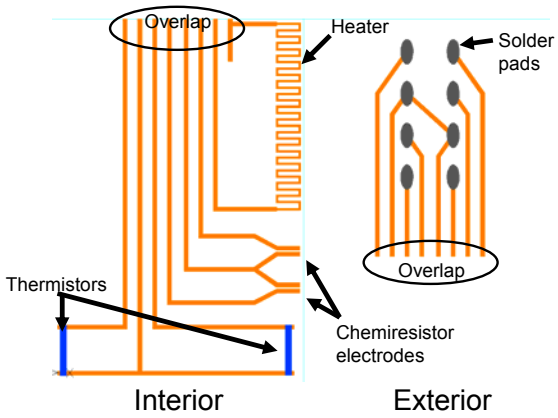

Figure 1. The interior and exterior design layouts combine to provide function and interconnections.

The overlap zone was used to connect the electrical path between thick films on the inner surface (which ends at the overlap) to the thick films on the exterior surface (which begins at the overlap). This overlap is monometallic in this case—both thick films being a pure gold commercial cofirable material (DuPont 5734).

The heater, which is subsequently embedded within the tube during rolling, is used to maintain a constant temperature for the chemiresistor sensor. The leads to the heater were 0.020" in width up to the reduced section, where the serpentine heater consisted of 0.010" wide lines. Chemiresistor electrodes were printed to provide 200 micrometer (0.008") gaps for the subsequent addition of the transducing polymer material (see Figure 2).

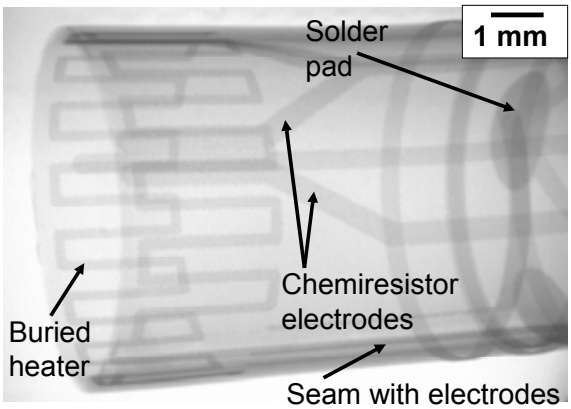

Figure 2. Several integral structures are visible by X-ray.

The chemiresistor electrodes were spaced apart from the heater so that when rolled, they would lie one layer above the embedded heater to allow temperature control. While the thermistors were not vended as a cofirable composition, we have used it several times with good results, as will be shown in a subsequent section.

A thermistor composition (DuPont 5092D, 5093D) was printed near the chemiresistor sensor to monitor the temperature. An upstream thermistor was also included in the design to monitor ambient incoming flows.

The output pads were printed from a cofirable solderable alloy (DuPont 5739) and covered the ends of the output lines from the other structures. They were arranged around the circumference of the middle of the tube. Individual leads were soldered to these pads, formed around the tube, and potted in a molding polymer for durability during testing as shown in Figure 3.

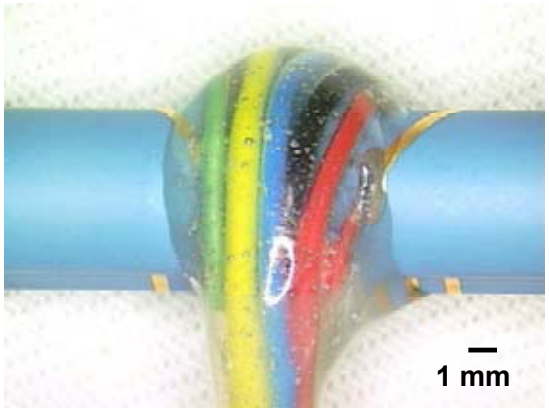

Figure 3. Potted leads increase the handling durability of the tube.

2.3 Fabrication

Having been completely printed, the LTCC tapes were sized in the green state. The leading edge of the substrate was then tapered using an abrasive surface. No thick film structures were placed near the inside seam in this design. The tube was manually rolled on an appropriately-sized smooth metal mandrel. A sufficient number of layers of a polymer film were wrapped around the tube to provide a pad or buffer, permitting us to use a conventional vacuum bagging technique for protection against the aqueous hydraulic fluid in an isostatic laminator. Without the buffer, the bag itself would impress additional undesirable features onto the exterior of the green tube. Following lamination, the buffer was easily removed and the green tube was removed from the mandrel. The tube was fired standing on-end and it supported itself during firing. A powdering inert setter material (Harmonics SPS) was used as a base, and minor deformation which occurred on the lower end was in a cut-off zone. Multiple devices were processed on a single tube and separated after firing.

2.4 Suspended vs. Surface-Printed Thermistors

Elevated structures are useful to a number of different applications. Examples are provided in the literature, including anemometry [5] and a stripline resonator [6]. In the cases cited, the thick film features have been supported on a thin layer of unfired LTCC for cofiring. Thick films may also be applied over a sacrificial material and cofired. During the cofiring cycle, the sacrificial material is removed or is inert and the thick film features that were attached to them are suspended above the substrate with a thermal mass that is very small.

In this study, suspended thermistors were fabricated on a thick film dielectric layer and subsequently separated and assembled into the tube, using a conductive epoxy as shown in Figure 4. These suspended thermistors were compared to the surface-printed thermistors in the following sections to evaluate the temperature and flow-sensing capabilities. A modification in which the suspended themistors are completely cofired into place is underway.

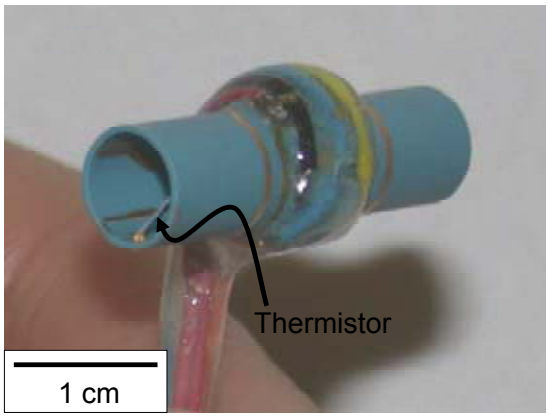

Figure 4. An assembled suspended thermistor is visible near the end of the tube.

2.5 Chemiresistor Fabrication

The chemiresistor sensors are comprised of two electrodes separated by a finite distance. A conductive polymer ("ink") is deposited over this gap to create an electrical pathway between the two electrodes.

The chemiresistor ink is a mixture of polymer and carbon black dissolved and dispersed in a solvent. Typically the mass of carbon and polymer totals 0.1 g and is mixed in 5 ml of solvent. The solvent is chosen based on the polymers' solubility. For example, for the polar polymer poly (N-vinyl pyrolidone) (PNVP), water was used as the solvent. For the other two polymers that were selected for our application, poly(ethylene-vinyl acetate) (PEVA) and poly(isobutylene) (PIB), trichloroethylene (TCE) was used as the solvent.

The polymer/solvent mixture is heated to approximately 40 °C to expedite the dissolution. After the polymer dissolves, a measured quantity of carbon black is added to the mixture. The vials are then placed in a sonicating bath for an hour to increase the dispersion of the carbon in the solution. The ink is then ready to deposited on the chemiresistor electrodes. For this application three polymer inks, (PNVP, PIB, & PEVA) were created using a 40%/60% carbon black/polymer ratio by weight.

The chemiresistor electrodes on the LTCC surfaces were cleaned with acetone and methanol. A 10 μL micropipette was used to wick a small amount

of ink from the vials. The micropipette was placed directly above the chemiresistor electrodes, and a slight pressure was placed on the top of the micropipette to push a bead of ink out of the pipette. If a resistance is not measured across the electrodes, more ink can be deposited or the prior deposition can be wiped off with acetone followed by another deposition. Figure 5 shows an image of the polymer ink deposition onto dual chemiresistor electrodes within the rolled LTCC smart channel.

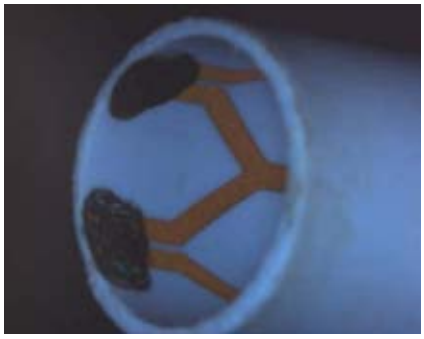

Figure 5. Deposition of polymer inks onto dual chemiresistor electrodes in the LTCC smart channel.

Seven LTCC smart channels were fabricated using different polymer combinations and thermistor configurations (Table 1).

Table 1. Seven LTCC smart-channel devices were fabricated for testing.

Device	Thermistor Configuration	Polymers
110705-1	Suspended	PEVA & PNVP
110705-2	Suspended	PEVA & PNVP
110705-3	Suspended	PEVA & PIB
110705-4	Suspended	PEVA & PIB
072705-4	Surface-printed	PEVA & PIB
072705-5	Surface-printed	PEVA & PIB
072705-7	Surface-printed	PEVA & PNVP

3.0 Calibration and Testing

The LTCC sensors were calibrated to temperature, gas flow, and chemical concentrations. Devices were calibrated to temperature in an oven that was monitored with a T-Type thermocouple. For flow calibrations, flow rates were monitored with an FMA-A208 Mass Flow Meter from Omega. Varying concentrations of different constituents (e.g., water vapor, TCE, m-Xylene) were introduced into the flow stream using bubblers and flow meters. All data were recorded with a CR1000 Campbell Scientific datalogger. The CR1000 was also programmed to control the temperature in the vicinity of the chemiresistor sensors using the embedded heater. The temperature of the chemiresistor sensors was maintained at 40 °C by toggling heater power on or off over 60 msec intervals.

For flow and chemical sensing, two LTCC devices were calibrated simultaneously in series. Figure 6 shows a schematic of the test apparatus for the flow and chemical calibrations.

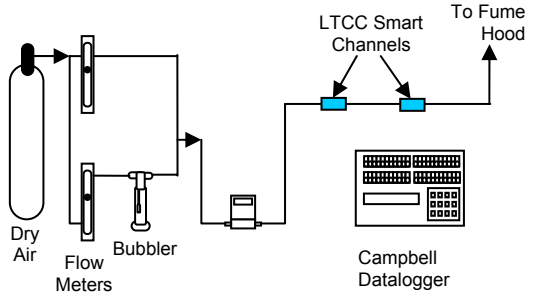

Figure 6. Sketch of the LTCC smart-channel flow and chemical-concentration test apparatus.

The following sections provide additional details regarding the calibration and testing of the temperature, flow, and chemical sensors.

3.1 Temperature Sensing

3.1.1 Calibration Procedure

Two thermistors on each of the LTCC smart channels were calibrated to temperature by placing the devices inside an oven set to 60 °C. The temperature inside the oven was allowed to stabilize before slowly decreasing after the oven was turned off. The resistances of the LTCC thermistors and the oven temperature were recorded using the CR1000. The temperature was plotted as a function of thermistor resistance for each device and a linear regression was applied.

3.1.2 Results

Figure 7 shows the temperature calibrations for four devices, each containing two thermistors. Two devices contained surface-printed thermistors, while the other two devices contained suspended thermistors. All of the thermistor resistances show an excellent linear regression with temperature. The surface-printed thermistor resistances were on the order of several thousand ohms, whereas the suspended thermistor resistances were on the order of several hundred ohms. The corresponding temperature regression for each thermistor (Table 2) was programmed into the CR1000 for additional

testing of each device with flow and chemical concentrations.

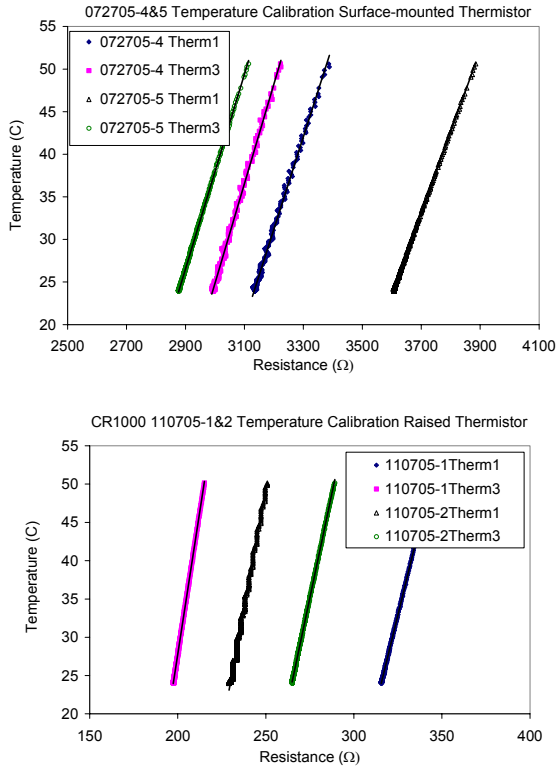

Figure 7. Temperature calibration of surface-printed thermistors (top) and suspended thermistors (bottom).

3.2 Flow Sensing (Anemometry)

3.2.1 Calibration Procedure

The LTCC smart channels were calibrated to flow using different gases at various flow rates. The flow rates ranged from 50 mL/min to 600 mL/min in 50 mL/min increments. Sensors were calibrated to each flow rate for 10 minutes. Voltage was applied to the heating element of each device to maintain a constant thermistor temperature of 40 °C (near the heater). The applied voltage was monitored with the CR1000 datalogger every 60 msec, and a running average of recorded voltages was taken for a two second period. The average voltage was plotted against the actual flow rate to generate calibration curves. This procedure was repeated for the following gases: dry air, moist air at 100% relative humidity, dry air with 50% TCE, and dry air with 50% m-Xylene.

Table 2. Summary of linear regressions for temperature-calibrated thermistors.

Sensor	Linear Regression	R^2
72705-4Therm1	0.1096x - 319.51	0.9901
72705-4Therm3	0.1164x - 324.35	0.9906
72705-5Therm1	0.0966x - 324.48	0.9983
72705-5Therm3	0.1138x - 303.43	0.9975
72705-7Therm1	0.1345x - 385.23	0.9865
72705-7Therm3	0.1133x - 395.82	0.9925
110705-1Therm1	0.9429x - 273.51	0.9994
110705-1Therm3	1.4974x - 271.85	0.9994
110705-2Therm1	1.1798x - 246.55	0.9877
110705-2Therm3	1.0814x - 262.28	0.9988
110705-3Therm1	0.8761x - 262.42	0.9966
110705-3Therm3	1.4659x - 274.84	0.9989
110705-4Therm1	1.2382x - 281.05	0.9996
110705-4Therm3	1.3121x - 273.31	0.9997

3.2.2 Test Results

Figure 8 shows the flow calibrations for two LTCC smart channels—one device contained surface-printed thermistors, and the other device contained suspended thermistors. The device with surface-printed thermistors yielded more variability in the applied voltage for different gases and flow rates. The suspended thermistors produced much better linear regressions between the applied flow rates and the applied voltage for all the gases tested. We postulate that the suspended thermistors are more sensitive to changes in flow rates since they are within the flow stream. This was also observed in previous studies [5]. The surface-printed thermistors are within a viscous sublayer of flow and are less sensitive to the bulk changes in flow rates. In addition, because the viscosity is different among the different gases used in the calibrations, the flow calibrations for the surface-printed thermistors vary significantly with the different gases.

Therefore, these tests demonstrate that suspended thermistors perform better than surface-printed thermistors for the purposes of anemometry in LTCC smart channels. Table 3 summarizes the flow calibrations for two representative devices exposed to different gas constituents and flow rates. The R^2 values confirm that the regressions for the suspended thermistors are superior to the regressions for the surface-printed thermistors.

Table 3. Flow calibrations for representative LTCC smart channels with surface-printed thermistors vs. suspended thermistors using different gas constituents and flow rates.

Gas Constituent	Linear Regression			
	Surface-printed Thermistor (072705-4)	R^2	Suspended Thermistor (110705-1)	R^2
Dry Air	7.8762x - 2974.7	0.91	1.4875x - 702.79	0.98
Moist Air with 100% RH (water vapor)	6.3221x - 2164.8	0.89	1.5658x - 777.45	0.97
Dry Air with 50% TCE by Volume	10.032x - 3327.6	0.67	1.695x - 832.63	0.99
Dry Air with 50% m-Xylene by Volume	8.6134x - 2832	0.76	1.6344x - 802.07	0.98

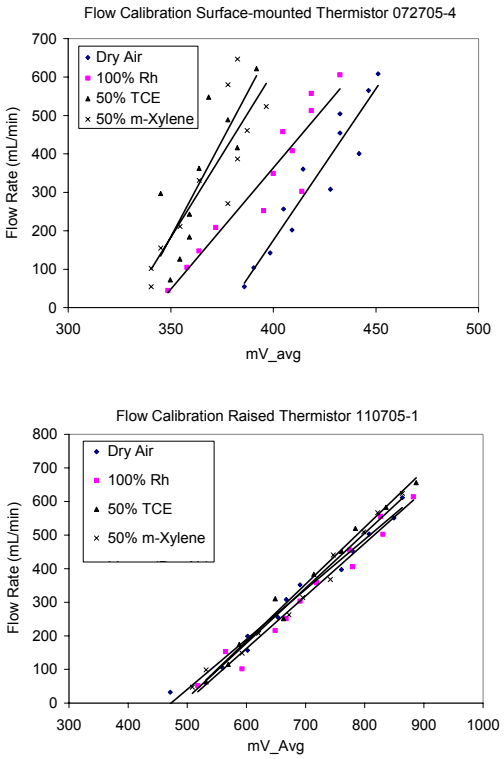

Figure 8. Flow calibration of surface-printed thermistors (top) and suspended thermistors (bottom).

3.3 Chemical Sensing

The chemiresistor consists of a chemically-sensitive polymer that is dissolved in a solvent and mixed with conductive carbon particles [7]. The resulting ink is then deposited and dried onto thick-film gold traces printed onto an LTCC tape. When chemical vapors (volatile organic compounds) come into contact with the polymers, the chemicals absorb into the polymers, causing them to swell. The swelling changes the resistance of the electrode, which can be measured and recorded (Figure 9). The amount of swelling corresponds to the concentration of the chemical vapor in contact with the chemiresistor. The process is reversible if the chemical vapors are removed, but some hysteresis and drift can occur.

The LTCC smart channels evaluated in this paper include two sets of chemiresistor electrodes. Different polymers can be deposited onto each pair of electrodes. By choosing polymers with different affinities to different volatile organic compounds, we can use various chemometric and multivariate regression techniques to discriminate among different chemicals [8],[9].

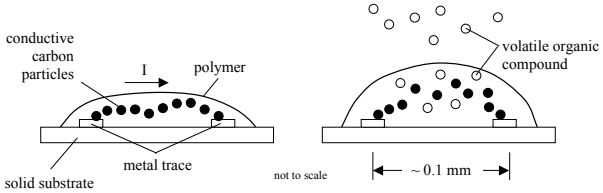

Figure 9. Chemiresistor detection of volatile organic compound vapors. Left: Electrical current (I) flows across a conductive thick-film carbon-loaded polymer deposited across a pair of electrodes. Right: Chemicals absorb into the polymer, causing it to swell (reversibly) and break some of the conductive pathways, which increases the electrical resistance. [7]

3.3.1 Calibration Procedure

Table 1 summarizes the different polymer combinations that were used for each pair of chemiresistor sensors and for each LTCC smart-channel. The PEVA/PNVP polymer combination was used to discriminate solvents such as TCE from water. PEVA has a strong affinity for chlorinated solvents and hydrocarbons, while PNVP has a strong affinity for polar compounds such as water. The PEVA/PIB combination was evaluated for discrimination among TCE and m-Xylene, an aromatic hydrocarbon. Based on these combinations, the chemiresistor sensors were

exposed to combinations of either dry air, water vapor, and TCE, or dry air, TCE, and m-Xylene. The concentrations of water vapor that were used included 0%, 50%, and 100% relative humidity (RH). The concentrations of TCE and m-Xylene that were used included 0%, 50%, and 100% of the constituent's saturated vapor pressure (at 23 °C) in dry air by volume.

The chemiresistor sensors were exposed to chemicals by placing two LTCC smart channels in series with gas flowing at 200 mL/min though each channel. The channels were purged initially for approximately 60 minutes by flowing clean dry air through the lines. During this time the sensors stabilized and a baseline resistance was recorded, R_b. Then the sensors were exposed to a known chemical concentration of water vapor, TCE, or m-Xylene for approximately 60 minutes.

The relative change in resistance for each chemiresistor sensor was used for the calibrations. The equation for the relative change in chemiresistor resistance is as follows:

$$\frac{\Delta R}{R_b} = \frac{R - R_b}{R_b}$$

where R is the measured resistance and R_b is the baseline resistance taken prior to exposure.

3.3.2 Test Results

A typical response of the chemiresistor sensor to chemical exposure is illustrated in Figure 10. The PEVA chemiresistor (device 072705-4) is exposed to dry air and then 25%, 50%, and 100% saturated TCE vapor by volume with dry-air purges in between each exposure. The chemiresistor response is fairly rapid (on the order of seconds), although at such high concentrations, it can take on the order of minutes to reach equilibrium. In Figure 10, it appears that the PEVA resistances did not reach complete equilibrium before each purge.

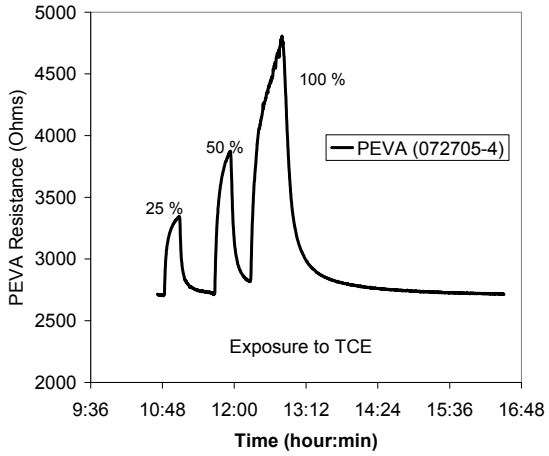

Figure 10. Exposure of PEVA chemiresistor (device 072705-4) to different concentrations of TCE with a clean-air purge in between each exposure.

Figure 11 and Figure 12 show the calibration of two different pairs of chemiresistors to different gas constituents. The PIB/PEVA chemiresistor pair was calibrated to m-Xylene and TCE, and the PNVP/PEVA chemiresistor pair was calibrated to TCE and water vapor (at different relative humidities). Figure 11 shows that the PIB and PEVA polymers are more sensitive to exposure to TCE versus exposure to m-Xylene, but both polymers appear to respond similarly. Therefore, using these two polymers for discrimination of m-Xylene and TCE is not optimal.

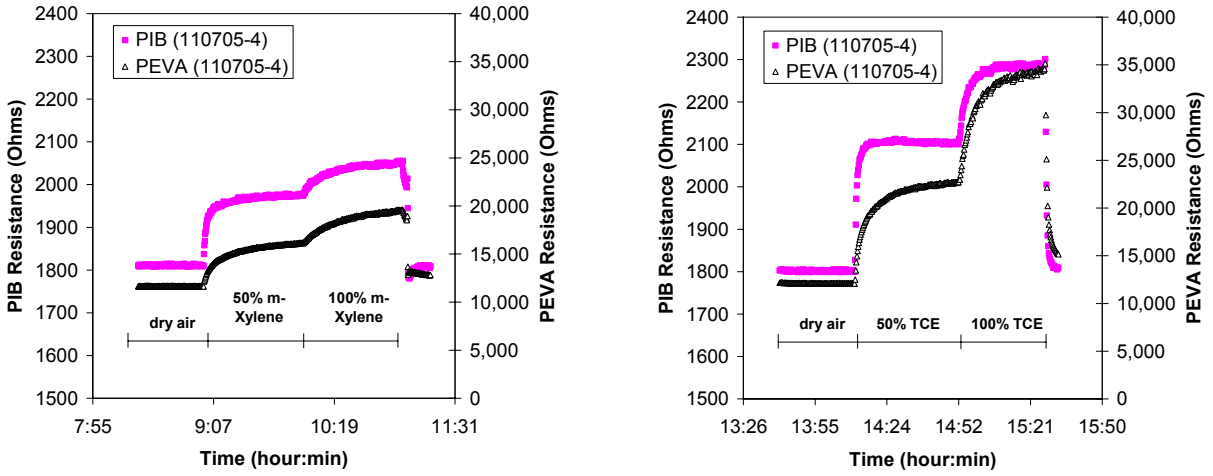

Figure 11. Calibration of PIB/PEVA chemiresistors (on device 110705-4) to m-Xylene (left) and TCE (right).

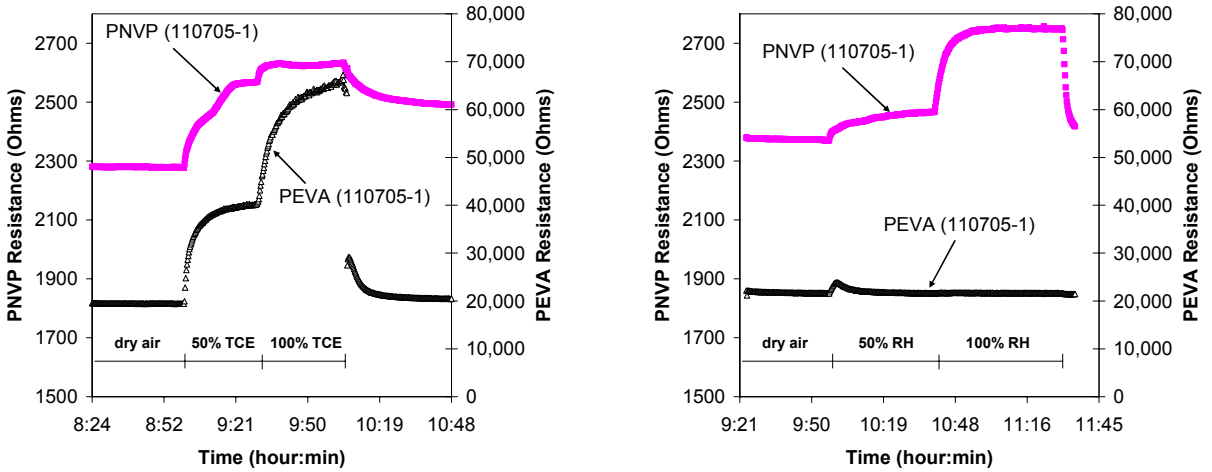

Figure 12. Calibration of PNVP/PEVA chemiresistors (on device 110705-1) to TCE (left) and water vapor (right).

Figure 12 shows that the PEVA polymer has a very strong response to TCE, but very little response to water vapor (the small "blip" in the PEVA response to water vapor at the onset of the 50% relative-humidity exposure was due to the use of a flow line that was previously connected to the TCE bubbler). In contrast, PNVP responds to TCE, but it has a much more stable and definitive response to water vapor. Therefore, the use of the combined PNVP and PEVA chemiresistors should allow reasonable discrimination between TCE and water vapor.

The results of the PNVP/PEVA calibrations (for device 110705-1) were used to develop multivariate polynomial regressions to estimate the TCE and water-vapor concentrations as a function of the relative change in resistances for both PNVP and PEVA. The commercial statistical software package Statistica® was used to generate multivariate regressions with a forward stepwise regression analysis to calculate relative-humidity and TCE concentrations:

Relative Humidity:

$$RH(\%) = -0.163 + 1450\left(\frac{\Delta R}{R_b}\right)_{PNVP} - 5130\left(\frac{\Delta R}{R_b}\right)^2_{PNVP} - 137\left(\frac{\Delta R}{R_b}\right)_{PEVA} + 39.4\left(\frac{\Delta R}{R_b}\right)^2_{PEVA}$$

TCE (% saturated vapor):

$$TCE(\%) = 0.584 + 42.2\left(\frac{\Delta R}{R_b}\right)_{PEVA}$$

Results showed that the relative humidity was a function of both PNVP and PEVA, but the TCE concentration was a function of PEVA only. Because the PEVA responded significantly to TCE (and minimally to water vapor), the forward stepwise regression analysis found that the TCE concentration could be calculated using PEVA alone. However, because PNVP responded to both water vapor and TCE, additional terms were needed to calculate the relative humidity to compensate the response of PNVP to TCE. The coefficient of determination (R^2) for both regressions is greater than 0.99.

The effectiveness of these regressions was tested by exposing the LTCC smart channel (110705-1) to both water vapor and TCE in successive exposures with dry-air purges in between. Figure 13 shows the actual and predicted concentrations as a function of time.

The regression for water vapor concentration (relative humidity) does a good job in predicting the prescribed relative humidity values during the experiment, but there are some erroneous jumps in the predicted relative humidity during the exposure to TCE (Figure 13). The regression for relative humidity was based on steady values of resistances achieved when the chemiresistors had reached equilibrium during the calibrations. Therefore, sharp changes in the resistances of PEVA when the TCE is turned on or off can erroneously affect the predicted relative humidity since the resistance values were not in equilibrium.

The predicted TCE concentration (% saturation) is quite good throughout the entire experiment. The regression correctly predicts a TCE concentration near zero when the chemiresistors are exposed only to water vapor, and the regression

predicts fairly accurate values of TCE concentration during the TCE exposures. The predicted TCE concentration at an exposure of 100% saturated TCE vapor is about 10% larger than the actual value.

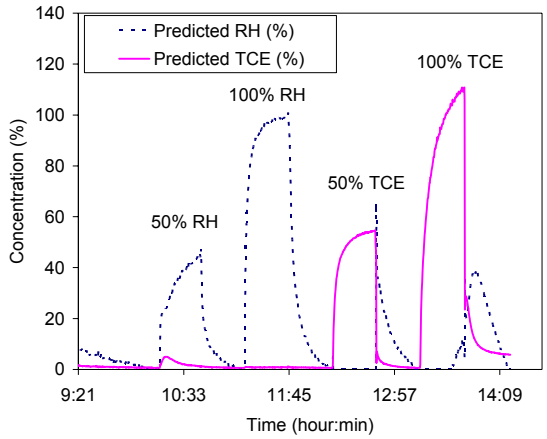

Figure 13. Predicted concentrations of water vapor (% relative humidity, RH) and saturated TCE vapor (%) as a function of time during successive exposures with dry-air purges in between. Actual concentrations are shown as labels above each peak.

4.0 Summary and Conclusions

Smart channels consisting of temperature, flow, and chemical sensors have been fabricated from LTCC. Tubular channels have been investigated in this paper, but flat channels are also being evaluated. Thick-film thermistors were integrated into the channels as temperature sensors, and a heating element was used in conjunction with the thermistors to provide anemometry. Both surface-printed and suspended thermistors were fabricated and evaluated.

Results showed that all of the thermistor resistances yielded linear responses to changes in temperature. However, the suspended thermistors were superior to the surface-printed thermistors in providing linear regressions of flow rate as a function of power (voltage) added to the heater for different gases.

Chemiresistor sensors were integrated into the LTCC channels to provide quantitative detection of volatile organic compounds. Pairs of chemiresistors were included in each channel to evaluate discrimination capabilities among different chemicals. Results showed that the PNVP/PEVA polymer combination yielded reasonable quantitative predictions of water-vapor and TCE concentrations using multivariate regressions.

Future work will focus on improving the design of the suspended thermistors to refine a single-step fabrication process. Flat LTCC smart channels will also be developed for integration with other devices and applications in planar configurations.

Acknowledgments

The authors would like to thank Dennis De Smet for his technical assistance. Sandia is a multiprogram laboratory operated by Sandia Corporation, a Lockheed Martin Company for the United States Department of Energy's National Nuclear Security Administration under contract DE-AC04-94AL85000.

References

[1] R.P. Manginell, P.R. Lewis, D.R. Adkins, R.J. Kottenstette, D. Wheeler, S. Sokolowski, D. Trudell, J. Byrnes, M. Okandan, J.M. Bauer, and R.G. Manley, "Recent Advancements in the Gas-Phase MicroChemLab,™" in Proceedings of SPIE Vol. 5591, edited by L.A. Smith and D. Sobek, Bellingham, WA, December 2004.

[2] M.R. Gongora-Rubio, P. Espinoza-Vallejos, L. Sola-Laguna, and J.J. Santiago-Aviles, "Overview of Low Temperature Co-Fired Ceramics Tape Technology for Meso-System Technology," Sensor. Actuat. A, 89 222–241, 2001.

[3] K.A. Peterson, K.D. Patel, C.K. Ho, S.B. Rohde, C.D. Nordquist, C.A. Walker, B.D. Wroblewski, and M. Okandan, "Novel Microsystem Applications with New Techniques in Low-Temperature Co-Fired Ceramics," *Int. Journal of Applied Ceramic Technology*, 2 (5) 371–389, 2005.

[4] K. A. Peterson, S.B. Rohde, K.B. Pfeifer, T.S. Turner, "Novel LTCC fabrication techniques applied to a rolled ion mobility spectrometer," *Electrochem. Soc. Series*, 27, 156-171, October 2003.

[5] M. Gongora-Rubio, L.M. Sola-Laguna, P.J. Moffett, J.J. Santiago-Aviles, "The utilization of low temperature co-fired ceramics (LTCC-ML) technology for meso-scale EMS, a simple thermistor based flow sensor," *Sensors and Actuators A*, v73, no3, 215-221, 1999.

[6] Y.C.Lee and C.S. Park, "A Novel High-Q Stripline Resonator for Millimeter-Wave Applications," *IEEE Microwave and Wireless Components Letters*, V13, No.12, 499-501, 2003.

[7] C.K. Ho and R.C. Hughes, 2002, "*In-Situ* Chemiresistor Sensor Package for Real-Time Detection of Volatile Organic Compounds in Soil and Groundwater," *Sensors*, 2, 23-34, 2002.

[8] T.P., Vaid, T.P, M.C. Burl, and N.S. Lewis, "Comparison of the performance of different discriminant algorithms in analyte discrimination tasks using an array of carbon black-polymer composite vapor detectors," *Analytical Chemistry*, 73(2), 321-331, 2001.
[9] J.W. Grate and B.M. Wise, "A method for chemometric classification of unknown vapors from the responses of an array of volume-transducing sensors," *Analytical Chemistry*, 73(10), 2239-2244, 2001.

Appendix 3. Macro-Meso-Microsystems Integration in LTCC

Low Temperature Cofired Ceramic Microfluidic Microsystems for High Temperature and High Pressure Applications

Kamlesh D. Patel*, Kenneth A. Peterson, and Kyle W. Hukari

Sandia National Laboratories
7011 East Ave
Livermore, CA 94550
Phone: 925-294-37373, Fax: 925-294-3020
Email: kdpatel@sandia.gov
*-Corresponding author

Abstract

As an alternative material to glass, silicon, and plastics, Low Temperature Cofired Ceramic (LTCC) substrate technology is becoming increasingly important for enabling microfluidic microsystems and devices for integrated chemical and biological analysis. LTCC's simple fabrication method and unique ability to withstand high temperatures and high pressures make it well-suited for applications not possible with traditional materials. As part of Sandia's initiative to develop an automated sample preparation system for the μChemlab™ bioagent detector, an integrated microfluidic lyser using LTCC technology has been fabricated, which enables the use of aqueous buffers at high temperatures without boiling by using a pressurized system. Thermal lysing of bacterial spores in a flow-through microfluidic device at temperatures as high as 220°C and pressures up to 10.3 MPa (1,500 psi) represents a new method for solubilizing spore proteins for identification and analysis, eliminating the reliance on harsh chemical reducing agents for lysing. This paper will present results on the development of a microfluidic LTCC-based lyser by taking advantage of the inherent properties of LTCC substrates. Specifically, the performance and implementation of a prototype LTCC lyser for solubilizing bacterial spore proteins will be reported.

Key words

High temperature, lysis, microfluidics protein solubilzation, spores.

Introduction

The use of Low Temperature Cofired Ceramic (LTCC) materials for packaging and interconnect technology in the microelectronics industry is well-established. However, the application of LTCC technology for developing new biological and chemical microsystems is becoming more prevalent [1]. A common trend today for biological and chemical analysis systems is to shrink entire laboratory systems to a chip-size lab-on-a-chip. A μ-TAS (Total Analysis System) device incorporates all the necessary steps for analysis such as sample transport, filtration, dilution, separation, and detection. These devices require smaller sample amounts, perform faster and/or even better analyses, and cost less to operate than conventional benchtop methods. Our research at Sandia National Laboratories is focused on merging microfluidics and MEMS technology with the extensive industry knowledge of LTCC fabrication, metal patterning, fugitive layer firing, and lamination techniques to provide unique opportunities for enabling new and improved μTAS devices [2]. Recently, Golonka and coworkers have developed a simple LTCC-based analyzer with optical fiber detection. [3]. Their work and previous work by others [4[, [5] demonstrate the usefulness of LTCC substrates as a practical detection platform for chemical reactions. Similarly, LTCC devices have also been demonstrated for important biological applications requiring integrated microfluidic channels, heaters, and sensor for on-chip DNA amplification [6], [7].

Listed in Table I are some of the inherent advantages and disadvantages of LTCC substrates over traditional

Appendix 3. Macro-Meso-Microsystems Integration in LTCC

materials, such as glass, silicon and plastics, for the development of microfluidic devices. The key distinction for LTCC substrates is its simple lamination-style fabrication method and unique properties to withstand high temperatures and high pressures (>5,000 psi or 34,500 kPa). [2] Unlike glass and silicon, LTCC in its green form is very pliable making it easy to work with for designing features into the surface. The ability to stack and laminate multiple layers provides a straight-forward solution for creating complex 3-D fluidic networks with integrated sensors. Such a task in silicon and glass requires very complex and difficult fabrication methods. And unlike plastics, ceramics can withstand high temperatures and have a high strength making them suitable for extreme environments.

Table I. Distinct advantages and disadvantages of microfluidic devices fabricated in LTCC.

Advantages
Chemically inert to most solvents and samples Low to slightly negative surface charge Good thermal conductivity (w.r.t. plastic, glass) Low thermal coefficient of expansion Straight-forward fabrication method Print conductive thick-film traces and vias Develop multilevel fluidic networks easily Integrate electronic circuit directly Withstand fabrication temperatures to ~900°C Withstand high internal pressures Build complex geometries by lamination Fabricate devices in non-planar dimensions
Nearly unlimited channel miniaturization w/sacrificial materials
Disadvantages
Opaque and difficult for optical detection Punched channels geometries minimum size is 100 µm and channel height limited to tape thickness (25-50 µm) Shrinkage upon firing (12-15%) Contains low amount of lead

This paper demonstrates a microfluidic device that makes use of LTCC's high-temperature and high-pressure properties. Fabricating such a device in traditional materials would be inherently difficult due to their limitations. For this paper, we present our initial results on the development and characterization of a simple high temperature thermal lyser for the solubilization of bacterial spores for subsequent protein analysis with capillary gel electrophoresis (CGE). The design and test results of the prototype device will be presented, as well as its performance as a lyser compared to conventional benchtop techniques.

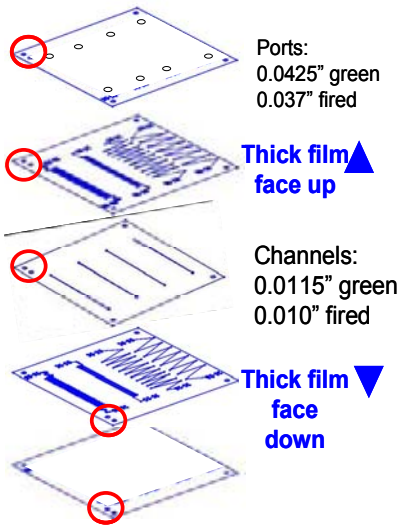

Fig. 1. Assembly of ceramic lyser using 0.010" thick Greentape™ from DuPont.

Experimental

A. Fabrication of the ceramic lyser

The flow-through ceramic lyser is a relatively simple device. It has a microfluidic channel with dimensions of 250 µm by 250 µm in its cross-section and 4 cm long. Each end of the microchannel is connected to liquid via ports. Upon firing, the final diameter fits an o-ring faced nanoport fitting for connection to the fluid lines. A thin-film gold trace is printed over the microchannel connected to electrical pads. Wires soldered to the pad deliver current to the thick-film traces to resistively heat the entire device.

For maximum heating efficiency, resistive heaters are placed on top and bottom of the microchannel. Fig. 1 shows the assembly of the five required layers to fabricate the device: a top and bottom layer, two intermediate layers with printed thick-film heaters, and a center layer with a punched channel. Liquid is introduced into the device through via holes punched in the top two layers as illustrated in the figure. The DuPont 951 tape used is 0.010 inches in thickness with shrinkage of about 14%. Standard fabrication procedures for punching the channels, laminating the layers, and cycling the oven-temperature ramps and dwells are used [1]. Fig. 2 shows the final sintered product after firing, but prior to dicing into individual pieces. The four different heater designs tested are shown.

B. Heater performance measurements

Prior to assembly, the individual heater designs were tested for the maximum temperature and duration to achieve stable temperature. Using a DC power supply, each heater design was tested and compared at 12 and 24 volts. The

Appendix 3. Macro-Meso-Microsystems Integration in LTCC

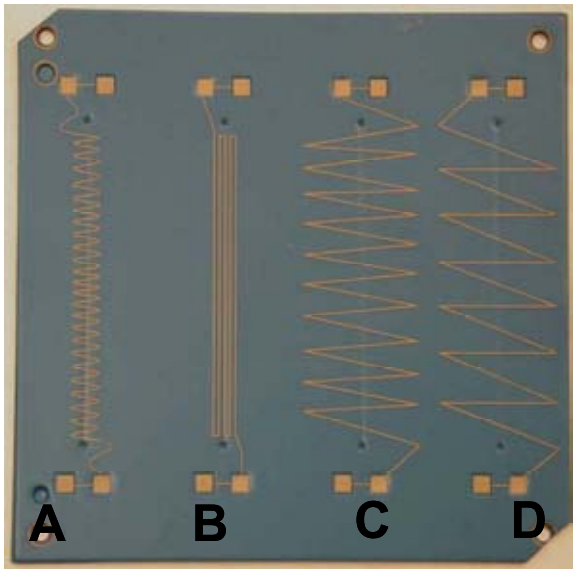

Fig. 2. The four heater designs of the ceramic lyser after firing. In this particular image, the intermediate layer and top layer heaters were independently addressable by pads on each level. This shows a clear picture of the four different heater designs in relation to the microchannel.

heater traces above and below the microchannel were connected in parallel to the power supply. A thin-wire thermocouple placed on the surface was used to measure the temperature of the device. The device was suspended in air with no extra external insulation to minimize heat loss. However, air drafts from the laboratory across the device were kept to a minimum.

C. Thermal lyser setup

The setup for testing the performance of the device is shown in Fig. 3. The sample is dispensed from a 250 µL glass syringe using a syringe pump (KW scientific). The syringe pump can be programmed to deliver a constant flow rate to the ceramic lyser. A glass capillary tube (Polymicro Technologies, Phoenix, AZ) with custom swaging ferrules [27] is used to connect the syringe to the lyser inlet port. The ports used are mated to the surface by either using an epoxy seal or by mechanically compressing an o-ring sandwiched between the port and LTCC surface. The entire device is supported on a Styrofoam base. Temperature is monitored using a surface thermocouple attached directly beneath microchannel between the Styrofoam backing and LTCC lyser. The solubilized spores or lysate exit through a small diameter capillary flow restrictor. The primary purpose for the capillary flow restrictors is to increase the pressure inside the microchannel. Raising the pressure increases the solvent boiling point to achieve a superheated solution allowing higher temperatures (increased thermal energy) to be reached before boiling or steam generation. The lysate is collected in a small vial for subsequent analysis by CGE.

D. Spore and standard protein preparation

Spore preparations were either purchased (Raven Biological, Omaha, NB.) or prepared as described. In-house preparations of *B. Anthracis* (delta sterne) and *B. Subtillis* were performed as previously described by Nicolson and Setlow [8]. Briefly, initial growth for cultures took place in Luria-Bertani media (20 g L-1, LB Broth, Difco). Small scale cultures incubated overnight at 37°C were diluted and used to inoculate large scale cultures at an optical density (O.D.) of 0.05 at 600 nm. When cultures reached an O.D. between 0.4 and 0.6 at 600 nm, cells were spun down for 10 minutes at 5,000 x g and resuspended in an equal volume of sporulation media [8], [9]. Cultures remained incubated at 37°C for 48 hours. Samples were centrifuged at 10,000 x g and the supernatant decanted. Purification included 3 washes with sterile deionized H_2O, 1 wash with 1 M KCl / 0.5 M NaCl, 1 wash with 1 M NaCl, 1 wash with 2 M NaCl, 1 wash with 0.25% Sodium dodecylsulfate (SDS) solution, and 3 washes with sterile deionized H_2O to remove extraneous vegetative cell lysates. All washes occurred in ¼ the original culture volume with centrifugation at 10,000 x g for 10 minutes. Purified spores were then resuspended in sterile deionized H_2O and stored at 4 °C.

To use the spores, samples were pelleted by centrifugation and resuspended in an aqueous carrier buffer containing 5 mM boric acid and 5 mM SDS at a pH of 8.5-8.8 (adjusted dropwise with NaOH). The spores were diluted to a final concentration of $1x10^5$ spores per mL concentration.

Protein standards CCK (Cholecystikinin flanking peptide), α-lactalbumin, ovalbumin, BSA (bovine serum albumin), purchased from Sigma-Aldrich (St. Louis, MO), were suspended in an identical carrier buffer as above and passed through the lyser to see the effects of high-temperature and pressure on the protein separation. The concentration of the proteins was in the nanomolar range.
After 10-15 µL of lysate or sample is collected, an aliqout is reacted with fluorescamine (Molecular Probes, Eugene OR), a fluorogenic fluorescent labeling dye which reacts rapidly with proteins [10]. Once fully labeled, the samples are hand injected on a hand-portable microchannel electrophoresis instrument described previously [11], [12] to perform microchannel gel electrophoresis.

Appendix 3. Macro-Meso-Microsystems Integration in LTCC

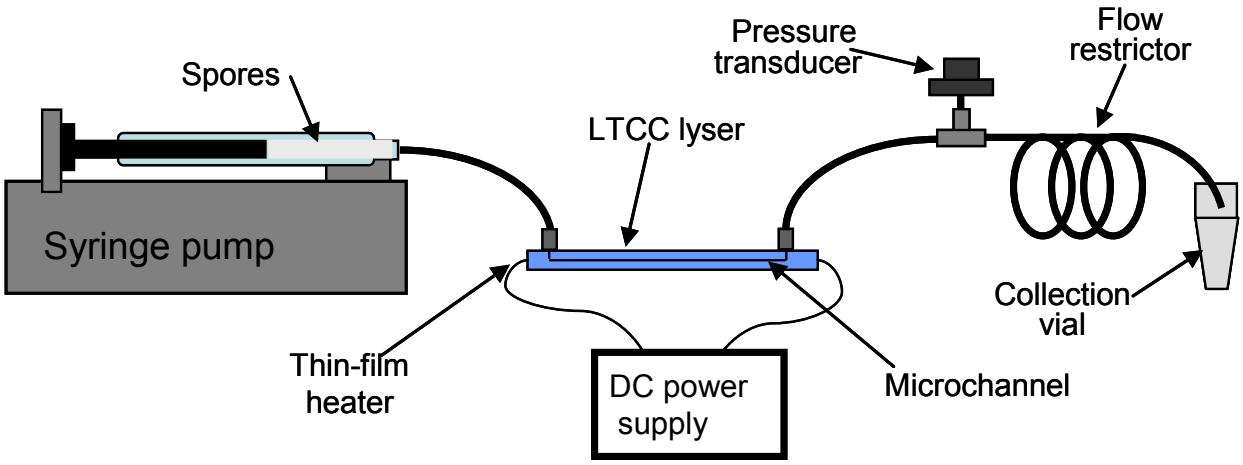

Fig. 3. Layout of the setup to test the performance of the LTCC lyser. Spores are delivered to the lyser at a constant flow rate. The heater inside the device heats the spores to high temperatures. The capillary flow restrictor elevates the pressure in the device to prevent boiling of the carrier fluid (aqueous buffer).

Results and Discussion

A. Heater performance.

One of the key advantages of LTCC materials is that thick-film metal traces can be easily cofired on the surface. Fig. 2 shows the four heater designs printed on the surface and tested. The measured electrical resistance for each heater pair is between 85 to 90 Ohms. Fig. 4 shows the temperature response curve verses time of a surface-mounted thermocouple for each heater design at two applied voltages. The time to reach a stable temperature at 12 V applied takes over 3 minutes; where as for 24 V applied, the temperature reaches greater than 150°C in less than 1 minute.

In comparing the four heaters, design A is the most effective in reaching higher temperatures. As a result, design A is the one used for the lysing experiments due the even coverage over microchannel. Fig. 5 shows the temperature response curve with respect to current applied to the heater on the device. To observe the cooling effect, carrier buffer is passed through the device at 6 µL/min under pressure. From the figure, it is clear that at low current settings (lower temperatures), the liquid velocity through the device is sufficient to suppress the temperature. However increasing the current above 0.15 A, there is a near linear relationship between current and temperature. These currents values are high enough to overcome the cooling effect due to the flowing liquid.

B. High temperature lyser

A major step in efficient sample preparation is the lysis and solubilization of a bioagent for analysis. This step is complicated by the wide variability in the susceptibility of biological agents to lysis and solubilization [13]. As a result, a variety of techniques have been developed for the lysis of bacterial agents including chemical and detergent lysis [14], [15], enzyme treatment [16], sonication [17], heating [18], and glass bead milling [19]. Bacterial spores are extremely resistant to lysis and solubilization, and typically require a combination of these aforementioned techniques to prepare them for analysis [20], [21].

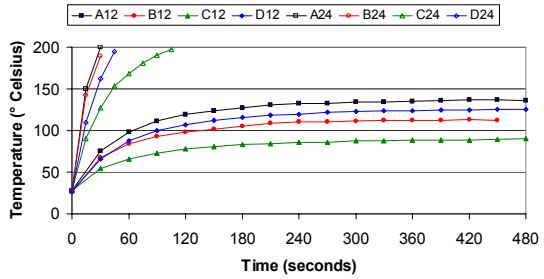

Fig 4. Temperature response of a surface-mounted thermocouple for the four heater designs (A-D). Design A has the best performance at both voltages tested.

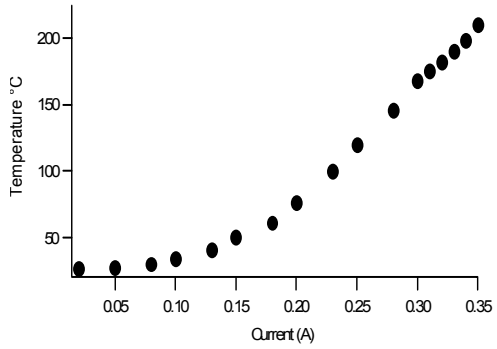

Fig 5. Temperature response of a surface-mounted thermocouple for heater design A with fluid flowing through the device.

Consequently, many of these lysis techniques often complicate subsequent analysis due to addition of chemical additives, such as TCEP, DDT, BME, or enzymes to the samples, which can interfere with the amplification, labeling, or separation [18]. Our ceramic lyser concept avoids unnecessary additives and simply uses increased thermal energy to break open the spores and solubilize the spore proteins for analysis.

The concept of high temperature lysing for bacterial spores was first introduced by West and coworkers at Sandia National Laboratories [22], [23]. They used a simple capillary tube with a heater coil to heat a capillary and the solution within to temperatures above 180°C. To reach these temperatures without boiling, the carrier fluid was an ethylene glycol base, which has a boiling point of 197°C. [24]. A significant improvement of the ceramic thermal lyser over the capillary system was that it could use conventional aqueous 5mM borate buffer instead of an uncharacterized ethylene glycol carrier fluid. Since the ceramic device uses aqueous buffers, the channel required pressurization to raise the effective boiling point of the buffer.

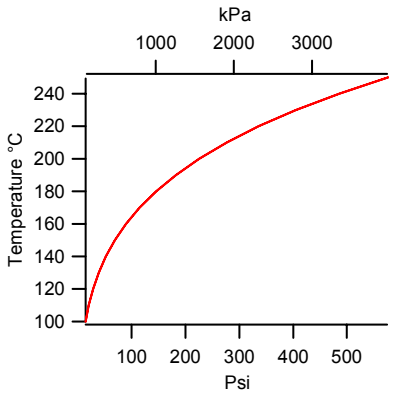

Fig. 6. Boiling point curve for water with respect to pressure.

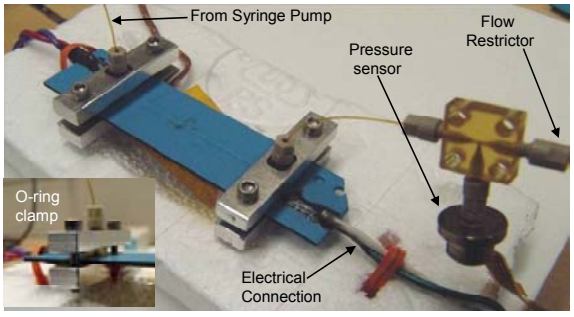

Fig. 7. High temperature LTCC thermal lyser for solubilizing spores. Spores are pumped into the device using a syringe pump and collected in a vial for subsequent analysis (not shown).

Fig. 6 shows the boiling point change for water with pressure [25]. The region below 220°C and 350 psi is the range in which the ceramic lyser is designed to operate to achieve spore lysis.

Fig. 7 shows an image of the ceramic lyser in operation. The device shown uses o-ring seals. The aluminum cross-members provide the compression force to seal the o-ring to the LTCC surface. Although cumbersome to assembly, this design is superior to surface glued fittings, which weaken at high temperatures. The o-ring design can achieve pressures as high as 10,345 kPa (1,500 psi) at 220°C with no observable leaks.

C. Standard protein analysis

It is well-known that above 60°C, most proteins will denature and loose their tertiary structure or 3-D shape [26]. However, the peptide bond between amino acids is a strong covalent bonded that can survive much higher temperatures. To be certain that the combination of temperature and pressure are not causing strange and unwanted effects, standard proteins with a range of molecular weights are passed through the lyser at high temperature and high pressure, simulating the lysate. Fig. 8 shows a series of electropherograms of the separated protein mixture by CGE. Aliquots of the same sample are collected at four different temperatures. The run at 23°C served as the control. Operating at 6 µL/min flow rate and approximately 2,700 kPa (300 psi) back pressure, the residence time of the protein mixture inside the device is approximately 25 seconds. The electropherogram of the proteins pass through the lyser at 131°C is similar to the electropherogram for the run at room temperature; there are no significant differences. However, the run at 185°C begins to show some peak broadening and perhaps the start of protein degradation. The highest temperature of 220°C shows significant degradation of the protein peaks. The peak broadening is most likely caused by the proteins fragmenting into multiple smaller components causing the peaks to broaden and decrease the overall height of the peak. From these results, it seems that 220°C is the limit before proteins degrade. However, more tests are necessary to determine if the fragmentation is due to the autocleaving of the peptide bond or undesired chemistry with the surface or buffer system. Referring back to Fig. 6, 220°C is above to the boiling point for pure water at 300 psi. Unfortunately, the exact boiling point of our carrier fluid and the effects of boiling a protein solution at high temperature under pressure are unknown. Nevertheless, it can be concluded from this set of experiments that operating the lyser up to 185°C will not cause appreciable degradation of the proteins.

D. Spore lysis

Based on the results from the standard protein runs, the ceramic lyser was set to operate at a temperature of 150°C, 2414 kPa (350 psi) backpressure, and a flow rate set to 2.5 µL/min for lysing *Bacillus subtilius* spores. With a flow rate of 2.5 µL/min, the residence time of the spores in the lyser is approximately one minute. A suspension of spores at 1 x 10^5 per mL concentration in a glass syringe has a cloudy appearance. However, the same solution exiting the lyser is clear. These results are similar to the results reported previously. [1], [27] Once, a sufficient amount of sample is collected, it is labeled with a fluorescent dye and then injected into the CGE instrument.

To determine the lysing efficiency, the device was compared to spores prepared using conventional methods. To prepare the spores using common protocols, the spores are first heated for 30 minutes at 100°C (atmospheric pressure) in a 20mM solution of TCEP, a common reducing agent, to assist breaking the disulfide linkages found on the proteins in the spore coat. The sample is then centrifuged, washed, and filtered to remove the TCEP followed by a fluorescent labeling step and injection into a CGE instrument. Fig. 9 shows a comparison between the thermal lysing technique and conventional benchtop method. Comparing the two electropherograms, they both have the same general profile suggesting that the two techniques work in a similar fashion. However, the intensities of the protein peaks in the thermal lysis electropherogram are much higher, which suggests a better and more complete lysis. Also, new peaks are observed between 125-150 seconds. Whether these are due to degraded fragments of larger proteins or newly resolved proteins is not clear. Nevertheless, high thermal lysing with a LTCC device does provide a distinct advantage in spore lysing efficiency.

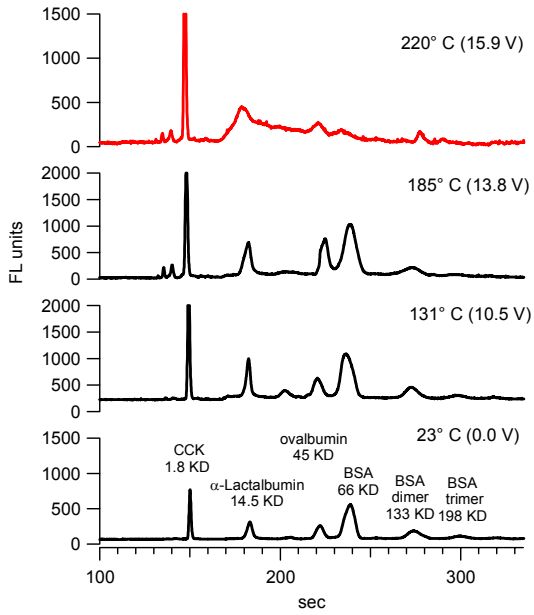

Fig 8. A series of electropherograms of standard proteins run through the lyser at different temperatures. Protein degradation is seen at temperatures near 220°C.

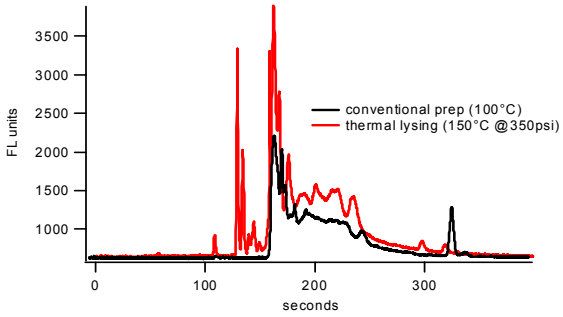

Fig 9. Comparsion of the lysing efficiency of the ceramic lyser to conventional benchtop methods.

Conclusion

It has been shown that LTCC materials are quite useful for developing new microfluidic microsystems for analysis of chemical and biological samples. Particularly, the unique capability of LTCC to withstand high temperatures and internal pressures opens the door for new microfluidic applications not possible with traditional materials. The ceramic lyser is a good example of this. We have shown that using high temperatures to lyse spores is an effective technique; however, more work is necessary to prove this is a reliable and robust method. We plan to continue our efforts in developing LTCC microsystems. For the ceramic lyser concept, the immediate goal is to integrate a working device into an automated sample prep system as part of an unattended bioagent detection system.

Acknowlegement

The authors would like thank the Dennis DeSmit and Timothy A. Turner for their assistance in fabrication of these devices.

References

[1] M. R. Gongora-Rubio, P. Espinoza-Vallejos, L. Sola-Laguna, and J. J. Santiago-Aviles, "Overview of low temperature cofired ceramics tape technology for meso-system technology (MsST)", Sens. Actuators A, 89, pp 222–241, 2001.

[2] K. A. Peterson, K. D. Patel, C. K. Ho, S. B. Rohde, C. D. Nordquist, C. A. Walker, B. D. Wroblewski, and M. Okandan, "Novel Microsystem Applications with New Techniques in Low-Temperature Co-Fired Ceramics", Int. J. Appli. Ceram. Technol., Vol. 5, pp 345-363, 2005.

[3] L. J. Golonka, H. Roguszczak, and T. Zawada, "LTCC based microfluidic systems with optical detection", Sens. Actuators B, Vol. 111-112, pp 392-402, 2005.
[4] M. R. Gongora-Rubio, L. M. Sola-Laguna, P. J. Moffett, and J. J. Santiago-Aviles, "The utilization of low temperature cofired ceramic (LTCC) technology for meso-scale EMS, a simple thermistor based flow sensor" , Sens. Actuators A, Vol. 73, pp 215–221, 1999.
[5] M. R. Gongora-Rubio, M. B. Fontes, Z. Mendes da Rocha, E. M. Richter, and L. Angnes, ''LTCC Manifold for Heavy Metal Detection System in Biomedical and Environmental Fluids'', Sens. Actuators. B, Vol. 103, pp 468–473, 2004.
[6] K. Budniewski, L. J. Golonka, H. Roguszczak, T. Zawada, and T. Dobosz, "Microchamber PCR device in LTCC: modeling and preliminary experiments," in Proceeding VI Optoelectronic and Electronic Sensors Conference, Wroclaw, pp 90–93, 2004.
[7] C. F. Chou, R. Changrani, P. Roberts, D. Sadler, J. Burdon, F. Zenhausern, S. Lin, A. Mulholland, N. Swami, and R. Terbrueggen, "A miniaturized cycle PCR device: modeling and experiments", Microelectron.Eng., Vol. 61/62, pp 921–925, 2002.
[8] W. L. Nicholson and P. Setlow, "Sporulation, Germination and Outgrowth, in *Molecular Biology Methods for Bacillus*," C.R. Harwood and S.M. Cutting, Ed. New York: John Wiley & Sons Ltd, 1964, pp 391–450.
[9] S. M. Cutting and P. M. VanderHorn, "Genetic analysis, in Molecular Biology Methods for Bacillus", C.R. Harwood and S.M. Cutting, Ed. New York: John Wiley & Sons Ltd, 1990.
[10] S. Udenfriend, et al., "Fluorescamine: a reagent for assay of amino acids, peptides, proteins, and primary amines in the picomole range", Science, Vol. 178, No. 3, pp 871-2, 1972.
[11] R. F. Renzi *et al*., "Hand-portable analytical instrument for re-usable chip-based electrophoresis Part 1: system design and integration", Anal. Chem., Vol. 77, pp 435-441, 2005.
[12] J. A. Fruetel *et al*., "Microchip separations of protein biotoxins using an integrated hand-held device." Electrophoresis, Vol. 26, No. 6, pp 1144-54, 2005.
[13] A. Candeli, *et al*., "Sensitivity to lytic agents and DNA base composition of several aerobic spore-bearing bacilli." Zentralbl. Bakteriol. Naturwiss., Vol. 133, No. 3, pp 250-60, 1978.
[14] W. L. King and G. W. Gould, "Lysis of bacterial spores with hydrogen peroxide", J. Appl. Bacteriol., Vol. 32, No. 4, pp 481-90, 1969.
[15] D. P. Weeks, N. Beerman, and O. M. Griffith, "A small-scale five-hour procedure for isolating multiple samples of CsCl-purified DNA: application to isolations from mammalian, insect, higher plant, algal, yeast, and bacterial sources", Anal. Biochem., Vol. 152, No. 2, pp 376-85, 1986.
[16] B. Cummings and T. Wood, "A simple and efficient method for isolating genomic DNA from endomycorrhizal spores", Gene Anal. Tech., Vol. 6, No.5, pp 89-92, 1989.
[17] E. M. Fykse, J. S. Olsen, and G. Skogan, "Application of sonication to release DNA from Bacillus cereus for quantitative detection by real-time PCR", J. Microbiol. Methods, Vol. 55, No. 1, pp 1-10, 2003.
[18] C. Ryu, *et al*., "Sensitive and rapid quantitative detection of anthrax spores isolated from soil samples by real-time PCR", Microbiol. Immunol., Vol. 47, No. 10, pp 693-9, 2003.
[19] D. D. Song, and N. A. Jacques, "Cell disruption of Escherichia coli by glass bead stirring for the recovery of recombinant proteins", Anal. Biochem., Vol. 248, No. 2, pp 300-1, 1997.
[20] D. L. Popham, and P. Setlow, "The cortical peptidoglycan from spores of Bacillus megaterium and Bacillus subtilis is not highly cross-linked", J. Bacteriol., Vol. 175, No. 9, pp 2767-9, 1993.
[21] W. L. Nicholson et al., "Resistance of Bacillus endospores to extreme terrestrial and extraterrestrial environments", Microbiol. Mol. Biol. Rev., Vol. 64, No. 3, pp 548-72, 2000.
[22] J. A. West, K. W. Hukari, and K. D. Patel, 2004 Patent application West, U.S. patent application # 11/059,079, 02/16/2005.
[23] K. D Patel, K. W. Hukari, and K. A. Peterson, ''Low-Temperature Cofired Ceramic Substrate Technology for Microfluidic Systems: Development of a High-Temperature Ceramic Lyser for Solubilizing Spores,'' Conference on MicroScale BioSeparations, February 13–17, 2005, New Orleans, LA.
[24] http://en.wikipedia.org/wiki/Ethylene_glycol, 2006.
[25] L. Haar, J. S. Gallagher, and G. S. Kell, "NBS.NRC Steam Tables," Hemisphere Publishing Corp., New York, 1984.
[26] M.T. Taylor, et al., "Lysing bacterial spores by sonication through a flexible interface in a microfluidic system", Anal. Chem., Vol. 73, No. 3, pp 492-6, 2001.
[27] J.A. West, K.W. Hukari, and K.D. Patel, "A Simple Flow-through Capillary Device for Bacterial Spore Lysis", *Electrophoresis,* submitted for publication.

Additional Journal Information

1) Submission Date, Sponsors, Contact Information

Manuscript received June 07, 2006. Sandia is a multiprogram laboratory operated by Sandia Corporation, a Lockheed Martin Company, for the United States Department of Energy's National Nuclear Security Administration under contract DE-AC04-94AL85000. This research has been funded through Sandia's Laboratory Research and Development program.

K. D. Patel is with the Sandia National Laboratories, Livermore, CA 94550 USA (phone: 925-294-3737; e-mail: kdpatel@sandia.gov). K. A. Peterson is with Sandia National Laboratories, New Mexico, NM 87199 USA (phone: 505-845-8549; email: peterska@sandia.gov). Kyle W. Hukari is with Arcxis Biotechnologies, Livermore CA, 94551.

Distribution

2	MS9018	Central Technical Files	8944
2	MS0899	Technical Library	4536